View metadata, citation and similar papers at core.ac.uk
brought to you by CORE
provided by University of Saskatchewan's Research Archive

WEATHER EFFECT CONSIDERATIONS IN RELIABILITY EVALUATION OF ELECTRICAL TRANSMISSION AND DISTRIBUTION SYSTEMS

A Thesis Submitted to the
College of Graduate Studies and Research
in Partial Fulfillment of the Requirements
for the Degree of

Master of Science

in the Department of Electrical Engineering
University of Saskatchewan
Saskatoon

By
Janak Raj Acharya

© Copyright Janak Raj Acharya, August 2005. All rights reserved.

PERMISSION TO USE

In presenting this thesis in partial fulfilment of the requirements for a Postgraduate degree from the University of Saskatchewan, I agree that the Libraries of this University may make it freely available for inspection. I further agree that permission for copying of this thesis in any manner, in whole or in part, for scholarly purposes may be granted by the professor or professors who supervised the thesis work or, in their absence, by the Head of the Department or the Dean of the College in which the thesis work was done. It is understood that any copying or publication or use of this thesis or parts thereof for financial gain shall not be allowed without author's written permission and without approved by the University of Saskatchewan. It is also understood that due recognition shall be given to the author and to the University of Saskatchewan in any scholarly use which may be made of any material in this thesis.

Requests for permission to copy or to make other use of material in this thesis in whole or part should be addressed to:

Head of the Department of Electrical Engineering
University of Saskatchewan
57 Campus Drive
Saskatoon, SK S7N 5A9

ABSTRACT

The weather environment has a significant impact on the reliability of a power system due to its effect on the system failure mechanisms of overhead circuits and on the operational ability of an electric power utility. The physical stresses created by weather increase the failure rates of transmission or distribution lines operating in adverse weather conditions, resulting in increased coincident failures of multiple circuits. Exceptionally severe weather can cause immense system damages and significantly impact the reliability performance. Recognition of the pertinent weather impacts clearly indicates the need to develop appropriate models and techniques that incorporate variable weather conditions for realistic estimation of reliability indices.

This thesis illustrates a series of multi-state weather models that can be utilized for predictive reliability assessment incorporating adverse and extremely adverse weather conditions. The studies described in this thesis are mainly focused on the analyses using the three state weather model. A series of multi-state weather models are developed and utilized to assess reliability performance of parallel redundant configurations. The application of weather modeling in reliability evaluation is illustrated using a practical transmission system. The thesis presents an approach to identify weather specific contributions to system reliability indices and illustrates the technique by utilizing a test distribution system. The analysis of a range of reliability distributions with regard to major event day segmentation is presented.

The research work illustrated in this thesis clearly illustrates that reliability indices estimated without recognition of weather situations are unrealistic and that at minimum the three state weather model should be applied in reliability evaluation of systems residing in varying weather environments. The conclusions, concepts and techniques presented in this thesis should prove useful in practical application.

ACKNOWLEDGEMENTS

I first and foremost express my sincere gratitude and appreciation to my research supervisor, Professor Roy Billinton, for his valuable guidance, advice, criticism and encouragement throughout the course of this research work and in the preparation of this thesis. I also express sincere thanks to the Advisory Committee members, Professors Garry Wacker, Sherif O. Faried and Anh V. Dinh, for their valuable comments and suggestion in the preparation of this thesis. I would also like to thank Professor Leon Wegner for acting as my external examiner.

I am grateful to my parents, brothers and sisters in Nepal for their constant support and encouragement. I wish to gratefully acknowledge the inspiration, encouragement and consistent help in many ways received from my cousin Nirmala, brother-in-law Prem and nephew Aseem throughout my graduate studies. Thanks also to my colleagues in the University of Saskatchewan for sharing their time with me.

I thankfully acknowledge the financial assistance provided by the Natural Science and Engineering Research Council through a research grant to Professor Roy Billinton.

TABLE OF CONTENTS

LIST OF TABLES

LIST OF FIGURES

LIST OF ACRONYMS AND SYMBOLS

Acronyms

AENS	Average Energy Not Supplied
APL	Alberta Power Limited
ASAI	Average System Availability Index
ASUI	Average System Unavailability Index
CAIDI	Customer Average Interruption Duration Index
CCDF	Composite Customer Damage Function
CDF	Customer Damage Function
CEA	Canadian Electricity Association
ECOST	Expected Customer Cost
EEI	Edition Electric Institute
EENS	Expected Energy Not Supplied
HLI	Hierarchical Level I
HLII	Hierarchical Level II
HLIII	Hierarchical Level III
IEAR	Interruption Energy Assessment Ratio
IEEE	Institute of Electrical and Electronic Engineers
IOR	Index of Reliability
MED	Major Event Day
MTTF	Mean Time To Failure
RBTS	Roy Billinton Test System
SAIDI	System Average Interruption Duration Index
SAIFI	System Average Interruption Frequency Index

Symbols

A	Adverse weather, or average duration of adverse weather
λ_{avg}	Average component failure rate
L_{avg}	Average load
cust	Customers
λ	Failure rate
λ^a or $\lambda^{'}$	Failure rate in adverse weather
λ^m	Failure rate in major adverse weather
λ^n	Failure rate in normal weather
f/yr	Failures per year
F_m	Fraction of bad weather failures occurring in major adverse weather
F_b	Fraction of total line failures occurring in bad weather
f_m	Frequency of occurrence of major adverse weather
hr	Hour
intr	Interruption
kWh	Kilowatt-hour
M	Major adverse weather, or average duration of major adverse weather
MWh	Megawatt-hour
N	Normal weather, or average duration of normal weather
NA	Not available
occ	Occurrence
P_a	Steady state probability of adverse weather
P_m	Steady state probability of major adverse weather
P_n	Steady state probability of normal weather
U	Unavailability
yr	Year

Chapter 1

INTRODUCTION

1.1 Background

Electric power transmission systems are among the most complex networks and the largest systems that exist in the world. The electrical power industry is undergoing considerable changes with respect to structure, operation, re-regulation and deregulation. Networking with neighbouring power systems is highly utilized in order to assure supply continuity and to achieve economic system operation. Transmission systems are highly interconnected and modern utilities purchase economic energy from sources outside their own systems. Transmission systems often traverse a long distance to transport the energy over various networks to load centres. Parallel redundancy of transmission lines is a common way of improving the reliability of power supply. Multiple transmission line outages can significantly alter the transmission system operating configuration and possibly result in supply interruptions to a large number of customers. One of the major causes of transmission line outages is extreme adverse weather conditions.

Power supply interruptions to consumers are generally due to problems that arise in the distribution system or the bulk power system. Experience indicates that disturbances on the bulk system are rare but have a great impact when they do occur. On the other hand, problems occurring in the distribution system are relatively frequent and impact smaller numbers of customers. Distribution systems are usually concentrated in small geographic areas and therefore are directly affected by prevailing adverse weather situations.

In the past, electric utility customers have tended to tolerate service disturbances with relatively few complaints. In the current electricity market, consumers are using more sophisticated computerized processes and are becoming increasingly sensitive to power interruptions. Customers in a competitive energy market may require different levels of supply reliability at the lowest associated cost. The balance between the reliability and economic aspects can be achieved by integrating reliability evaluation into the planning, design and operating phases.

1.2 Power system reliability evaluation

Power system reliability refers to the ability of the system to satisfy the system load requirement as economically as possible and with a reasonable assurance of continuity and quality. It involves the two basic aspects of system adequacy and system security as shown in Figure 1.1. System adequacy relates to the existence of sufficient facilities within the system to meet the consumer demand, whereas system security refers to the ability of the system to respond to disturbances arising within the system [1].

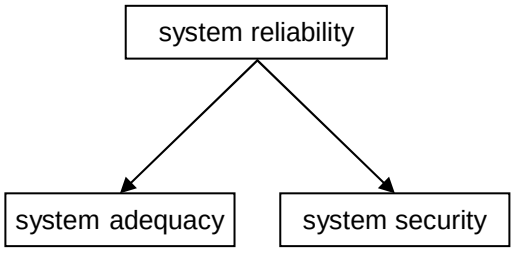

Figure 1.1 System adequacy and system security

A complete power system is composed of the main three functional segments designated as generation, transmission and distribution. A reliability study can be done within an individual functional zone or the zones can be combined to form hierarchical levels. Hierarchical Level I (HLI) analyses are concerned only with generating capacity adequacy. The ability of the generation and transmission systems to perform their

function is designated as HLII analysis. An overall assessment considering all three functional segments is known as HLIII analysis. Reliability evaluation in this thesis is limited to the domain of adequacy assessment within the transmission and distribution functional zones.

Reliability analysis of a power system can be conducted using either deterministic or probabilistic techniques. The early techniques used in practical application were deterministic and some of them are still in use today. The basic weakness inherent in the deterministic methods is the inability to respond or recognize the stochastic or random nature of component failures, customer demands or the overall system behaviour. These limitations have led utilities to apply probabilistic approaches that overcome these problems. Probabilistic methods are now reasonably well developed and most modern power utilities extensively apply these techniques. The research described in this thesis extends the probabilistic evaluation of transmission and distribution systems by incorporating adverse weather considerations.

1.3 Importance of weather considerations in reliability assessment

Transmission and distribution systems are usually overhead facilities that operate in a wide range of weather conditions. The failure rates of transmission and distribution lines are greatly enhanced in severe weather situations. Adverse weather conditions such as gales, lightning, snow, frost, icing, high wind, etc. can significantly increase the likelihood of multiple overlapping outages. The coincident failure of multiple circuits during these periods is generally known as failure bunching. Failure bunching in transmission or distribution systems can significantly impact the reliability performance.

There is a number of reliability indices traditionally used to quantify reliability performance at different levels. The fundamental load point indices are the average failure rate, outage duration and annual outage time. The most commonly used reliability indices to measure aggregate electric power utility performance are the

System Average Interruption Frequency Index (SAIFI), the System Average Interruption Duration Index (SAIDI), the Customer Average Interruption Duration Index (CAIDI), and the Index of Reliability (IOR) [2]. Additional system indices together with their definitions are presented in [1].

The Canadian Electricity Association (CEA) classifies the causes of power interruptions into ten groups. These are designated as adverse weather, scheduled outage, loss of supply, tree contact, lightning, defective equipment, human element, foreign interference, and other/unknown [2]. Adverse weather is one of the major causes of power interruptions. The CEA publishes an annual Service Continuity Report on Distribution System Performance in Electrical Utilities. The individual utility data are confidential to the members. The overall Canadian performance is, however, provided in the annual report and includes details on outage causes and relevant indices. The report presents the annual reliability indices of SAIFI, SAIDI, CAIDI and IOR together with the interruption cause contributions for the participating utilities and for Canada as a whole. Figures 1.2-1.3 present the Canadian individual cause contributions to SAIFI, SAIDI and CAIDI for 2003 [2].

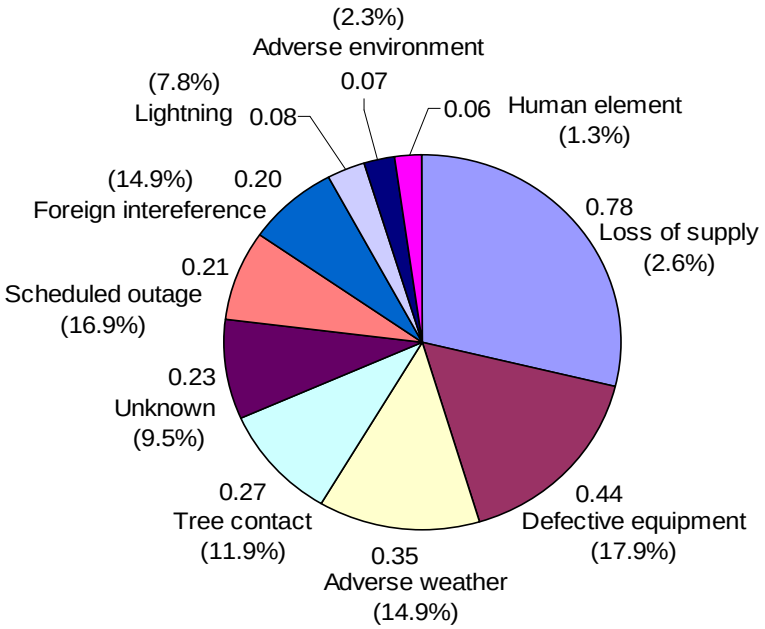

Figure 1.2 Contributions to SAIFI for 2003

Figure 1.2 shows the contributions to SAIFI for each of the ten cause codes. The values shown in the parentheses are the percentages of interruptions. The total SAIFI for the year was 2.67. Figure 1.2 shows that adverse weather caused approximately 15% of the total interruptions and contributed 0.35 to the total SAIFI.

Figure 1.3 shows the contributions to SAIDI and CAIDI for 2003. The total SAIDI was 10.65 hours per year, which represents a substantial increase of 61.9% over the 2002 figure of 4.06 hours. This increase was primarily due to the August 14th blackout and Hurricane Juan. The contribution of adverse weather in 2003 was 13%. The average customer interruption duration per interruption (CAIDI) was 3.99 hours. The CAIDI associated with adverse weather conditions was 7.01 hours, and as shown in Figure 1.3, is the largest cause code contribution.

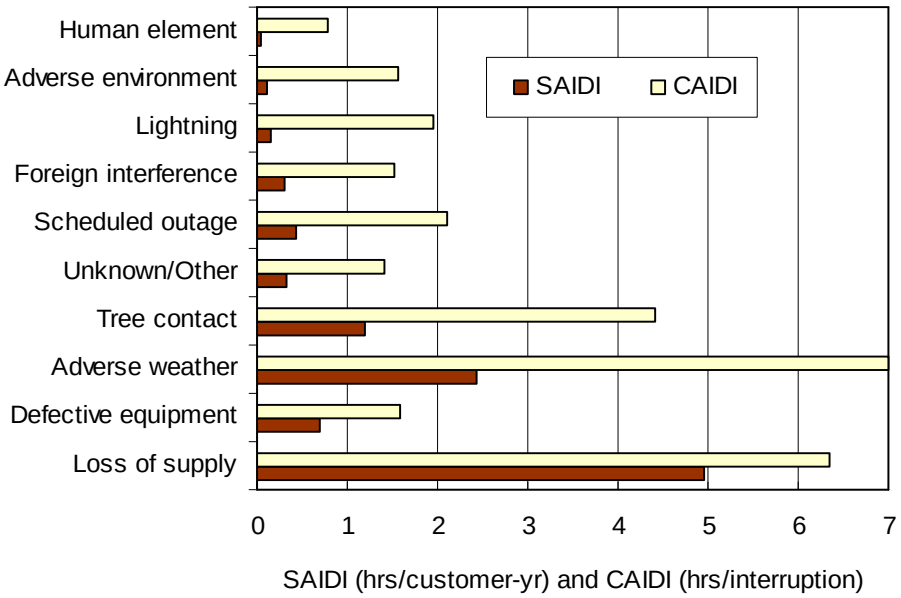

Figure 1.3 Contributions to SAIDI and SAIFI for 2003

Figures 1.2-1.3 clearly illustrate that adverse weather has a significant impact on overall system reliability. The CEA 2000 Service Continuity Report [3] states that the SAIFI in 1998 was 3.58 and was 2.40 with the ice storm excluded. The storm had an even greater

impact on the SAIDI, which was 30.31 hours in total and 3.32 hours excluding the ice storm. Extraordinary events such as “Ice Storm 98” are designated as major events and are normally excluded from an assessment of basic utility performance and reviewed separately.

The above comments illustrate the impact of adverse weather on power system reliability as a whole. The British Electricity Board noted that virtually all the failures in their distribution systems occur in adverse weather conditions, such as lightning, wind, and ice storms [4]. A study of data (1986-1990) from Alberta Power Limited (APL) illustrates that, for 144kV transmission lines, about 33% of all interruptions were caused by adverse weather. In the case of 240kV lines, 45% of all outages were due to adverse weather situations. An analysis of APL’s bulk electric system for the period 1988-1991 revealed that among the weather related outages, 61% were credited to lightning, 35% were due to wind and wet snow, and 4% were caused by frost and icing [5]. These data bases are insufficient to generalize the effects of a specific weather condition, but they clearly indicate that a large proportion of outages are attributable to abnormal weather periods.

The number of customers interrupted, the extent of damage to plant and the duration of outages due to problems created by weather conditions vary considerably due to factors such as weather severity levels, density of customers, system infrastructures, topology etc. Extreme adverse weather situations and their implications for various utilities based on the 44 responses of six participating utilities in a survey conducted by the Edison Electric Institute (EEI) are shown in Tables A.1-A.3 [6] in Appendix A. This clearly shows the magnitude of physical destruction, the number of customers out of service and the periods of supply interruption.

A great deal of experience indicates that most customer supply interruptions are due to failures that occur in the distribution system. It has been observed that in Canada, customer interruptions caused by generation and transmission system outages constitute approximately twenty percent of the total customer interruptions. The remaining eighty

percent of the interruptions are due to distribution system failures [7]. This is primarily due to the localized effect of the weather environments in which the distribution systems are situated. It is, therefore, important to incorporate the weather conditions in reliability evaluations of transmission and distribution systems and recognize the impact on the resulting reliability of the overall power systems.

1.4 Historical development of weather effect considerations

The basic concepts of incorporating weather-related failures were first introduced in [8] with an application to a two-component redundant system. This paper proposed a two state weather model to consider adverse weather in the calculation of the system failure rate. It was stated that the assessment of system failure rate without considering weather conditions could be quite optimistic. The techniques presented initiated considerable future research work in quantitative reliability assessment of transmission and distribution systems.

The ideas presented in [8] can be applied to distribution or transmission systems residing in common weather environments. Failure bunching evaluation is difficult to conduct for transmission systems that occupy large geographic areas and traverse a wide range of weather conditions. This problem was addressed in [9] by incorporating regional weather effects on large-scale systems with transmission lines passing through different geographical regions having different weather conditions.

References 8 and 10 provided the basic framework for the developments in [11, 12]. A three state weather model was postulated in [11] in order to incorporate the effect of severe storm disasters, which were not considered in [8]. Reference 11 also applied the technique to a three line parallel redundant system using a two weather state model. The effects of weather on common mode failures are illustrated in [13]. A previously published three state weather model [14] is extended to multi-state weather models in

[15] in which the continuously varying weather is incorporated more precisely and illustrated using a range of multi-state weather models.

1.5 Evaluation method

The application of probability techniques for transmission and distribution system reliability evaluation was introduced in [8, 16] using a series of approximate equations. These publications presented methods for calculating the failure frequency, the average outage duration and the unavailability of simple series and parallel systems. The application of Markov processes to transmission system reliability evaluation was introduced in [10]. This paper noted that the developed approximate equations did not provide consistent results. These equations were modified in [11, 12] where the Markov method was used as the standard evaluation approach against which the accuracy of the approximate equations was assessed. The equations were further modified in [14] and results were shown to be more accurate than those presented in previous literature. The Monte Carlo Simulation technique was used in [9] in order to incorporate the regional weather effects. In this thesis the Markov approach [10, 17] which is regarded as a benchmark method in power system reliability, is utilized to develop and illustrate a series of weather models.

1.6 Research objectives

The primary objectives of the research work described in this thesis are to examine the existing weather models and extend them to reflect the effect of continuously changing stress created by weather in reliability assessment of transmission and distribution systems. The research in this area was initiated in the 1960s, and significant developments have been made since that time. The research described in this thesis can be regarded as a continuation of the work that was recently presented in [18] at the University of Saskatchewan. Previous studies have incorporated the effects of adverse and major adverse weather by developing two and three weather state models. These

models were explicitly examined using a two line parallel redundant system. This thesis examines these models using both two component and three component parallel configurations. It also examines the impact of incorporating weather considerations on the customer related reliability indices of a practical distribution system. The research described in this thesis extends the existing weather models to multi-state weather models in order to recognize the range of weather severity levels. An additional objective is to investigate the separate contributions of individual weather states to the unreliability of a system. The research also examines the underlying lognormal distribution assumptions used in IEEE Standard 1366 [19] to classify major event days associated with widespread customer outage situations.

1.7 General overview of the thesis

This thesis is divided into eight chapters. Following the introduction in Chapter 1, Chapter 2 introduces the basic concepts of weather modeling. Reliability evaluation of a two component redundant system and a three component redundant system incorporating normal and adverse weather is described using the Markov approach. The results are presented by the fundamental reliability indices of failure rate, outage duration and unavailability.

Chapter 3 describes the consideration of extreme weather conditions. A two component parallel system and a three component parallel system are analysed to examine the effect of incorporating extreme weather conditions utilizing the Markov approach. A number of systems with different failure rates and repair times residing in the same weather environment are studied to examine the effects of weather considerations. The impact of the frequency of occurrence and duration of the extreme weather is discussed.

Chapter 4 illustrates the application of weather modeling to a practical transmission or distribution system. The significance of using the two state and three state weather models over the conventional single state representation in evaluating load point indices

and system indices is presented. A comparative illustration of results obtained for different weather models is provided.

Chapter 5 presents the concept of creating a multi-state weather model as a direct extension of the three weather state model described in Chapter 3. A series of multi-state weather models are developed and used to predict the basic reliability indices of the system failure rate, outage duration and unavailability. The influence of incorporating multi-state weather models is illustrated using Error Factor curves.

Chapter 6 introduces an approach to segment the reliability indices into a series of weather specific indices. The system performance indicators SAIFI and SAIDI are divided into the three segments of normal weather, adverse weather and extreme weather indices. A test distribution system is used to illustrate the method introduced in this chapter. The impact of the time to repair following the system outage due to extreme weather is illustrated. The studies also discuss the effects of the frequency of occurrence of major adverse weather. The influence of coincident multiple circuit failures inherent in radially operated distribution systems is described.

Chapter 7 briefly discusses the methods of classifying a Major Event Day [19]. A set of theoretical reliability distributions and a number of histograms associated with utility data are presented and the applicability of the lognormal distribution used in [19] is discussed.

Chapter 8 presents the summary of the thesis and highlights the conclusions.

Chapter 2

BASIC WEATHER MODELING CONCEPTS

2.1 Introduction

Electrical transmission and distribution networks exist in the two basic forms of underground facilities using cables and overhead facilities on appropriate tower structures. Cables normally operate in a relatively stable environment, while overhead circuits operate in a wide range of weather conditions and are subjected to varying degrees of physical stress due to continuously changing weather patterns. The variation in stress manifests itself in terms of highly variable overhead line failure rates. The stress created by severe weather is much higher than in fair weather and increases with the bad weather intensity level, leading to increases in line failure rates. The likelihood of coincident line failures during high stress periods increases significantly. The phenomenon of multiple line failures during these periods is generally referred to as failure bunching. It is important to appreciate that these overlapping failures are independent events and should not be misunderstood as common mode failures which are an entirely different failure process in parallel circuits on common tower structures.

Parallel redundancy of transmission or distribution elements is a common way of improving the reliability of power supply. As noted earlier, overhead circuits are under the influence of the weather environment to which they are exposed; therefore, reliability assessments without recognizing weather conditions can be highly optimistic and erroneous. This chapter describes basic concepts of weather modeling and illustrates the inclusion of weather conditions in reliability analyses of parallel redundant systems.

2.2 Two state weather modeling

The failure rate of a transmission or distribution line is a continuous function of the weather conditions. It is not realistic to attempt to model and collect data for all possible weather intensity levels. IEEE Standard 346 divides the weather environment into three classes designated as normal weather, adverse weather and major storm disaster [20].

Normal weather: It includes all weather conditions not designated as adverse or major adverse weather.

Adverse weather: Designates weather conditions which cause an abnormally high rate of forced outages for exposed components while such conditions persist, but do not qualify as major storm disasters. Adverse weather conditions can be defined for a particular system by selecting the proper values and combinations of conditions reported by the weather bureau: thunderstorms, tornadoes, wind velocities, precipitation, temperature etc.

Major storm disaster: Designates weather which exceeds design limits of plant and which satisfies all of the following:

- extensive mechanical damage to plant
- more than a specified percentage of customers out of service
- service restoration times longer than a specified time

The utilization of a two state fluctuating weather model [8] was a major step in recognizing the failure bunching phenomenon and provided the basic framework to include multi-state weather conditions. The following describes the consideration of two weather conditions designated as normal and adverse weather.

Randomly occurring weather conditions can be represented as shown in Figure 2.1.

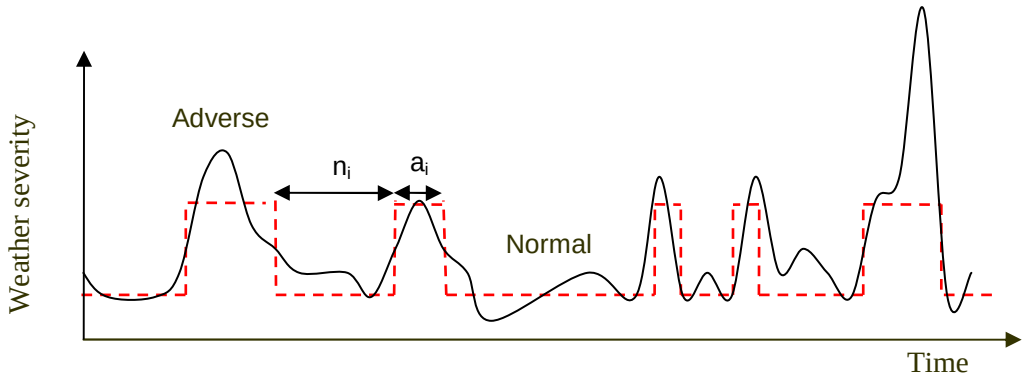

Figure 2.1 Chronological weather pattern

In Figure 2.1,

n_i = duration of the i^{th} normal weather period

a_i = duration of the i^{th} adverse weather period

The adverse weather periods are assumed to occur randomly and the probability distributions associated with the weather durations are assumed to be exponential. The randomly occurring normal and adverse weather periods can be modeled by the periodic weather pattern shown in Figure 2.2.

In Figure 2.2,

N = average duration of normal weather

A = average duration of adverse weather

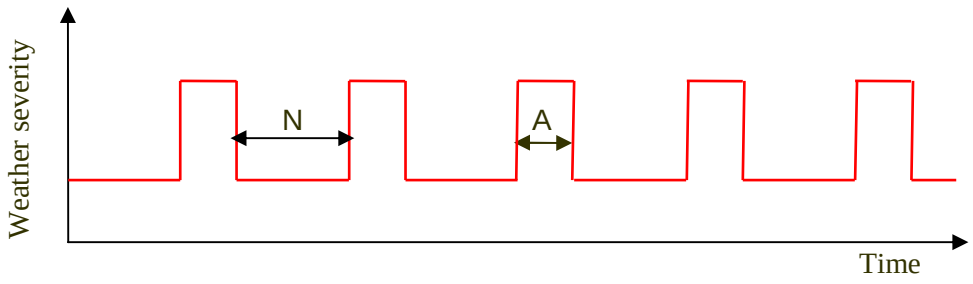

Figure 2.2 Average weather profile

Provided that the necessary conditions are valid, the fluctuating weather can be represented by the Markov model shown in Figure 2.3. The basic concepts of the Markov approach are given in [17]. The weather statistics required for the two state weather model are the average durations of normal weather and adverse weather.

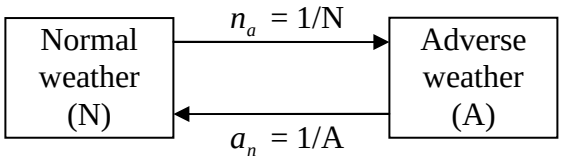

Figure 2.3 Two state weather model

2.3 Failure rate considerations

The normal and adverse weather failure rates are expressed in failures per year of time in the respective weather state, not in the number of failures per year. The average failure rate and the weather specific failure rates are related as shown in Equation 2.1.

$$\lambda_{avg} = P_n \lambda + P_a \lambda' \qquad (2.1)$$

where,

λ_{avg} = average component failure rate expressed in failures per year

$P_n = N/(N + A)$ = steady state probability of normal weather

$P_a = A/(N + A)$ = steady state probability of adverse weather

λ = failure rate expressed in failures per year of normal weather

λ' = failure rate expressed in failures per year of adverse weather

It is extremely difficult to determine the transmission line failure rates associated with a particular weather condition from available historical data. They can, however, be estimated using Equations 2.2 and 2.3 using the fraction of the total number of failures that can be attributed to adverse weather (F) and normal weather (1-F).

$$\lambda = \lambda_{avg}\,(1-F)/P_n \tag{2.2}$$

$$\lambda^{'} = \lambda_{avg}\;F/P_a \tag{2.3}$$

Figure 2.4 shows the two state representation of the component failure rate.

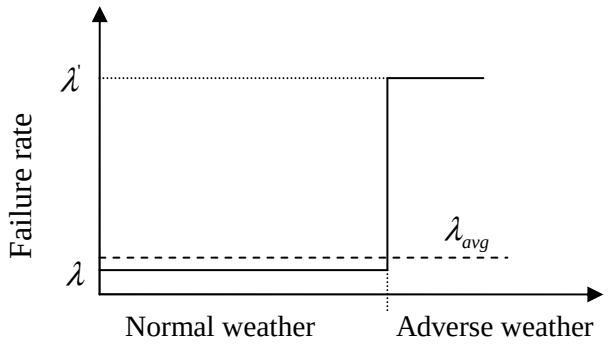

Figure 2.4 Failure rate representation in the two state weather model

2.4 Evaluation techniques

There are various techniques that can be employed to incorporate the failure bunching effect of the weather environment. The basic approximate equation approach was initially introduced to recognize weather effects. It is probably the most popular method in practical application. One of the reasons behind its popularity is that this two state weather representation can be easily included in existing software applications.

The two state weather model has been used for many years [8, 10]. It has been realized, however, that the two state model does not fully reflect the actual weather severity. This led to the development of three or more state weather models. Three state weather modeling is illustrated in [14, 18]. An important conclusion drawn from these publications is that numerical results obtained using the approximate approach are inconsistent. In certain cases, relatively wide assumptions are made to simplify the equation derivation process and the representation of actual system behaviour may be lost.

On the other hand, the Markov approach reflects the stochastic system behaviour with relatively few assumptions. The most relevant assumptions are that the time duration of each system state is exponentially distributed, and the transition rates are constant. One disadvantage of this approach is that the number of system states increases significantly as the failure modes or the number of system components increase. In this thesis, only two or three components are considered in the failure bunching process and the system element is represented by the two operating states designated as up and down. When a system model contains a large number of states, it can be solved using a relatively simple computer program. The weather modeling studies in this chapter and in the subsequent chapters were analysed using the Markov approach.

2.5 Markov analysis of a two component system

Figure 2.5 shows the system state space diagram of a two component system with a two state weather model.

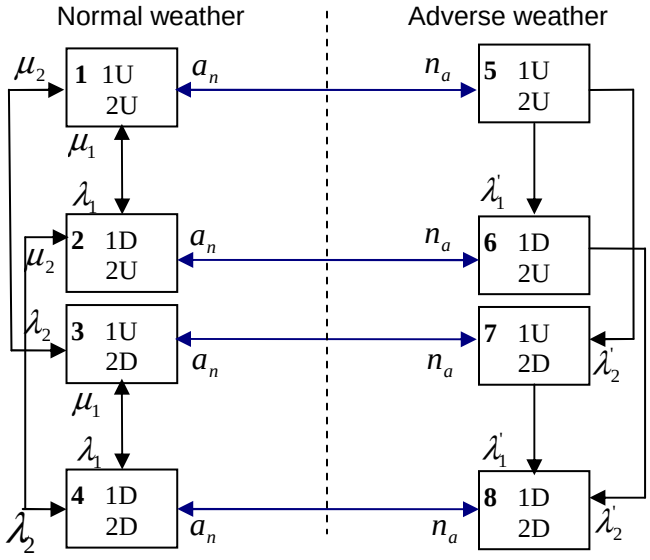

Figure 2.5 System state space diagram with a two state weather model

The letters U and D inside the rectangles in Figure 2.5 denote the component currently being in the up-state (operating) and down-state (failed) respectively. The parameters n_a and a_n are the transition rates between normal and adverse weather. The failure rates in normal and adverse weather are λ and λ' given by Equation 2.2 and Equation 2.3 respectively and μ is the repair rate in normal weather, which is the reciprocal of the component repair time. The repair activity is assumed to be carried out only in normal weather. The repair rate in the adverse weather state is therefore zero.

The steady state probabilities can be determined using the frequency balance approach. The procedure is described in detail in [17].

$$(\lambda_1 + \lambda_2 + n_a) P_1 - \mu_1 P_2 - \mu_2 P_3 - a_n P_5 = 0 \quad (2.4a)$$

$$-\lambda_1 P_1 + (\mu_1 + \lambda_2 + n_a) P_2 - \mu_2 P_4 - a_n P_6 = 0 \quad (2.4b)$$

$$-\lambda_2 P_1 - \mu_1 P_4 + (\lambda_1 + \mu_2 + n_a) P_3 - a_n P_7 = 0 \quad (2.4c)$$

$$-\lambda_2 P_2 - \lambda_1 P_3 + (\mu_1 + \mu_2 + n_a) P_4 - a_n P_8 = 0 \quad (2.4d)$$

$$-n_a P_1 + (a_n + \lambda_2' + \lambda_1') P_5 = 0 \quad (2.4e)$$

$$-n_a P_2 - \lambda_1' P_5 + (a_n + \lambda_2') P_6 = 0 \quad (2.4f)$$

$$-n_a P_3 - \lambda_2' P_5 + (a_n + \lambda_1') P_7 = 0 \quad (2.4g)$$

$$-n_a P_4 - \lambda_2' P_6 - \lambda_1' P_7 + a_n P_8 = 0 \quad (2.4h)$$

Equation 2.4 is a system of dependent simultaneous equations and therefore, to solve for the eight variables, an additional independent equation is needed. This additional equation is

$$P_1 + P_2 + P_3 + P_4 + P_5 + P_6 + P_7 + P_8 = 1 \quad (2.5)$$

The above linear equations can be expressed in the matrix form:

$$[X][Pb] = [0] \quad (2.6)$$

where,

$[Pb]$= Transpose of $[P_1 \quad P_2 \quad P_3 \quad P_4 \quad P_5 \quad P_6 \quad P_7 \quad P_8]$

$[X]$=

$$\begin{bmatrix} \lambda_1+\lambda_2+n_a & -\mu_1 & -\mu_2 & 0 & -a_n & 0 & 0 & 0 \\ -\lambda_1 & \mu_1+\lambda_2+n_a & 0 & -\mu_2 & 0 & -a_n & 0 & 0 \\ -\lambda_2 & 0 & \lambda_1+\mu_2+n_a & -\mu_2 & 0 & 0 & -a_n & 0 \\ 0 & -\lambda_2 & -\lambda_1 & \mu_1+\mu_2+n_a & 0 & 0 & 0 & -a_n \\ -n_a & 0 & 0 & 0 & \lambda_1'+\lambda_2'+a_n & 0 & 0 & 0 \\ 0 & -n_a & 0 & 0 & -\lambda_2' & \lambda_2'+a_n & 0 & 0 \\ 0 & 0 & -n_a & 0 & -\lambda_1' & 0 & \lambda_1'+a_n & 0 \\ 0 & 0 & 0 & -n_a & 0 & -\lambda_2' & -\lambda_1' & a_n \end{bmatrix}$$

Equation 2.5 can be substituted for any Equation from 2.4a to 2.4h. If Equation 2.4h is replaced by Equation 2.5, each element in the last row of the matrix [X] becomes 1 and the system of equations is represented by Equation 2.7.

$$[X][Pb] = [Y] \tag{2.7}$$

where,

$[Y]$ = Transpose of $[0 \quad 0 \quad 0 \quad 0 \quad 0 \quad 0 \quad 0 \quad 1]$

Now, $[Pb] = [X]^{-1}[Y]$ (2.8)

The stochastic transitional probability matrix possesses a feature that can be employed in order to obtain matrix [X]. The stochastic transitional probability matrix constructed using the state space diagram shown in Figure 2.5 is as follows.

$$[P] =$$

$$\begin{bmatrix}
1-\lambda_1-\lambda_2-n_a & \lambda_1 & \lambda_2 & 0 & n_a & 0 & 0 & 0 \\
\mu_1 & 1-\mu_1-\lambda_2-n_a & 0 & \lambda_2 & 0 & n_a & 0 & 0 \\
\mu_2 & 0 & 1-\lambda_1-\mu_2-n_a & \lambda_1 & 0 & 0 & n_a & 0 \\
0 & \mu_2 & \mu_1 & 1-\mu_1-\mu_2-n_a & 0 & 0 & 0 & n_a \\
a_n & 0 & 0 & 0 & 1-\lambda_1-\lambda_2-a_n & \lambda_1 & \lambda_2 & 0 \\
0 & a_n & 0 & 0 & 0 & 1-\lambda_2-a_n & 0 & \lambda_2 \\
0 & 0 & a_n & 0 & 0 & 0 & 1-\lambda_1-a_n & \lambda_1 \\
0 & 0 & 0 & a_n & 0 & 0 & 0 & 1-a_n
\end{bmatrix}$$

The matrix [X] can be produced by subtracting the transpose of [P] from the identity matrix.

$$[X] = [I] - \text{Transpose of } [P] \qquad (2.9)$$

The probabilities associated with each state can also be determined using limiting state probability analysis [17].

The system failure rate can be obtained using the stochastic transitional probability matrix [17]. The system states 4 and 8 represent the down state for the two component parallel redundant system. If the rows and columns corresponding to the system down states are removed, the resulting matrix is [Q] as given below.

$$[Q] =$$

$$\begin{bmatrix}
1-\lambda_1-\lambda_2-n_a & \lambda_1 & \lambda_2 & n_a & 0 & 0 \\
\mu_1 & 1-\mu_1-\lambda_2-n_a & 0 & 0 & n_a & 0 \\
\mu_2 & 0 & 1-\lambda_1-\mu_2-n_a & 0 & 0 & n_a \\
a_n & 0 & 0 & 1-\lambda_1-\lambda_2-a_n & \lambda_1 & \lambda_2 \\
0 & a_n & 0 & 0 & 1-\lambda_2-a_n & 0 \\
0 & 0 & a_n & 0 & 0 & 1-\lambda_1-a_n
\end{bmatrix}$$

The truncated matrix [Q] is subtracted from the identity matrix and inverted. Equation 2.10 gives the resulting matrix [N].

$$[N] = [I - Q]^{-1} \tag{2.10}$$

State 1 is considered to be the starting state. The total expected time before entering the absorbing state is the Mean Time To Failure (MTTF) and is obtained by summing the first row of the matrix [N].

$$MTTF = \sum_{i=1}^{6} N_{1,i} \tag{2.11}$$

The average system failure rate, designated as λ_W, is the reciprocal of the MTTF as shown in Equation 2.12.

$$\lambda_W = 1/MTTF \tag{2.12}$$

The average system outage duration (r_W) is the average time spent in the down state and is obtained by dividing the cumulative probability of the failed state by the frequency of encountering the failed state. It is shown in Equation 2.13.

$$r_W = \frac{P_4 + P_8}{P_4\ (\mu_1 + \mu_2)} \tag{2.13}$$

The average system unavailability (U_W) is the probability of the system being in the down state. Equation 2.14 gives the unavailability for the two component parallel redundant system.

$$U_W = P_4 + P_8 \tag{2.14}$$

The average system unavailability is usually expressed in hours per year by multiplying U_W by 8760 hours per year.

2.6 Markov analysis of a three component system

The state space diagram for the three component system residing in two weather states is shown in Figure 2.6. The absence of a repair rate in the adverse weather state indicates that repair is not considered during adverse weather. The individual state connections between the two different weather conditions are not shown. The two thick arrows between the two weather states indicate these transitions. For example, consider state 1 and state 9. States 1 and 9 represent the system states in which both components are in the up-state, but are in two different weather conditions. The parameter n_a indicates the transitions from state 1 in normal weather to state 9 in adverse weather. Similarly a_n demonstrates the transitions from state 9 to state 1. Likewise, states 2 and 10, 3 and 11, 4 and 12 and so on form the set of similar operating states and are defined similar to that described for the set of states 1 and 9.

The average system failure rate can be evaluated using the transitional probability matrix associated with the state space diagram in Figure 2.6. The procedure is similar to that described for the two component system in Section 2.5. The stochastic transitional probability matrix is given in Appendix B.1. The system MTTF is used to obtain the average system failure rate as shown in Equation 2.15. System states 8 and 16 are the down states for redundant operation of the three component system. The average system outage duration and unavailability are calculated as shown in Equation 2.15.

$$\lambda_W = 1/MTTF \tag{2.15a}$$

$$r_W = \frac{P_8 + P_{16}}{P_8\ (\mu_1 + \mu_2 + \mu_3)} \tag{2.15b}$$

$$U_W = P_8 + P_{16} \tag{2.15c}$$

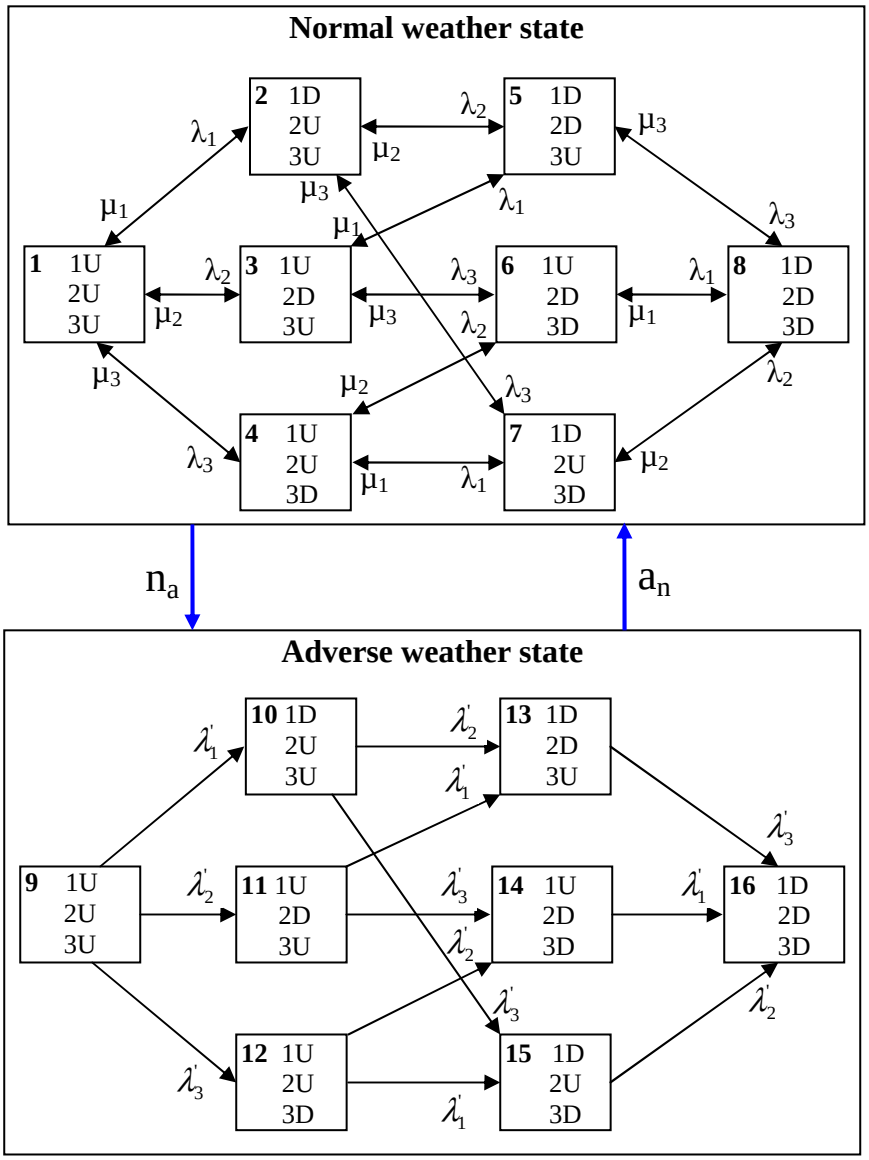

Figure 2.6 State space diagram for a three component system with a two state weather model

2.7 Sensitivity study

The simple transmission system shown in Figure 2.7 is used to illustrate the application of two state weather modeling. In the following analysis, transmission lines 1 and 2 are used to form a two line parallel configuration, or a second order mincut. Line 3 is added to form a three line parallel system, or a third order mincut. A mincut can be defined as the assembly of system components in which all components must fail to cause the system to fail.

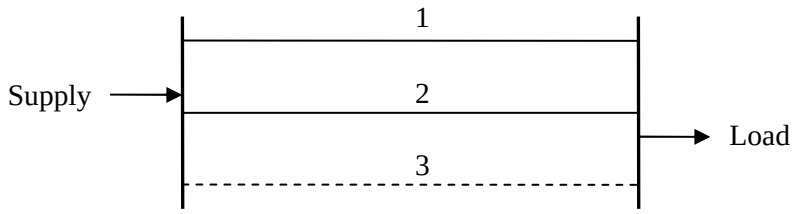

Figure 2.7 A simple parallel transmission system

The following data are used in the analysis:

Average failure rate for each component = 1.0 f/yr

Average repair time for each component = 7.5 hrs

Average duration of normal weather = 200 hrs

Average duration of adverse weather = 2 hrs

The system failure rate of the two line system without considering weather conditions can be evaluated using the Markov approach or approximated by Equation 2.16 [17]. Similarly Equation 2.17 can be used to determine the average system failure rate of the three line parallel system.

Two line parallel system: $\overline{\lambda}_{system} = \lambda_1\lambda_2(r_1 + r_2)$ (2.16)

Three line parallel system: $\overline{\lambda}_{system} = \lambda_1\lambda_2\lambda_3(r_1r_2 + r_2r_3 + r_3r_1)$ (2.17)

The ratio of the system failure rate considering weather effects (λ_W) and the system failure rate without incorporating weather conditions ($\overline{\lambda}_{system}$) is designated as the Error Factor as expressed by Equation 2.18

$$\text{Error Factor} = \frac{\lambda_W}{\overline{\lambda}_{system}} \tag{2.18}$$

Table 2.1 shows the weather specific failure rates, average system failure rate and Error Factor for the two component parallel redundant system. The percentage of line failures occurring in adverse weather is varied from 0 to 100% in 10% increments.

Table 2.1 Failure rate and Error Factor for a second order mincut

% of line failures in adverse weather	Normal weather failure rate (λ)	Adverse weather failure rate (λ')	System failure rate (λ_W) (failures/yr)	Error Factor
0	1.010	0.00	0.0017	1.01
10	0.909	10.10	0.0022	1.27
20	0.808	20.20	0.0035	2.06
30	0.707	30.30	0.0058	3.37
40	0.606	40.40	0.0089	5.18
50	0.505	50.50	0.0128	7.48
60	0.404	60.60	0.0176	10.27
70	0.303	70.70	0.0232	13.52
80	0.202	80.80	0.0295	17.25
90	0.101	90.90	0.0367	21.42
100	0.000	101.00	0.0446	26.05

The Error Factor as a function of the percentage of line failure occurring in adverse weather is presented pictorially in Figure 2.8. It can be seen from Figure 2.8 that the system failure rate increases with the percentage of failures occurring in adverse weather and that disregarding adverse weather conditions can severely underestimate the predicted average system failure rate.

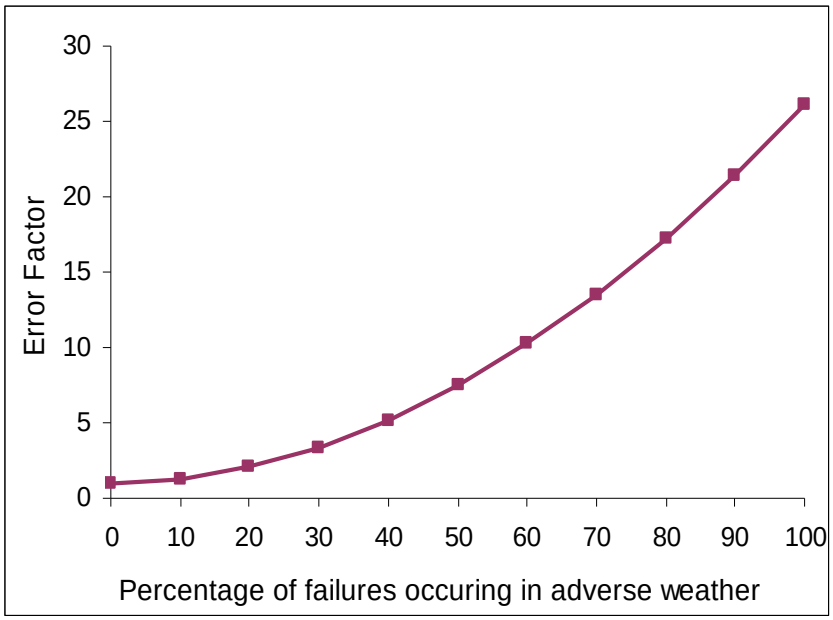

Figure 2.8 Error Factor for a second order mincut

Table 2.2 shows the average system outage duration and unavailability of the two component system for varying failure percentages assigned to adverse weather. These indices are shown graphically in Figure 2.9. Figure 2.9 shows that the average outage duration initially increases sharply as more failures occur in adverse weather and then becomes relatively stable for further increases in adverse weather failures. The unavailability, however, increases gradually as more failures occur in adverse weather.

Table 2.2 System outage duration and unavailability for a second order mincut

% of line failures in adverse weather	Average outage duration (hours)	Unavailability (hours/year)
0	3.79	0.0065
10	4.36	0.0095
20	5.01	0.0177
30	5.37	0.0310
40	5.56	0.0493
50	5.65	0.0725
60	5.71	0.1005
70	5.74	0.1331
80	5.76	0.1704
90	5.78	0.2121
100	5.79	0.2583

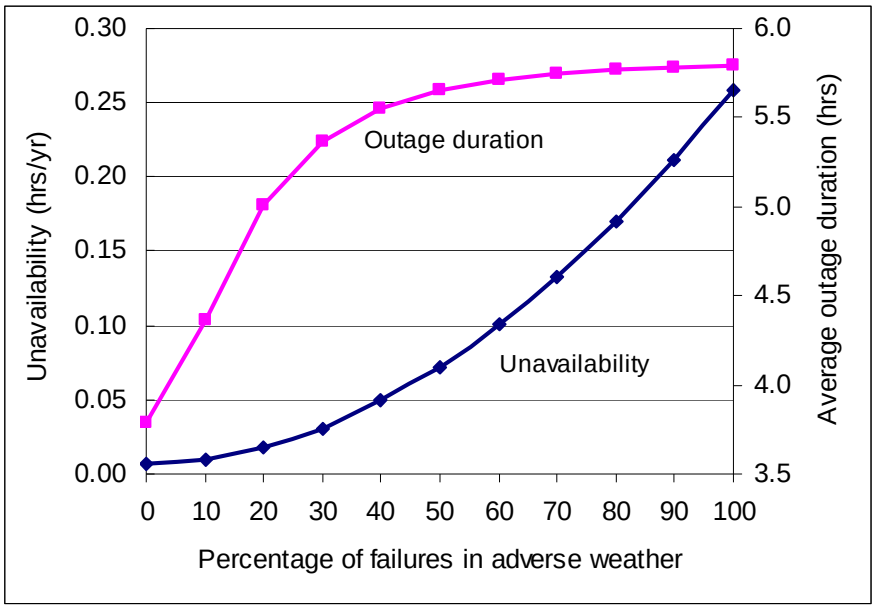

Figure 2.9 Unavailability and outage duration for a second order mincut

Table 2.3 presents the average system failure rate and the Error Factor for a three component parallel redundant system with a two state weather model.

Table 2.3 Average system failure rate for a third order mincut

% of line failures in adverse weather	Normal weather failure rate (λ)	Adverse weather failure rate (λ')	System failure rate (λ_w) (failures/yr)	Error Factor
0	1.010	0.00	0.000002	1.02
10	0.909	10.10	0.000007	3.25
20	0.808	20.20	0.000034	15.46
30	0.707	30.30	0.000100	45.59
40	0.606	40.40	0.000222	101.12
50	0.505	50.50	0.000416	189.11
60	0.404	60.60	0.000695	316.24
70	0.303	70.70	0.001075	488.76
80	0.202	80.80	0.001567	712.61
90	0.101	90.90	0.002184	993.33
100	0.000	101.00	0.002938	1336.16

The Error Factor is displayed in Figure 2.10. Figure 2.10 illustrates that the Error Factor increases sharply with the percentage of failures in adverse weather. The influence of adverse weather on the higher order mincut can be illustrated by comparing the Error Factor in Figure 2.10 with that in Figure 2.8.

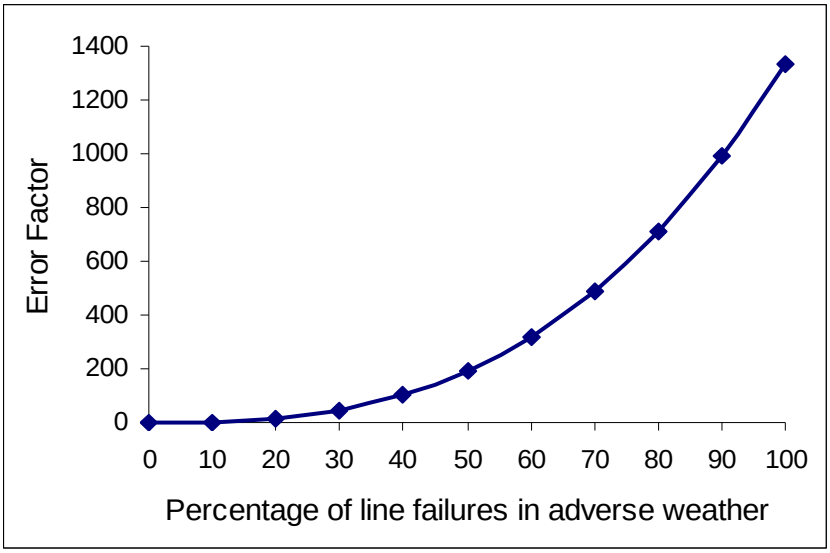

Figure 2.10 Error Factor for a third order mincut

The average system outage duration and unavailability are shown in Table 2.4. These indices are shown graphically in Figure 2.11.

Table 2.4 System outage duration and unavailability for a third order mincut

% of line failures in adverse weather	Average outage duration (hours)	Unavailability (hours/year)
0	2.52	0.000006
10	3.81	0.000027
20	4.31	0.000147
30	4.42	0.000443
40	4.46	0.000993
50	4.49	0.001866
60	4.50	0.003130
70	4.51	0.004848
80	4.52	0.007079
90	4.52	0.009880
100	4.52	0.013302

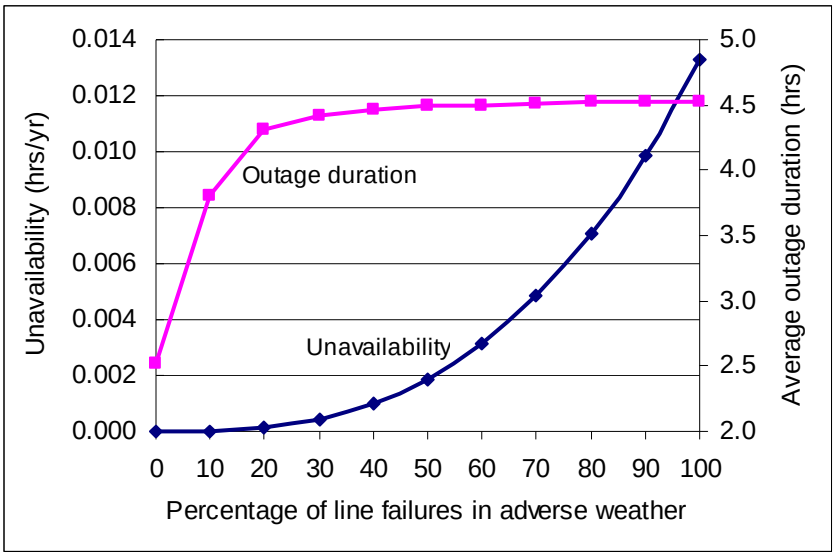

Figure 2.11 Unavailability and average outage duration

As shown in Figure 2.11, the unavailability increases as the percentage of failures occurring in adverse weather increases. The unavailability increases faster as more failures occur in adverse weather. The average system outage duration initially increases rapidly with adverse weather failures and then becomes almost constant with further increases in the percentage of failures in adverse weather.

2.8 Summary

The basic concepts used to incorporate the weather environment in a reliability study of outdoor transmission or distribution systems are introduced in this chapter. Weather conditions are divided into the two categories of normal and adverse weather to create a simple fluctuating two state weather model. Reliability models for systems containing two and three lines in parallel in two weather conditions are developed and utilized to compute the fundamental reliability indices using the Markov approach. The Error Factor is used to provide a comparative analysis of the system failure rates with and without considering the weather effects.

The application of the two state weather model is illustrated using two different redundant systems consisting of two and three lines. The reliability indices of the average system failure rate, outage duration and unavailability are evaluated incorporating adverse weather. The effect of failure bunching due to adverse weather on the average system failure rate is clearly demonstrated using the Error Factor. The studies show that failure bunching has even greater influence in a third order mincut. The impact on the average outage duration and unavailability are also described. The analysis in this chapter clearly shows the importance of incorporating adverse weather in the reliability assessment of multi-line systems exposed to a fluctuating weather environment. The influence of separately incorporating extremely adverse weather conditions is described in Chapter 3.

Chapter 3

EXTREME WEATHER CONSIDERATIONS

3.1 Introduction

The previous chapter illustrates the concept that environmental stresses have great influence on transmission line forced outage rates and that the effect of failure bunching can be incorporated in a reliability assessment by utilizing a two state weather model including normal and adverse weather. It is important to note that disastrous weather conditions such as major hurricanes, high intensity tornadoes, heavy thunderstorms, ice storms etc. cannot be aggregated with other generally less destructive periods of adverse weather. These extreme conditions, while less probable, can have great impacts on power system operations. This dictates a need to examine the effect of violent weather events on the predicted reliability indices of transmission and distribution configurations operating in a wide range of randomly occurring weather conditions. In this chapter, a three state weather model is developed to include major adverse weather. This is a direct extension of the two state weather model incorporating normal and adverse weather.

A three state weather model was introduced in [11] and further work was conducted in [14, 18]. The focus in these publications was on weather modeling using the basic approximate equations in the context of a second order mincut. This chapter examines the application of a three state weather model to second order mincuts and extends the analysis to incorporate third order mincuts, using the Markov method. The analyses described in this chapter illustrate the influence of incorporating major adverse weather conditions on the reliability performance of a parallel transmission system. The results are presented in terms of the system average failure rate, average outage duration and average annual unavailability.

3.2 Three state weather model

As noted in Chapter 2, the weather environment can be divided into the three categories of normal, adverse and major storm disaster [20]. Failures that occur in extremely severe weather can be incorporated using the three state weather model shown in Figure 3.1. The terms extreme weather or major adverse weather are used to describe extremely adverse weather situations. Adverse and extreme weather conditions are collectively designated as bad weather in this thesis.

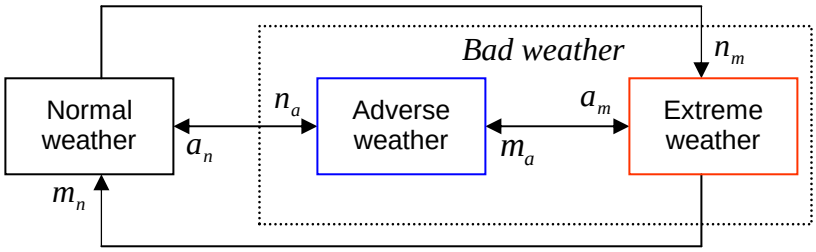

Figure 3.1 Three state weather model

The transition rates between the various weather states in Figure 3.1 are as follows:

a_n = adverse weather to normal weather

a_m = adverse weather to major adverse weather

n_a = normal weather to adverse weather

n_m = normal weather to major adverse weather

m_a = major adverse weather to adverse weather

m_n = major adverse weather to normal weather

The steady state probabilities associated with a specific weather state can be determined using the frequency balance approach in conjunction with the state space diagram shown in Figure 3.1. Unlike the case of the two state weather model, the steady state probabilities in the three state weather model cannot be simply obtained using the average durations of the weather states. It is possible, however, to estimate the steady state probabilities using the actual durations of each weather state. In this case, the

probability of a weather state is the ratio of the total time associated with that weather state and the total period of observation. The frequency balance approach or limiting state probability technique [17] can be used to determine the steady state probabilities when the transition rates between the different weather states in the Markov model shown in Figure 3.1 are known. The transition rates can also be used to compute the average weather durations and frequencies of occurrence [17]. The weather statistics required in the three state weather model are the weather transition rates. Detailed weather statistics are not available and the collection of such data is beyond the scope of this thesis work.

The following transition rates were assumed in order to create a realistic and practical three state weather model.

n_a = 1/200 occ/hr	a_n = 1/2 occ/hr
a_m = 1/8760 occ/hr	m_a = 1/2 occ/hr
n_m = 1/8760 occ/hr	m_n = 1/2 occ/hr

The steady state probabilities, average durations and frequencies of occurrence associated with the weather states are as follows.

Steady state probability:

Normal weather, $$P_n = \frac{D_1}{D_1 + D_2 + D_3}$$

Adverse weather, $$P_a = \frac{D_2}{D_1 + D_2 + D_3}$$

Extreme weather, $$P_m = \frac{D_3}{D_1 + D_2 + D_3}$$

where, $$D_1 = m_a a_n + m_n a_m + m_n a_n$$

$$D_2 = m_a n_a + m_a n_m + m_n n_a$$

$$D_3 = n_a a_m + n_m a_n + n_m a_m$$

Average duration:

Normal weather, $$N = 1/(n_a + n_m)$$

Adverse weather, $A = 1/(a_n + a_m)$

Extreme weather, $M = 1/(m_a + m_n)$

Frequency of occurrence:

Normal weather, $f_N = P_n (n_a + n_m)$

Adverse weather, $f_A = P_a (a_n + a_m)$

Extreme weather, $f_M = P_m (m_a + m_n)$

Table 3.1 shows the steady state probability, frequency of encountering and average duration of the different weather states for the data shown above.

Table 3.1 Weather statistics

Weather state	Steady state probability	Frequency of occurrence (Occ/year)	Average duration (hours)
Normal weather	0.989875	44.346	195.54
Adverse weather	0.010011	43.856	1.9995
Extreme weather	0.000114	0.9999	1.0

3.3 Failure rate representation

The failure rate of a component is a continuous function of the weather conditions to which it is exposed [1]. In the three state weather model, continuously varying weather conditions are grouped into three weather categories. The three relevant failure rates are defined as follows:

λ^n = normal weather failure rate expressed in failures per year of normal weather

λ^a = adverse weather failure rate expressed in failures per year of adverse weather

λ^m = major adverse weather failure rate expressed in failures per year of major adverse weather

The average component failure rate as a function of the failure rates in the various weather states is given by Equation 3.1.

$$\lambda_{avg} = P_n \lambda^n + P_a \lambda^a + P_m \lambda^m \qquad (3.1)$$

where, P_n, P_a and P_m are the steady state probabilities of normal, adverse and major adverse weather respectively.

The failure rates λ^n, λ^a and λ^m are given by Equation 3.2.

$$\lambda^n = \lambda_{avg} (1 - F_b) / P_n \qquad (3.2a)$$

$$\lambda^a = \lambda_{avg} F_b (1 - F_m) / P_a \qquad (3.2b)$$

$$\lambda^m = \lambda_{avg} F_b F_m / P_m \qquad (3.2c)$$

where, F_b is the fraction of total line failures occurring in bad weather and F_m is the fraction of bad weather failures occurring in major adverse weather.

The variation in the component failure rate as a result of considering the three state weather model can be represented in the general form shown in Figure 3.2 where the component failure rate increases significantly during adverse weather and extreme weather periods.

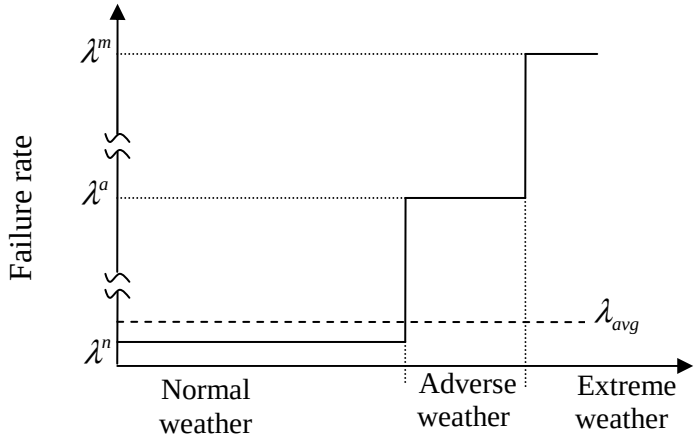

Figure 3.2 Failure rate representation in the three state weather model

Assuming that the average annual failure rate is 1.0 f/yr, the failure rates for the three weather states under the condition that the percentage of line failures occurring in bad weather vary from 0% to 100% and that 20% of the bad weather failures are allocated to major adverse weather (F_m = 20%) are shown in Table 3.2.

Table 3.2 Line failure rates in the three weather states

% of total line failures that occur in bad weather (F_b)	Normal weather failure rate (λ^n)	Adverse weather failure rate (λ^a)	Extreme weather failure rate (λ^m)
0	1.0102	0	0
10	0.9092	7.992	175.22
20	0.8082	15.983	350.44
30	0.7072	23.975	525.66
40	0.6061	31.966	700.88
50	0.5051	39.958	876.10
60	0.4041	47.949	1051.32
70	0.3031	55.941	1226.54
80	0.2020	63.932	1401.76
90	0.1010	71.924	1576.98
100	0	79.915	1752.20

The magnitude of the failure rates in adverse weather and major adverse weather shown in Table 3.2 change according to the percentages of bad weather failures attributed to the major adverse weather period. The failure rate profile presented in Figure 3.2 represents the values in one row of Table 3.2.

3.4 Markov analysis of a two component system

The Markov model for a two component system with a three state weather model is shown in Figure 3.3. It should be noted that in Figure 3.3, repair is not performed in bad weather i.e. in neither adverse weather nor major adverse weather.

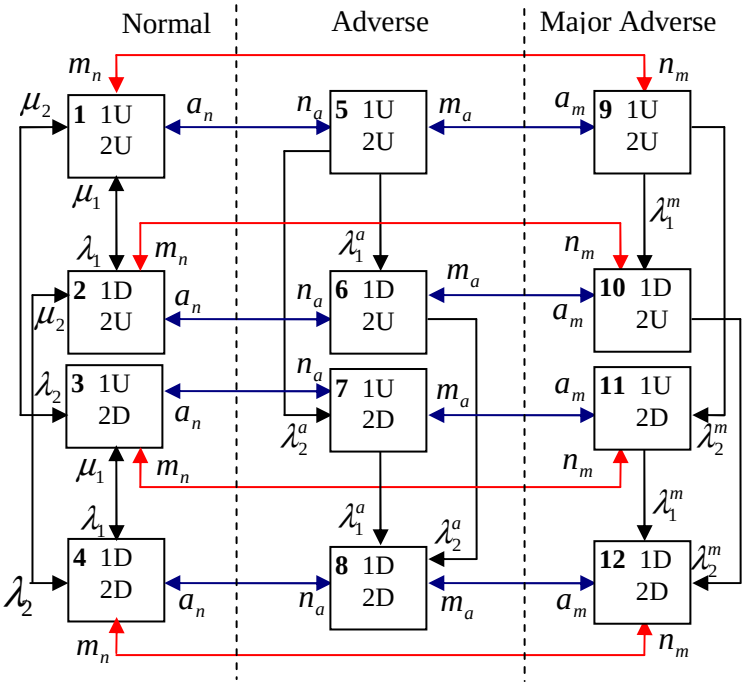

Figure 3.3 State space diagram for a two component system with a three state weather model

There are a number of possible approaches to determine the steady state probabilities associated with each state of a Markov model. The stochastic transitional probability matrix for the system is shown in Equation 3.3.

$$[P] = \begin{bmatrix} A & B & C \\ D & E & F \\ G & H & J \end{bmatrix} \tag{3.3}$$

where, $[B] = n_a [I]_{4x4}$ $[C] = n_m [I]_{4x4}$

$[D] = a_n [I]_{4x4}$ $[F] = a_m [I]_{4x4}$

$[G] = m_n [I]_{4x4}$ $[H] = m_a [I]_{4x4}$

$$[A]=\begin{bmatrix} 1-\lambda_1-\lambda_2-\eta_a-\eta_m & \lambda_1 & \lambda_2 & 0 \\ \mu_1 & 1-\mu_1-\lambda_2-\eta_a-\eta_m & 0 & \lambda_2 \\ \mu_2 & 0 & 1-\mu_2-\lambda_1-\eta_a-\eta_m & \lambda_1 \\ 0 & \mu_2 & \mu_1 & 1-\mu_1-\mu_2-\eta_a-\eta_m \end{bmatrix}$$

$$[E]=\begin{bmatrix} 1-\lambda_1^a-\lambda_2^a-a_n-a_m & \lambda_1^a & \lambda_2^a & 0 \\ 0 & 1-\lambda_2^a-a_n-a_m & 0 & \lambda_2^a \\ 0 & 0 & 1-\lambda_1^a-a_n-a_m & \lambda_1^a \\ 0 & 0 & 0 & 1-a_n-a_m \end{bmatrix}$$

$$[J]=\begin{bmatrix} 1-\lambda_1^n-\lambda_2^n-\eta_h-\eta_a & \lambda_1^n & \lambda_2^n & 0 \\ 0 & 1-\lambda_2^n-\eta_h-\eta_a & 0 & \lambda_2^n \\ 0 & 0 & 1-\lambda_1^n-\eta_h-\eta_a & \lambda_1^n \\ 0 & 0 & 0 & 1-\eta_h-\eta_a \end{bmatrix}$$

The absorbing states in Figure 3.3 are states 4, 8, and 12. The elimination of these states results in the [Q] matrix, which is subtracted from the identity matrix and inverted as shown in Equation 3.4.

$$[\mathrm{N}] = [\,I - Q\,]^{-1} \qquad (3.4)$$

State 1 is considered to be the starting state. The MTTF is given by the summation of the elements of the first row of [N] as shown in Equation 3.5. The average system failure rate, outage duration and unavailability are given in Equations 3.6-3.8.

$$\text{MTTF} = \sum_{i=1}^{9} N_{1,i} \tag{3.5}$$

$$\lambda_W = \frac{1}{\text{MTTF}} \tag{3.6}$$

$$r_W = \frac{P_4 + P_8 + P_{12}}{P_4\ (\mu_1 + \mu_2)} \tag{3.7}$$

$$U_W = P_4 + P_8 + P_{12} \tag{3.8}$$

The average system unavailability is usually expressed in hours per year and is obtained by multiplying U_W by 8760.

3.5 Markov analysis of a three component system

Figure 3.4 shows the system state space model of a three component system with a three state weather model. Figure 3.4 is a simplified form of the complete state space diagram. The individual system state transitions between the different weather states are not shown. The system state transitions between the weather categories in Figure 3.4 are the various weather transition rates. This can be illustrated as follows. Consider the states 1, 9 and 17. These states have similar operating modes with all the components in the up-state in the three weather conditions. While the system is operating in this mode, a change in weather condition could occur. The system could transit from state 1 to state 9 or state 17 depending on the variation in the weather environment. In this case, the arrow going downwards from normal weather to adverse weather originates at state 1 and terminates at state 9, and that going to major adverse weather begins at state 1 and ends at state 17. The rest of the transitions can be described in a similar manner.

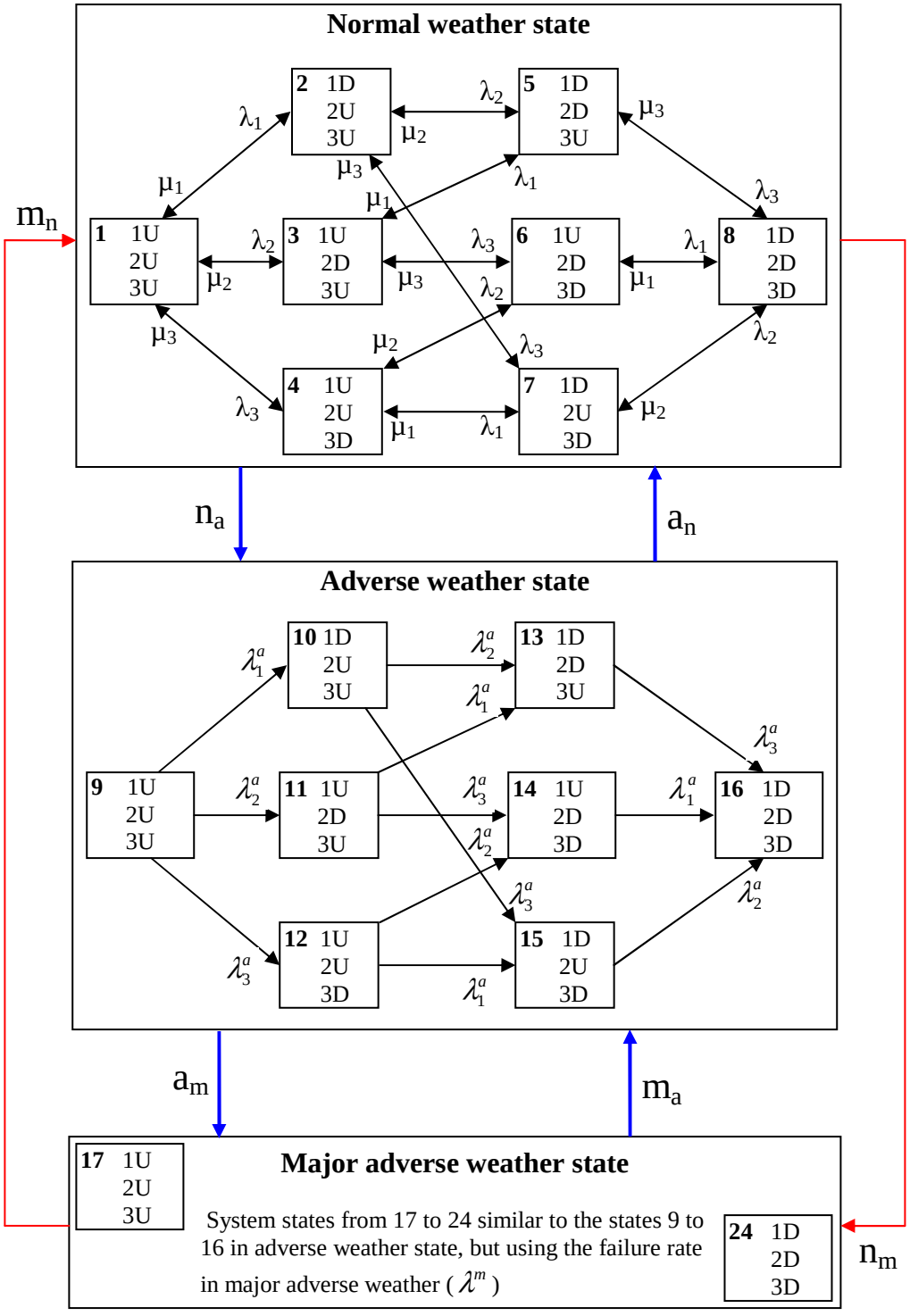

Figure 3.4 System state space diagram for a three component system with a three state weather model

The stochastic transitional probability matrix in this case is given in Appendix B.2. The system states 8, 16 and 24 represent the system down states for the parallel redundant configuration. These states are removed from the stochastic transitional probability matrix, resulting in a truncated matrix which is subtracted from the identity matrix and inverted. The final matrix [N] is used to determine the MTTF using Equation 3.9.

$$\text{MTTF} = \sum_{i=1}^{21} N_{1,i} \tag{3.9}$$

The reciprocal of MTTF is the average system failure rate as shown in Equation 3.10.

$$\lambda_W = \frac{1}{\text{MTTF}} \tag{3.10}$$

The average system outage duration and unavailability are given by Equations 3.11-3.12.

$$r_W = \frac{P_8 + P_{16} + P_{24}}{P_8\ (\mu_1 + \mu_2 + \mu_3)} \tag{3.11}$$

$$U_W = P_8 + P_{12} + P_{24} \tag{3.12}$$

3.6 Sensitivity analysis

The analyses presented in this section are focused on the average system failure rate, average system outage duration and the system unavailability. In addition to these reliability indices, the Error Factor is presented to provide a comparative measure of the average system failure rates. The weather data shown in Table 3.1 is used in the following analysis. The percentage of failures in bad weather (F_b) is varied from 0% to 100% and the percentage of bad weather failures occurring in major adverse weather (F_m) is allowed to vary from 0% to 50% in 10% increments.

Table 3.3 shows the average system failure rate obtained by varying the portion of failures in adverse weather and different percentages of bad weather failures attributed to major adverse weather. The condition that 0% of failures occur in major adverse weather is analogous to the two state weather model.

Table 3.3 Average system failure rate for a second order mincut (failures/year)

F_b (%)	F_m = 0%	F_m =10%	F_m =20%	F_m =30%	F_m =40%	F_m =50%
0	0.001725	0.001725	0.001725	0.001725	0.001725	0.001725
10	0.002176	0.002304	0.002799	0.003631	0.004772	0.006195
20	0.003516	0.004005	0.005839	0.008802	0.012713	0.017422
30	0.005726	0.006782	0.010606	0.016562	0.024160	0.033018
40	0.008790	0.010587	0.016898	0.026391	0.038124	0.051416
50	0.012691	0.015381	0.024544	0.037883	0.053893	0.071567
60	0.017410	0.021123	0.033399	0.050721	0.070949	0.092759
70	0.022932	0.027777	0.043340	0.064652	0.088913	0.114508
80	0.029241	0.035308	0.054260	0.079478	0.107503	0.136483
90	0.036321	0.043684	0.066067	0.095039	0.126513	0.158456
100	0.044156	0.052875	0.078682	0.111209	0.145787	0.180275

The effect on the average system failure rate as a function of the percentages of failures occurring in bad weather is clearly shown in Figure 3.5.

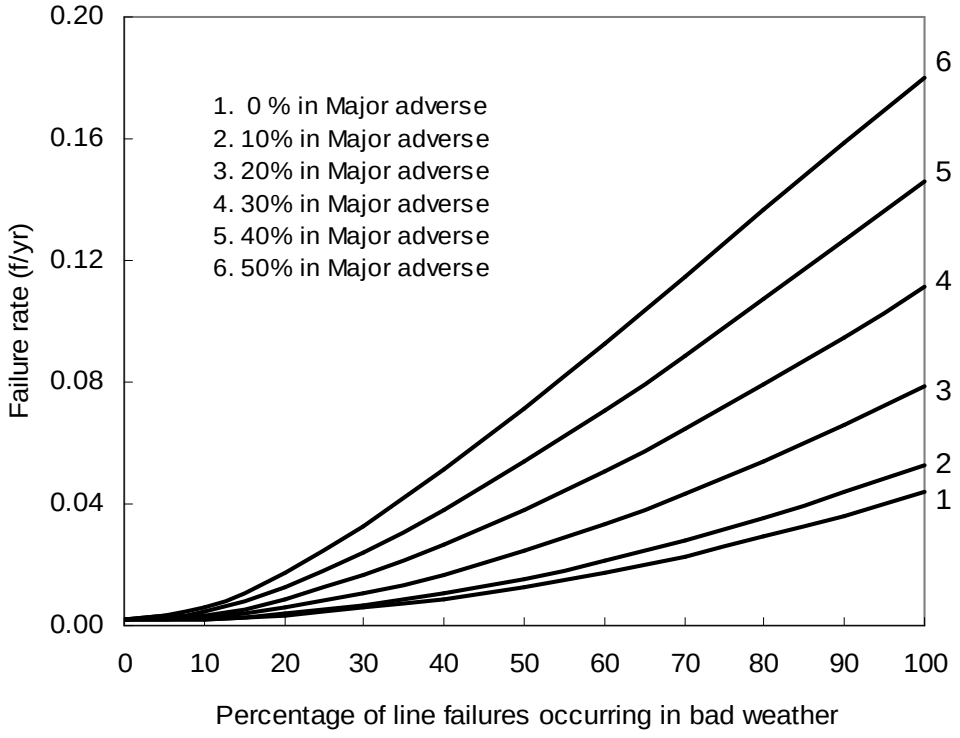

Figure 3.5 System failure rate for a second order mincut

Profile 1 in Figure 3.5 represents the system failure rate obtained using the two state weather model. The rest of the profiles are for the three state weather model with varying percentages of bad weather failures in major adverse weather. The failure rate increases with increase in the percentage of bad weather failures attributed to major adverse weather. It can be seen that the predicted system failure rate calculated using the two state weather model is increasingly optimistic when the percentage of bad weather failures occurring in major adverse weather increases. Figure 3.6 further illustrates this effect in terms of the Error Factor.

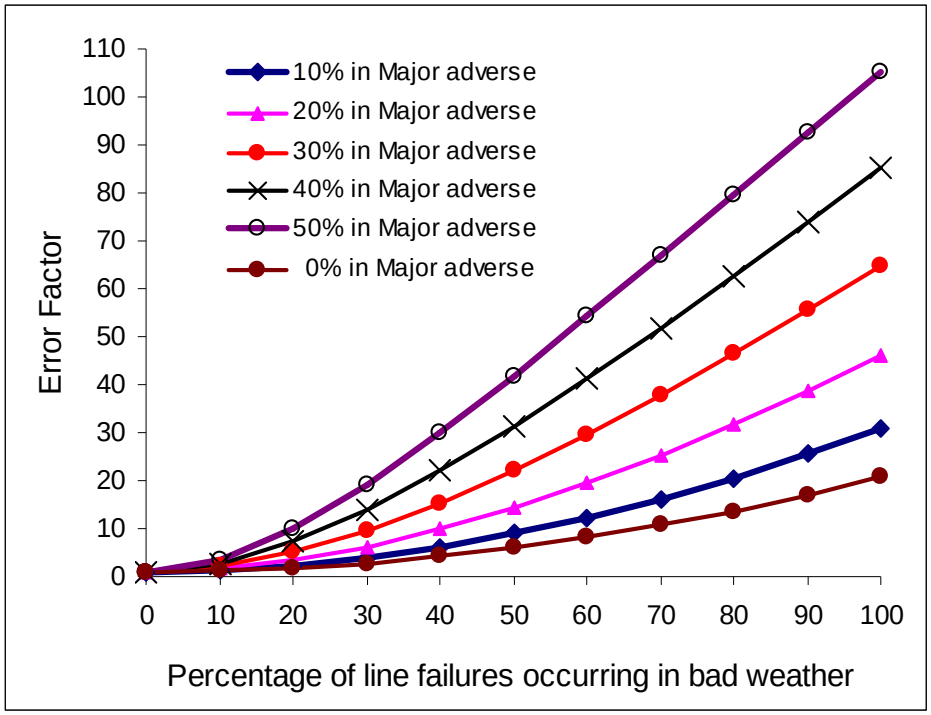

Figure 3.6 Error Factor for a second order mincut

The average system outage duration and unavailability are shown in Tables 3.4-3.5 and are further illustrated in Figures 3.7-3.8. In Figure 3.7, the average system outage duration initially increases considerably with the utilization of the three state weather model and then eventually appears to be constant as more failures are assigned to bad weather. The effect on the average system unavailability can clearly be seen in Figure

3.8. The average system failure rate in Figure 3.5, the Error Factor in Figure 3.6, and the system unavailability in Figure 3.8 all vary in a similar manner.

Table 3.4 Average system outage duration for a second order mincut (hours)

F_b (%)	F_m = 0%	F_m =10%	F_m =20%	F_m =30%	F_m =40%	F_m =50%
0	3.7884	3.7884	3.7884	3.7884	3.7884	3.7884
10	4.3618	4.4411	4.6801	4.9348	5.1396	5.2894
20	5.0046	5.1007	5.3176	5.4771	5.5738	5.6326
30	5.3682	5.4340	5.5627	5.6448	5.6909	5.7178
40	5.5545	5.5946	5.6678	5.7120	5.7363	5.7505
50	5.6539	5.6778	5.7198	5.7447	5.7583	5.7663
60	5.7103	5.7243	5.7485	5.7627	5.7706	5.7752
70	5.7442	5.7521	5.7656	5.7735	5.7780	5.7807
80	5.7654	5.7695	5.7764	5.7805	5.7828	5.7842
90	5.7792	5.7808	5.7835	5.7851	5.7861	5.7867
100	5.7884	5.7884	5.7884	5.7884	5.7884	5.7884

Table 3.5 System unavailability for a second order mincut (hours/year)

F_b (%)	F_m = 0%	F_m =10%	F_m =20%	F_m =30%	F_m =40%	F_m =50%
0	0.0065	0.0065	0.0065	0.0065	0.0065	0.0065
10	0.0095	0.0102	0.0131	0.0179	0.0245	0.0328
20	0.0176	0.0204	0.0311	0.0482	0.0709	0.0982
30	0.0308	0.0369	0.0590	0.0936	0.1376	0.1889
40	0.0489	0.0593	0.0959	0.1509	0.2189	0.2959
50	0.0718	0.0874	0.1405	0.2178	0.3106	0.4130
60	0.0995	0.1210	0.1921	0.2925	0.4097	0.5361
70	0.1318	0.1599	0.2501	0.3735	0.5141	0.6623
80	0.1687	0.2039	0.3137	0.4597	0.6221	0.7899
90	0.2101	0.2527	0.3824	0.5502	0.7324	0.9174
100	0.2558	0.3063	0.4558	0.6441	0.8443	1.0440

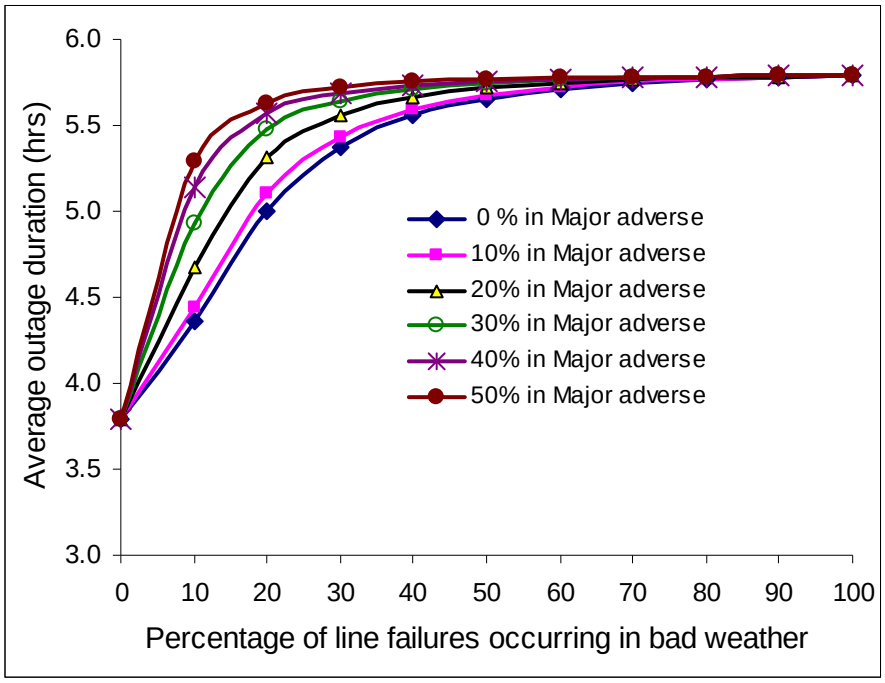

Figure 3.7 Average system outage duration for a second order mincut

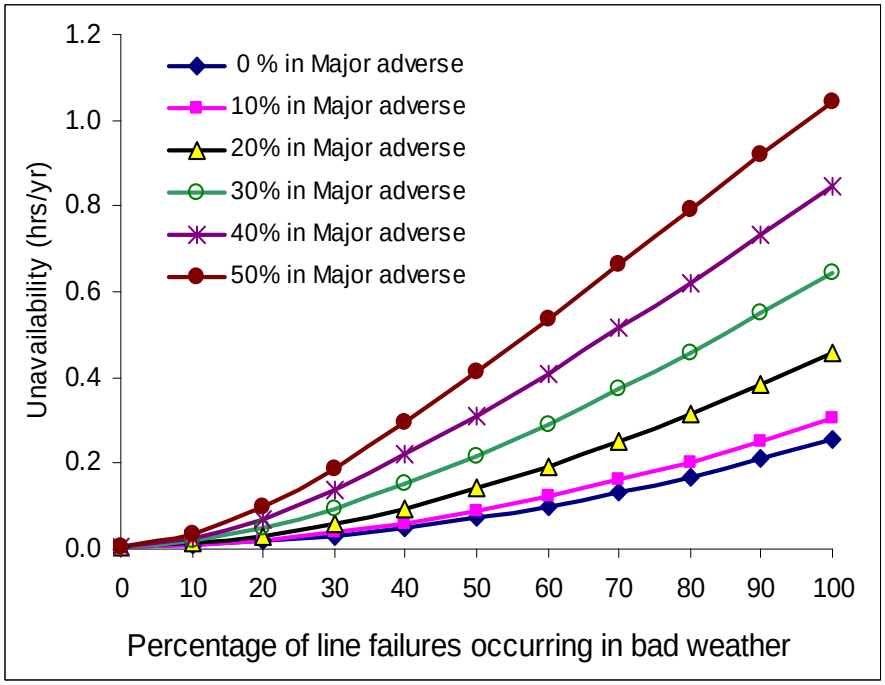

Figure 3.8 System unavailability for a second order mincut

The analysis can be extended to a third order mincut. Line 3, which is identical to lines 1 and 2, is added in Figure 2.7 to form a three line parallel redundant system. Table 3.6 shows the average system failure rate of the third order mincut for varying percentages of failures occurring in major adverse weather. The increase in the failure rate is clearly shown in Table 3.7 and Figure 3.9 using the Error Factor.

Table 3.6 Average system failure rate for a third order mincut (failures/year)

F_b (%)	F_m = 0%	F_m =10%	F_m =20%	F_m =30%	F_m =40%	F_m =50%
0	0.000002	0.000002	0.000002	0.000002	0.000002	0.000002
10	0.000007	0.000013	0.000053	0.000150	0.000324	0.000589
20	0.000034	0.000077	0.000350	0.000986	0.002056	0.003591
30	0.000100	0.000233	0.001047	0.002832	0.005674	0.009549
40	0.000222	0.000517	0.002228	0.005787	0.011181	0.018215
50	0.000416	0.000954	0.003938	0.009838	0.018389	0.029110
60	0.000695	0.001568	0.006189	0.014911	0.027045	0.041736
70	0.001075	0.002377	0.008980	0.020905	0.036893	0.055650
80	0.001567	0.003396	0.012293	0.027714	0.047694	0.070483
90	0.002184	0.004638	0.016106	0.035231	0.059242	0.085935
100	0.002938	0.006113	0.020393	0.043355	0.071359	0.101770

Table 3.7 Error Factor for a third order mincut

F_b (%)	F_m = 0%	F_m =10%	F_m =20%	F_m =30%	F_m =40%	F_m =50%
0	1.02	1.02	1.02	1.02	1.02	1.02
10	3.21	5.94	23.96	68.32	147.52	267.99
20	15.18	34.87	159.27	448.45	934.9	1632.97
30	44.71	106.17	475.95	1287.60	2580.04	4342.47
40	99.11	235.00	1013.2	2631.72	5084.45	8283.09
50	185.32	433.85	1790.55	4473.88	8362.18	13237.30
60	309.88	713.00	2814.55	6780.60	12298.52	18978.95
70	478.93	1080.87	4083.4	9506.56	16776.56	25306.52
80	698.29	1544.39	5590.01	12602.73	21688.52	32051.66
90	973.42	2109.20	7324.1	16020.81	26939.89	39078.39
100	1309.48	2779.88	9273.62	19715.53	32450.03	46279.00

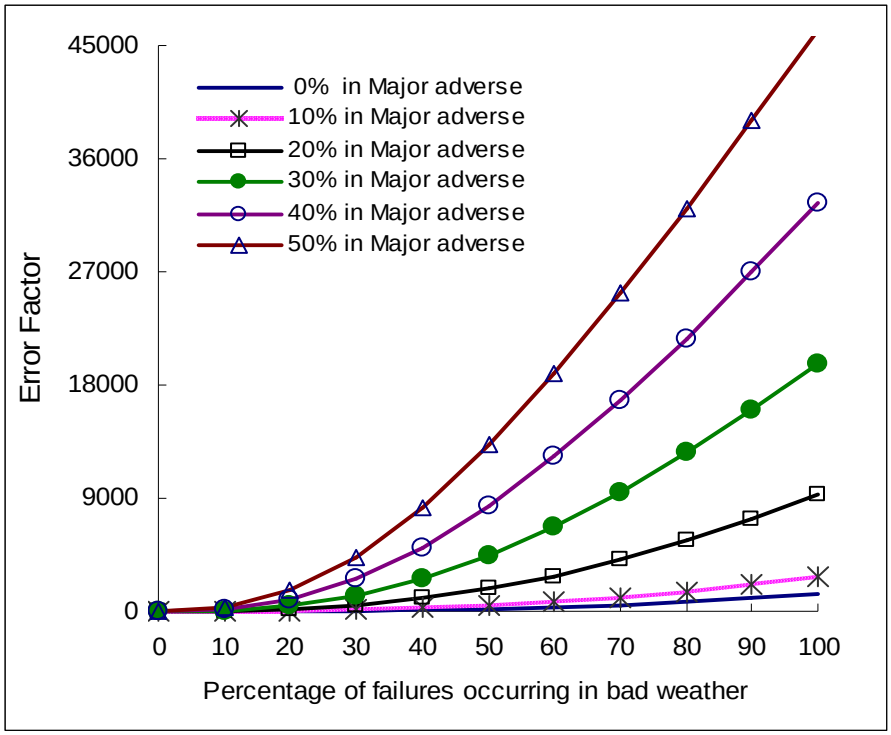

Figure 3.9 Error Factor for a third order mincut

Figure 3.9 illustrates that the Error Factor increases dramatically with increase in the percentage of failures occurring in bad weather. The profiles in Figure 3.9 can be compared with the corresponding profiles in Figure 3.6 for a second order mincut. In the case of a third order mincut, the Error Factor increases by a larger margin when the percentage of failures occurring in major adverse weather increases. This indicates that a third order mincut suffers more prominently from failure bunching than does a second order mincut.

Table 3.8 presents the system unavailability for a third order mincut. It is clear from Table 3.8 that the system unavailability increases rapidly as a result of incorporating bad weather conditions and recognizing major adverse weather failures. The average system outage duration for the same system is shown in Table 3.9. It can be seen from Table 3.9 that the average outage duration increases significantly as the fraction of bad weather failures increases but quickly becomes relatively constant.

Table 3.8 System unavailability for a third order mincut (hours/year)

F_b (%)	F_m = 0%	F_m =10%	F_m =20%	F_m =30%	F_m =40%	F_m =50%
0	0.000006	0.000006	0.000006	0.000006	0.000006	0.000006
10	0.000027	0.000054	0.000232	0.000672	0.001458	0.002655
20	0.000147	0.000339	0.001574	0.004448	0.009285	0.016227
30	0.000443	0.001045	0.004721	0.012793	0.025651	0.043186
40	0.000993	0.002324	0.010064	0.026167	0.050574	0.082407
50	0.001866	0.004300	0.017799	0.044503	0.083202	0.131725
60	0.003130	0.007078	0.027992	0.067467	0.122391	0.188887
70	0.004848	0.010741	0.040627	0.094610	0.166979	0.251887
80	0.007079	0.015359	0.055632	0.125444	0.215891	0.319049
90	0.009880	0.02099	0.072907	0.159487	0.268187	0.389017
100	0.013302	0.027678	0.092332	0.196290	0.323063	0.460718

Table 3.9 Average system outage duration for a third order mincut (hours)

F_b (%)	F_m = 0%	F_m =10%	F_m =20%	F_m =30%	F_m =40%	F_m =50%
0	2.5256	2.5256	2.5256	2.5256	2.5256	2.5256
10	3.8068	4.1154	4.4030	4.4707	4.4928	4.5026
20	4.3083	4.4185	4.4923	4.5084	4.5141	4.5169
30	4.4209	4.4740	4.5084	4.5162	4.5190	4.5205
40	4.4638	4.4947	4.5148	4.5195	4.5213	4.5222
50	4.4860	4.5055	4.5183	4.5214	4.5226	4.5232
60	4.4997	4.5123	4.5207	4.5227	4.5235	4.5240
70	4.5091	4.5170	4.5223	4.5237	4.5242	4.5245
80	4.5160	4.5205	4.5236	4.5244	4.5247	4.5249
90	4.5213	4.5233	4.5247	4.5250	4.5252	4.5253
100	4.5256	4.5256	4.5256	4.5256	4.5256	4.5256

3.7 Effect of failure rate and repair time

The forced outage rates and repair times of different transmission elements can vary from one utility to another depending on the transmission structures and available resources. It is of interest to analyse the effect when system elements with different reliability parameters operate in the same weather environment. The following analyses consider different combinations of the failure rates and repair times in a second order

mincut operating in three weather states. It is assumed that the percentage of bad weather failures in major adverse weather is 10%. The studies were conducted by varying the repair time using a constant component failure rate. Three cases are examined with the component failure rates held constant at 1.0, 0.5 and 5.0 f/yr. The repair times are assumed to be 3.75, 7.50 and 15.0 hours in each case.

Table 3.10 shows the average system failure rate and the Error Factor for the three different repair times. Table 3.10 was calculated using the average line failure rate of 1.0 f/yr. The average outage duration and unavailability are presented in Table 3.11. It can be seen from Table 3.10 that the failure rate initially increases proportionately as the repair time increases, but the difference decreases as the percentage of failures occurring in bad weather increases. This difference becomes insignificant when the most of the failures occur in bad weather. It is interesting to note that the Error Factor decreases significantly when the repair time increases and the percentage of failures in bad weather increases. In this case, the Error Factor does not clearly reflect the impacts of repair time on the average system failure rate.

Table 3.10 Average system failure rate and Error Factor, ($\lambda = 1.0$ f/yr)

F_b (%)	Average system failure rate (f/yr)			Error Factor		
	r = 3.75 hours	r = 7.5 hours	r = 15 hours	r = 3.75 hours	r = 7.5 hours	r = 15 hours
0	0.00086	0.00173	0.00344	1.01	1.01	1.01
10	0.00144	0.00230	0.00402	1.69	1.35	1.17
20	0.00315	0.00401	0.00571	3.68	2.34	1.67
30	0.00593	0.00678	0.00847	6.93	3.96	2.47
40	0.00975	0.01059	0.01226	11.39	6.18	3.58
50	0.01455	0.01538	0.01703	17.00	8.98	4.97
60	0.02031	0.02112	0.02274	23.72	12.34	6.64
70	0.02698	0.02778	0.02936	31.52	16.22	8.57
80	0.03453	0.03531	0.03685	40.33	20.62	10.76
90	0.04293	0.04368	0.04518	50.14	25.51	13.19
100	0.05214	0.05287	0.05433	60.91	30.88	15.86

Table 3.11 clearly shows how average outage duration and unavailability are impacted as a result of increase in the component repair time. It is obvious that both the average outage duration and unavailability will increase if service restoration is delayed.

Table 3.12 provides the average system failure rate and the Error Factor when the average failure rate is 0.5 f/yr. The average system unavailability and average outage duration in this case are shown in Table 3.13. The reliability indices when the average component failure rate is 5.0 f/yr are shown in Tables 3.14-3.15.

Table 3.11 Average system outage duration and unavailability, ($\lambda = 1.0$ f/yr)

F_b (%)	Average outage duration (hours)			Average unavailability (hours/yr)		
	r = 3.75 hours	r = 7.5 hours	r = 15 hours	r = 3.75 hours	r = 7.5 hours	r = 15 hours
0	1.89	3.79	7.58	0.002	0.007	0.026
10	2.82	4.44	8.04	0.004	0.010	0.032
20	3.46	5.10	8.61	0.011	0.020	0.049
30	3.69	5.43	9.01	0.022	0.037	0.076
40	3.79	5.59	9.24	0.037	0.059	0.113
50	3.84	5.68	9.38	0.056	0.087	0.16
60	3.86	5.72	9.46	0.078	0.121	0.215
70	3.88	5.75	9.51	0.105	0.160	0.280
80	3.88	5.77	9.54	0.134	0.204	0.352
90	3.89	5.78	9.56	0.167	0.253	0.433
100	3.89	5.79	9.58	0.203	0.306	0.521

Table 3.12 Average system failure rate and Error Factor, ($\lambda = 0.5$ f/yr)

F_b (%)	Average system failure rate (f/yr)			Error Factor		
	r = 3.75 hours	r = 7.5 hours	r = 15 hours	r = 3.75 hours	r = 7.5 hours	r = 15 hours
0	0.00022	0.00043	0.00086	1.01	1.01	1.01
10	0.00036	0.00058	0.00101	1.69	1.35	1.18
20	0.00080	0.00101	0.00144	3.72	2.36	1.68
30	0.00151	0.00173	0.00215	7.07	4.03	2.52
40	0.00251	0.00272	0.00314	11.70	6.35	3.67
50	0.00377	0.00398	0.00440	17.60	9.29	5.14
60	0.00529	0.00550	0.00592	24.72	12.85	6.91
70	0.00708	0.00728	0.00770	33.06	17.01	8.99
80	0.00911	0.00932	0.00973	42.58	21.76	11.36
90	0.01140	0.01160	0.01200	53.25	27.10	14.02
100	0.01393	0.01412	0.01452	65.06	32.99	16.96

The results shown in Table 3.10 can be compared with those in Table 3.12 and Table 3.14. It can be observed that the failure rate in Table 3.10 is larger than that in Table 3.12 and smaller than that in Table 3.14. The Error Factor is smaller for the large component failure rate. The average outage durations in Tables 3.11, 3.13 and 3.15 are very similar. This implies that the component failure rate does not affect the average outage duration. On the other hand, the system unavailability changes in accordance with the change in average system failure rate. The effect on the Error Factor for the three case studies is further illustrated in Figure 3.10.

Table 3.13 Average system outage duration and unavailability, ($\lambda = 0.5$ f/yr)

F_b (%)	Average outage duration (hours)			Average unavailability (hours/yr)		
	r = 3.75 hours	r = 7.5 hours	r = 15 hours	r = 3.75 hours	r = 7.5 hours	r = 15 hours
0	1.89	3.79	7.58	small	0.002	0.007
10	2.82	4.44	8.04	0.001	0.003	0.008
20	3.46	5.11	8.62	0.003	0.005	0.012
30	3.69	5.44	9.02	0.006	0.009	0.019
40	3.79	5.60	9.25	0.009	0.015	0.029
50	3.84	5.68	9.38	0.014	0.023	0.041
60	3.86	5.73	9.46	0.020	0.032	0.056
70	3.88	5.75	9.51	0.027	0.042	0.073
80	3.88	5.77	9.54	0.035	0.054	0.093
90	3.89	5.78	9.56	0.044	0.067	0.115
100	3.89	5.79	9.58	0.054	0.082	0.139

Table 3.14 Average system failure rate and Error Factor, ($\lambda = 5.0$ f/yr)

F_b (%)	Average system failure rate (f/yr)			Error Factor		
	r = 3.75 hours	r = 7.5 hours	r = 15 hours	r = 3.75 hours	r = 7.5 hours	r = 15 hours
0	0.02148	0.04269	0.08430	1.00	1.00	0.98
10	0.03503	0.05606	0.09733	1.64	1.31	1.14
20	0.07222	0.09276	0.13308	3.37	2.17	1.55
30	0.12896	0.14876	0.18762	6.03	3.48	2.19
40	0.20222	0.22105	0.25803	9.45	5.16	3.01
50	0.28964	0.30733	0.34209	13.53	7.18	4.00
60	0.38935	0.40576	0.43803	18.19	9.48	5.12
70	0.49984	0.51488	0.54445	23.35	12.03	6.36
80	0.61984	0.63343	0.66017	28.96	14.8	7.71
90	0.74829	0.76039	0.78421	34.96	17.76	9.16
100	0.88426	0.89486	0.91574	41.31	20.90	10.70

Table 3.15 Average system outage duration and unavailability, ($\lambda = 5.0$ f/yr)

F_b (%)	Average outage duration (hours)			Average unavailability (hours/yr)		
	r = 3.75 hours	r = 7.5 hours	r = 15 hours	r = 3.75 hours	r = 7.5 hours	r = 15 hours
0	1.89	3.79	7.58	0.041	0.162	0.644
10	2.79	4.42	8.02	0.098	0.249	0.787
20	3.42	5.06	8.57	0.248	0.471	1.150
30	3.67	5.40	8.96	0.474	0.806	1.695
40	3.77	5.57	9.20	0.764	1.235	2.392
50	3.82	5.66	9.34	1.110	1.745	3.220
60	3.85	5.71	9.44	1.503	2.326	4.162
70	3.87	5.74	9.49	1.938	2.967	5.203
80	3.88	5.77	9.53	2.410	3.663	6.331
90	3.89	5.78	9.56	2.914	4.406	7.538
100	3.89	5.79	9.58	3.447	5.192	8.814

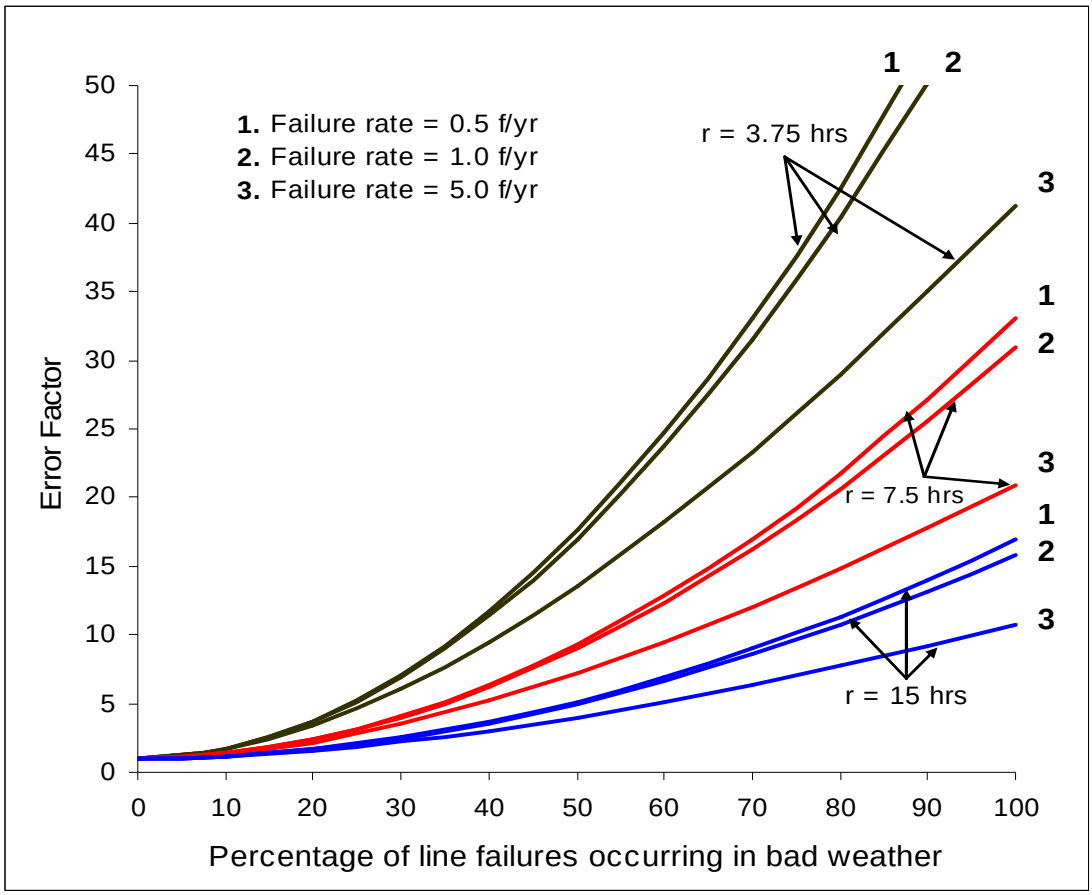

Figure 3.10 Variation of Error Factor with component reliability parameters

The Error Factor moves in the opposite direction to the system failure rate when the repair time increases. As discussed earlier, the average system failure rate increases with increase in the repair time, but the Error Factor decreases. The Error Factor is lower for systems having large component failure rates. This implies that the worst performing systems experience lower impacts compared to those with better reliability parameters.

3.8 Extreme weather severity analysis

Continuous exposure of a system element to unfavourable weather conditions for a prolonged duration can create different system failure mechanisms. On the other hand, the number of interruptions tends to increase as bad weather hits the system more frequently. It is evident that the number of storms varies from one place to another. Table 3.16 shows statistical data for storms that took place in the provinces of Canada between 1950─2003 [21].

Table 3.16 Number of severe weather events by province between 1950─2003

Provinces of Canada	Hail/Thun-derstorm	Hurricane	Snow Avalanche	Freezing-Rain	Blizzard and Snowstorm	Tornado	Provincial Total
Alberta, AB	18	0	2	2	5	3	30
British Columbia, BC	2	0	7	0	4	0	15
Manitoba, MB	5	0	0	0	2	2	9
New Brunswick, NB	0	5	0	1 (‘98)	4	0	10
Newfoundland, NF	0	3	1 (‘59)	3	8	0	15
Nova Scotia, NS	0	7	0	0	5	1 (‘54)	13
Ontario, ON	2	1 (‘54)	0	2	7	11	23
Prince Ed Island, PE	0	1 (‘90)	0	0	5	0	6
Quebec, QC	3	4	2	1 (‘98)	8	7	25
Saskatchewan, SK	5	0	0	2	1 (‘64)	2	10
Total	35	21	12	11	49	26	

In Table 3.16, the figure in the brackets indicates the year in which the weather event was experienced. These are not complete statistics, but they do provide a means of comparison. It is important to note that the impacts of disturbances caused by different storms are not the same and that they cannot be compared between different systems. Table 3.16 indicates that the number of stormy weather events and the types of storms in the various provinces vary significantly.

It is interesting to note that the territories NT, NU and YK did not receive any major storms in the categories given in Table 3.16 during the period 1950─2003. These provinces were excluded in the calculation of the frequencies of storm occurrence. Table 3.17 presents the frequencies of storms in the rest of the provinces. These data clearly show that Alberta, Quebec and Ontario are the most impacted provinces. The variation in the number of weather events indicates a need to examine the effect of the frequency of encountering major adverse weather.

Table 3.17 Frequencies of major storms in the Provinces of Canada

Statistics	BC, MB, NB, NF, PE, SK, NS	All (except NT, NU, YK)	Only AB, ON, QC
Average number by province	11	15.6	26
Average frequency (events/yr)	0.203 (once in 5 yrs)	0.289 (once in 3.46 yrs)	0.481 (once in 2 yrs)

The following analysis of a second order mincut considers the frequency of occurrence to vary in the range from 0.2 to 1.0 occurrence per year. The durations of normal and adverse weather are held constant at 200 hours and 2 hours respectively and the duration of major adverse weather changes in accordance with the variation in its frequency such that the steady state probability remains unchanged. Under the assumption that extreme weather occurs once per year with an average duration of one hour, the probability of extreme weather is 0.000114. The frequency of occurrence of major adverse weather is given by Equation 3.13.

$$f_m = P_n(n_m) + P_a(a_m) \qquad (3.13)$$

Assume, $n_m = a_m$

$$f_m = (P_n + P_a) n_m$$

$$n_m = f_m / (P_n + P_a)$$

Since, $(P_n + P_a) \approx 1.0$

$$n_m \approx f_m$$

The duration of major adverse weather (M) can be simply obtained by dividing the probability by the frequency of encountering the extreme weather. The resulting transition rates are as follows:

$n_m = a_m =$ 0.2 to 1.0 occ/yr

$n_a = 8760/200 - n_m$ occ/yr

$a_n = 8760/2 - a_m$ occ/yr

$m_n = m_a = 1/2M$ occ/yr

The weather state characteristics are given in Table 3.18. Table 3.19 shows the Error Factor when the frequency of encountering major adverse weather varies from 0.2 to 1.0 occ/yr in 0.2 occ/yr increments for the case when 10% of bad weather failures occur in major adverse weather. The Error Factor appears to be quite stable over the range in frequency of occurrence of extreme weather.

Table 3.18 Weather characteristics for variable frequency of extreme weather

Frequency of extreme weather (Occ/yr)	Duration of extreme weather (hr)	Steady state probability		
		Normal weather (P_n)	Adverse weather (P_a)	Extreme weather (P_m)
0.2	5.00	0.990008	0.009878	0.000114
0.4	2.50	0.990030	0.009856	0.000114
0.6	1.67	0.990052	0.009833	0.000114
0.8	1.25	0.990075	0.009811	0.000114
1.0	1.00	0.990097	0.009789	0.000114

Table 3.19 Error Factor for variable frequency of extreme weather

F_b (%)	Frequency of occurrence				
	0.2 Occ/yr	0.4 Occ/yr	0.6 Occ/yr	0.8 Occ/yr	1.0 Occ/yr
0	1.01	1.01	1.01	1.01	1.01
10	1.34	1.35	1.35	1.35	1.35
20	2.34	2.34	2.35	2.35	2.36
30	3.97	3.97	3.98	3.99	4.00
40	6.19	6.21	6.23	6.24	6.26
50	9.00	9.03	9.05	9.08	9.10
60	12.36	12.40	12.43	12.47	12.51
70	16.26	16.31	16.35	16.40	16.45
80	20.67	20.73	20.79	20.85	20.92
90	25.57	25.65	25.73	25.80	25.88
100	30.95	31.04	31.14	31.23	31.33

The results shown in Table 3.19 indicate that less often occurring weather events with longer durations and more often encountering weather events but with relatively short durations have similar impacts on the average system failure rate. In other words, the probability of normal weather which is very close to 1.0 increases by a small amount while that of adverse weather decreases by the same value, resulting in a small change in component failure rates in normal and adverse weather conditions. This change causes little or no effect on the predicted average system failure rate because the average system failure rate is largely dominated by the component failure rate in major adverse weather.

3.9 Summary

This chapter describes the importance of incorporating extreme adverse weather conditions in the reliability evaluation of transmission and distribution systems. A three state weather model is developed and illustrated by application to two line and three line parallel redundant systems. The studies described in this chapter reveal that estimated reliability indices can be quite optimistic if extreme weather conditions are not included in the analysis. This is clearly shown using a number of graphical illustrations.

A series of studies using a range of reliability parameters are presented for varying percentages of the total line failures occurring in bad weather. The portion of bad weather failures attributed to major adverse weather is 10% in these studies. The analyses show that the average system failure rate increases significantly with the repair time when the percentage of failures in bad weather is small. It, however, increases only marginally when relatively more failures occur in bad weather. On the contrary, the impact as a result of increase in the average component failure rate is small when the percentages of failures that are attributed to bad weather are small, but is significant when large percentages of the failures occur in bad weather. It should be noted that the impacts on the average system failure rate are not clearly reflected by a simple comparative study of Error Factors for different systems with different repair times. In these cases, the actual system failure rates should also be considered.

The influence on the reliability parameters due to varying the number of extreme weather events is also illustrated. The results obtained for a higher frequency of weather events occurring per year with short durations are compared with those for a lower frequency of weather events with longer durations. It is shown that the two cases have similar effects on the estimated average system failure rate. The analysis conducted in this chapter indicates that major storms have a significant influence on predicted reliability indices.

Chapter 4

PRACTICAL SYSTEM RELIABILITY ASSESSMENT

4.1 Introduction

The application of the two state weather model to two line and three line parallel redundant circuits is illustrated in Chapter 2. Chapter 3 describes the technique for incorporating extreme adverse weather conditions and applications to two line and three line parallel redundant configurations. Chapters 2 and 3 clearly demonstrate that the predicted reliability indices increase significantly when weather conditions are incorporated in the analysis. These chapters focus mainly on computation of the average system failure rate, the average outage duration and the unavailability of second order and third order mincuts using the two different weather models.

A transmission or distribution system is composed of a number of components that in different combinations contribute to supply interruptions. Although the basic indices are important elements, they do not in themselves reflect the significance and severity of customer outages. It is essential to evaluate customer oriented system indices that can be used to assess the overall system performance in decision making, design and planning. This chapter illustrates the application of weather modeling to a simple practical system. Two types of indices designated as load point indices and system indices are described and evaluated to illustrate the impacts due to the inclusion of weather conditions in the analysis.

4.2 Example system

The single line diagram of a simple transmission or distribution system is shown in Figure 4.1. This system consists of four lines, three buses and two load points. Bus 1 is the supply bus whereas Bus 2 and Bus 3 are the load buses to which load points L1 and L2 are connected respectively. The following analyses assume that the power supply is constantly available and the unavailability of the bus bars is not considered.

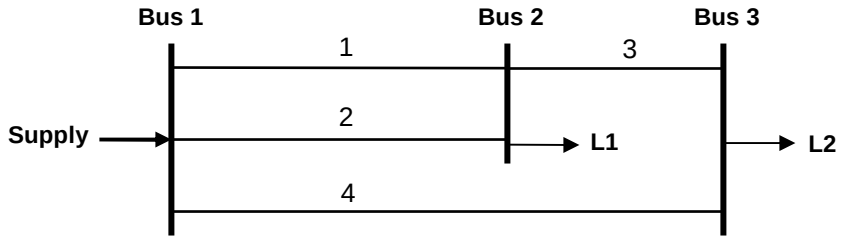

Figure 4.1 Simple transmission or distribution system

The minimal cut set approach can be used to identify the set of elements contributing to the failure of a load point. The minimal cuts identified for load points L1 and L2 are as follows:

Load point L1: 1-2-3, 1-2-4

Load point L2: 3-4, 1-2-4

The following data are used in the analysis:

Average line failure rate for component 1: $\lambda_1 = 1.5$ f/yr

Average line failure rate for component 2: $\lambda_2 = 1.5$ f/yr

Average line failure rate for component 3: $\lambda_3 = 1.0$ f/yr

Average line failure rate for component 4: $\lambda_4 = 2.0$ f/yr

Average repair time for each line = 10 hours

The hypothetical system load data are shown in Table 4.1.

Table 4.1 System load data

User sector	Load point L1			Load point L2		
	% Load	Load (kW)	Number of customers	% Load	Load (kW)	Number of customers
Agricultural	10	2000	50	5	800	20
Commercial	30	6000	150	25	4000	100
Industrial	20	4000	5	30	4800	6
Residential	40	8000	3200	40	6400	2560
Total	100	20000	3405	100	16000	2686

The customer types are agricultural, commercial, industrial and residential. The distribution of consumer load and the number of customers at each load point are shown in Table 4.1. The total system load of 36 MW is distributed over 5091 customers.

Table 4.2 presents the sector interruption costs, also known as customer damage functions (CDF), for typical outage durations of 1 hr, 4 hrs and 8 hrs [1]. The actual outage durations depending on the failure events may vary and the interruption cost relevant to the specific outage period should be evaluated. In this situation, an interpolation technique can be applied to determine this cost using Equation 4.1 [22].

Table 4.2 Sector customer damage function (CDF)

User sector	Interruption cost ($/kW)		
	1 hr	4 hrs	8 hrs
Agricultural	0.649	2.064	4.120
Commercial	8.552	31.317	83.008
Industrial	9.085	25.163	55.808
Residential	0.482	4.914	15.690

$$\log C_r = \left[\log C_y\{\log r - \log x\} - \log C_x\{\log r - \log y\}\right] \times 1/(\log y - \log x) \quad (4.1)$$

where,

r = duration of an outage event in hours

x = outage durations less than r hours

y = outage durations greater than r hours

C_r = interruption cost for an outage duration of r hours

C_x = interruption cost for an outage duration of x hours

C_y = interruption cost for an outage duration of y hours

The parameters x and y are 4 hrs and 8 hrs respectively for an outage duration falling between 4-8 hrs. For durations between 1-4 hrs, interpolation between 1 hr and 4 hours is required. The outage costs associated with various interruption durations for the different user sectors are given in Table C.17 in Appendix C.

The customer costs associated with an interruption at any load point involves the combination of costs associated with all customer types affected by that outage. This combined cost is referred to as a composite customer damage function (CCDF). The particular customer costs together with the percentage of load allocated to the respective classes of consumers results in the composite cost functions given by Equation 4.2.

$$CCDF = \sum P_S CDF_S \tag{4.2}$$

where,

P_S = percentage of total load at that load point

CDF_S = sector customer damage function

$$CCDF \text{ for L1} = 0.1CDF_{agr} + 0.3CDF_{com} + 0.2CDF_{ind} + 0.4CDF_{res} \tag{4.3}$$

$$CCDF \text{ for L2} = 0.05CDF_{agr} + 0.25CDF_{com} + 0.3CDF_{ind} + 0.4CDF_{res} \tag{4.4}$$

where,

CDF_{agr} = interruption cost for the agricultural sector

CDF_{com} = interruption cost for the commercial sector

CDF_{ind} = interruption cost for the industrial sector

CDF_{res} = interruption cost for the residential sector

4.3 Reliability indices

Reliability indices are important elements in the quantitative adequacy assessment of a system. Load point indices in conjunction with system indices can be used to measure distribution system adequacy. Load point indices provide the reliability at the individual load buses while system indices are indicators of total system reliability. Although the two sets of indices function differently, they complement each other. Load point indices are usually evaluated when the adequacy assessment is intended to identify and reinforce poorly performing buses in the system. On the other hand, system indices are used when the purpose of study is to assess global system adequacy and to provide a comparative analysis of different alternatives. Both sets of indices computed in this chapter are mainly focused on comparing the effects of various weather conditions. This section briefly describes the load point and system indices.

4.3.1 Load point indices

The traditional load point indices are the average failure rate, the average annual outage time or unavailability, and the average outage duration. The load point failure rate and unavailability are simply the sum of the failure rates and the unavailability of the individual failure events respectively. These indices are given by Equations 4.5-4.7.

Average failure rate, $\lambda = \sum \lambda_k$ (4.5)

Average annual outage time, $U = \sum U_k$ (4.6)

Average outage time, $r = \dfrac{\sum U_k}{\sum \lambda_k}$ (4.7)

where,

k denotes an outage event, or minimal cut

4.3.2 System indices

The load point indices provide an indication of the average performance at each individual load point in the system. These values can be aggregated to provide a set of overall system indices [1]. The system indices utilized in Canada and compiled by the Canadian Electricity Association (CEA) are noted in Chapter 1 of this thesis. These indices together with some other useful indicators [1] are defined as follows.

SAIFI: System Average Interruption Frequency Index

$$SAIFI = \frac{total\ number\ of\ customer\ interruptions}{total\ number\ of\ customers\ served}$$

$$= \frac{\sum \lambda_i N_i}{\sum N_i} \quad \text{(interruptions/customer-yr)} \qquad (4.8)$$

where λ_i is the failure rate and N_i is the number of customers at load point i

SAIDI: System Average Interruption Duration Index

$$SAIDI = \frac{sum\ of\ customer\ interruption\ durations}{total\ number\ of\ customers\ served}$$

$$= \frac{\sum U_i N_i}{\sum N_i} \quad \text{(hr/customer-yr)} \qquad (4.9)$$

where U_i is the annual outage time and N_i is the number of customers at load point i

CAIDI: Customer Average Interruption Duration Index:

$$CAIDI = \frac{sum\ of\ customer\ interruption\ durations}{total\ number\ of\ customer\ interruptions}$$

$$= \frac{\sum U_i N_i}{\sum \lambda_i N_i} = \frac{SAIDI}{SAIFI} \quad \text{(hrs/interruption)} \qquad (4.10)$$

ASAI: Average Service Availability Index

$$ASAI = \frac{customer\ hours\ of\ available\ service}{customer\ hours\ demanded}$$

$$= \frac{\sum N_i \times 8760 - \sum U_i N_i}{\sum N_i \times 8760} = 1 - \frac{SAIDI}{8760} \qquad (4.11)$$

ASUI = 1 – ASAI, where 8760 is the number of hours in a year

EENS: Expected Energy Not Supplied

$$EENS = \sum L_{avg(i)} U_i \qquad \text{(MWh/yr)} \qquad (4.12)$$

where $L_{avg(i)}$ is the average load connected to load point i

AENS: Average Energy Not Supplied

$$AENS = \frac{\sum L_{avg(i)} U_i}{\sum N_i} = \frac{EENS}{\sum N_i} \qquad \text{(MWh/Cust-yr)} \qquad (4.13)$$

ECOST: Expected Customer Cost

$$ECOST = \sum_{i=1}^{NL} \sum_{k=1}^{NE} L_{avg(i)}\, C_{rk}\, \lambda_k \qquad \text{(\$/yr)} \qquad (4.14)$$

where,

k = minimal cut or an outage event

λ_k = failure rate for the kth minimal cut or an outage event (f/yr)

C_{rk} = CDF for an outage duration of r hours due to failure event k (\$/kW)

NE = total number of outage events or minimal cuts of load point i

NL = total number of load points

It should be noted that the above indices can be evaluated at different levels in a system and can be used to assess the performance of a single feeder, a zone in the system or the

entire system. The energy and cost indices such as EENS, ECOST etc. can also be calculated for each outage event at the system lowest level.

4.4 Reliability assessment

The reliability indices described in the previous section are evaluated using the classical single weather state method and then by incorporating the weather conditions using the models developed in the previous chapters. In the classical approach, the component failure rate is assumed to be constant throughout the year. As described in the previous chapters, the component failure rate increases with weather severity. The impact of adverse weather is recognized using a two state weather model. The effects of extreme adverse weather conditions are incorporated in the analysis using the three state weather model.

4.4.1 Incorporating a single state weather model

The system and data described in Section 4.2 are used to calculate the various indices. Table 4.3 shows the reliability indices of average system failure rate, average outage duration and unavailability together with ECOST and EENS for the individual outage events (minimal cuts) at load point L1. The EENS was calculated using Equation 4.15 and ECOST using Equation 4.16.

$$EENS = L_{avg} U_k \tag{4.15}$$

$$ECOST = L_{avg}\, C_r\, \lambda_k \tag{4.16}$$

where,

λ_k = failure rate of minimal cut k

U_k = unavailability of minimal cut k

C_r = composite customer damage function for outage duration r

L_{avg} = average load at the load point

The sector composite interruption costs associated with various outage durations are given in Table C.17 in Appendix C. The indices associated with load point L2 are given in Table 4.4. This table clearly shows that the second order minimal cut largely dominates the indices. It is obvious that load point L1 is more reliable than load point L2. This effect is directly related to the degree of redundancy.

Table 4.3 Reliability indices for load point L1

Minimal cut	Failure rate (f/yr)	Average outage duration (hrs)	Unavailability (hrs/yr)	ECOST ($/yr)	EENS (kWh/yr)
1-2-3	0.000009	3.33	0.00003	2.51	0.6
1-2-4	0.000018	3.33	0.00006	5.01	1.2
Total	0.000027	3.33	0.00009	7.52	1.8

Table 4.4 Reliability indices for load point L2

Minimal cut	Failure rate (f/yr)	Average outage duration (hrs)	Unavailability (hrs/yr)	ECOST ($/yr)	EENS (kWh/yr)
3-4	0.004566	5.00	0.022831	1713.89	365.29
1-2-4	0.000018	3.33	0.000060	4.24	0.94
Total	0.004584	4.99	0.022891	1718.13	366.23

It is interesting to note that the failure rate and unavailability of mincut 1-2-4 are double those of mincut 1-2-3. This is because the failure rate of component 4 is double that of component 3. This shows the impact of this reliability parameter on the failure rate and unavailability. The system indices are listed below. The IEAR (Interruption Energy Assessment Rate) is given by the ratio of the ECOST and the EENS.

SAIFI = 0.002037 (intr/cust-yr)

SAIDI = 0.010143 (hrs/cust-yr)

EENS = 367.99 (kWh/yr)

ECOST = 1725.65 ($/yr)

IEAR = 4.67 ($/kWh)

ASAI = 0.999999

4.4.2 Incorporating a two state weather model

This section illustrates the effects of incorporating the two state weather model in the analysis. It, therefore, implies that the system can reside in normal or adverse weather conditions. The studies assume that component repair is performed only in normal weather. The failure events in the form of the minimal cuts are analysed using the Markov approach and the fundamental reliability indices of average system failure rate, outage duration and unavailability associated with each mincut are determined. Additional indices such as ECOST and EENS are also computed. The percentages of line failures in adverse weather are held at 50% and 90%, which are designated as Cases I and II respectively. Tables 4.5-4.8 show the results for the two cases.

Case I: 50% of failures occur in adverse weather

Table 4.5 Reliability indices for load point L1 (50% of failures in adverse weather)

Minimal cut	Failure rate (f/yr)	Average outage duration (hrs)	Unavailability (hrs/yr)	ECOST ($/yr)	EENS (kWh/yr)
1-2-3	0.000948	5.31	0.0050	462.62	100.00
1-2-4	0.001854	5.31	0.0099	904.75	198.00
Total	0.002802	5.31	0.01490	1367.37	298.00

Table 4.6 Reliability indices for load point L2 (50% of failures in adverse weather)

Minimal cut	Failure rate (f/yr)	Average outage duration (hrs)	Unavailability (hrs/yr)	ECOST ($/yr)	EENS (kWh/yr)
3-4	0.026270	6.88	0.1810	15097.89	2896.00
1-2-4	0.001854	5.31	0.0099	753.76	158.40
Total	0.028124	6.79	0.1909	15851.65	3054.40

Case II: 90% of failures occur in adverse weather

Table 4.7 Reliability indices for load point L1 (90% of failures in adverse weather)

Minimal cut	Failure rate (f/yr)	Average outage duration (hrs)	Unavailability (hrs/yr)	ECOST ($/yr)	EENS (kWh/yr)
1-2-3	0.004812	5.36	0.0258	2378.09	516.00
1-2-4	0.009248	5.36	0.0496	4570.36	992.00
Total	0.014060	5.36	0.0754	6948.45	1508.00

Table 4.8 Reliability indices for load point L2 (90% of failures in adverse weather)

Minimal cut	Failure rate (f/yr)	Average outage duration (hrs)	Unavailability (hrs/yr)	ECOST ($/yr)	EENS (kWh/yr)
3-4	0.07212	7.04	0.5083	42741.20	8132.80
1-2-4	0.00925	5.36	0.0496	3808.04	793.60
Total	0.08137	6.85	0.5579	46549.24	8926.40

The results presented in Tables 4.5-4.8 show that the load point indices increase considerably by incorporating the two state weather model. The increase in the percentage of failures in adverse weather has a significant effect on the load point indices.

The system indices obtained without considering the weather conditions together with those obtained using the two weather state model are shown in Table 4.9.

Table 4.9 System indices for the single and two state weather models

Condition	SAIFI (intr/cust-yr)	SAIDI (hrs/cust-yr)	ASAI	EENS (kWh/yr)	ECOST ($/yr)	IEAR ($/kWh)
Single state	0.002037	0.010143	0.999999	367.99	1725.65	4.67
2-state, Case I	0.013968	0.092512	0.999989	3352.4	17219.02	5.14
2-state, Case II	0.043742	0.288172	0.999967	10434.4	53497.69	5.13

It can be seen from Table 4.9 that there are quite large differences between the indices obtained using the basic formulae and those obtained using the two state weather model. The effect of adverse weather on these indices becomes more severe for larger percentages of failures occurring in adverse weather. The ASAI differs only marginally from that obtained using the single state weather model. It is evident that the system indices are dominated by the indices of load point L2 which is relatively unreliable.

4.4.3 Incorporating a three state weather model

The previous section illustrates the application of the two state weather model. It is clear that the load point indices are greatly influenced by the adverse weather conditions. Similar studies have been conducted to illustrate the effect of major adverse weather. The weather statistics are 200 hrs, 2hrs and 1 hr. The percentages of failures occurring in bad weather are held at 50% and 90% and the percentage of failures attributed to major adverse weather is varied from 10% to 50%. Tables 4.10-4.13 show the load point indices, energy indices and cost indices under the condition that 20% of bad weather failures occur in major adverse weather. The results for the cases when 10%, 30%, 40% and 50% of bad weather failures occur in extreme weather are presented in Tables C.1-C.16 in Appendix C.

Case I: 50% of line failures occurring in bad weather (F_b = 50%)

Table 4.10 Reliability indices for load point L1 (F_b = 50% and F_m = 20%)

Minimal cut	Failure rate (f/yr)	Average outage duration (hrs)	Unavailability (hrs/yr)	ECOST ($/yr)	EENS (kWh/yr)
1-2-3	0.007683	5.36	0.0412	3796.94	824
1-2-4	0.013351	5.36	0.0716	6598.06	1432
Total	0.021034	5.36	0.1128	10395.00	2256

Table 4.11 Reliability indices for load point L2 (F_b = 50% and F_m = 20%)

Minimal cut	Failure rate (f/yr)	Average outage duration (hrs)	Unavailability (hrs/yr)	ECOST ($/yr)	EENS (kWh/yr)
3-4	0.046157	6.96	0.3215	26940.91	5145.60
1-2-4	0.013351	5.36	0.0716	5496.34	1145.60
Total	0.059508	6.61	0.3931	32437.25	6291.20

Case II: 90% of line failures occurring in bad weather (F_b = 90%)

Table 4.12 Reliability indices for load point L1 (F_b = 90% and F_m = 20%)

Minimal cut	Failure rate (f/yr)	Average outage duration (hrs)	Unavailability (hrs/yr)	ECOST ($/yr)	EENS (kWh/yr)
1-2-3	0.029009	5.37	0.1558	14371.06	3116.00
1-2-4	0.047159	5.37	0.2533	23362.57	5066.00
Total	0.076168	5.37	0.4091	37733.63	8232.00

Table 4.13 Reliability indices for load point L2 (F_b = 90% and F_m = 20%)

Minimal cut	Failure rate (f/yr)	Average outage duration (hrs)	Unavailability (hrs/yr)	ECOST ($/yr)	EENS (kWh/yr)
3-4	0.116821	7.04	0.8240	69232.79	13184.00
1-2-4	0.047159	5.37	0.2533	19459.69	4052.80
Total	0.163980	6.57	1.0773	88692.48	17236.80

Table 4.14 shows the system indices for varying percentages of bad weather failures occurring in major adverse weather for 50% and 90% of the failures occurring in bad weather. The system indices shown in Table 4.14 can be compared with those in Table 4.9 where the indices were computed using the single and two state weather models. The differences are illustrated graphically in the next section.

Table 4.14 System indices obtained using the three state weather model

Failure condition		SAIFI (intr/ cust-yr)	SAIDI (hrs/ cust-yr)	ASAI	EENS (kWh/yr)	ECOST ($/kW)	IEAR ($/kWh)
For F_b = 50%	F_m = 10%	0.0186	0.1207	0.999986	4373.76	22311.48	5.1012
	F_m = 20%	0.0380	0.2364	0.999973	8547.20	42832.25	5.0112
	F_m = 30%	0.0692	0.4191	0.999952	15135.2	74965.72	4.9532
	F_m = 40%	0.1081	0.6460	0.999926	23312.8	114597.90	4.9157
	F_m = 50%	0.1518	0.8990	0.999897	32430.8	158870.39	4.8987
For F_b = 90%	F_m = 10%	0.0559	0.3625	0.999959	13111.4	66625.80	5.0815
	F_m = 20%	0.1149	0.7037	0.999920	25468.8	126426.11	4.9639
	F_m = 30%	0.1898	1.1348	0.999870	40951.2	201672.80	4.9247
	F_m = 40%	0.2709	1.5993	0.999817	57683.6	282424.69	4.8961
	F_m = 50%	0.3518	2.0612	0.999765	74320.4	362621.88	4.8792

4.5 Significance of using the two and three state weather models

The variations in SAIFI, SAIDI, EENS and ECOST with changing percentages of bad weather failures in extreme weather are illustrated pictorially in Figures 4.2-4.5. The system indices for the two cases when the system resides in two weather states are also shown. Figure 4.2 illustrates that the SAIFI increases significantly when a large number of failures occur in extreme weather. The effect is more acute when the failure percentages in bad weather increase from 50% to 90%. Figure 4.2 clearly shows that the two state weather model severely underestimates the predicted SAIFI. Similar variations in SAIDI, EENS and ECOST are illustrated in Figures 4.3, 4.4 and 4.5 respectively.

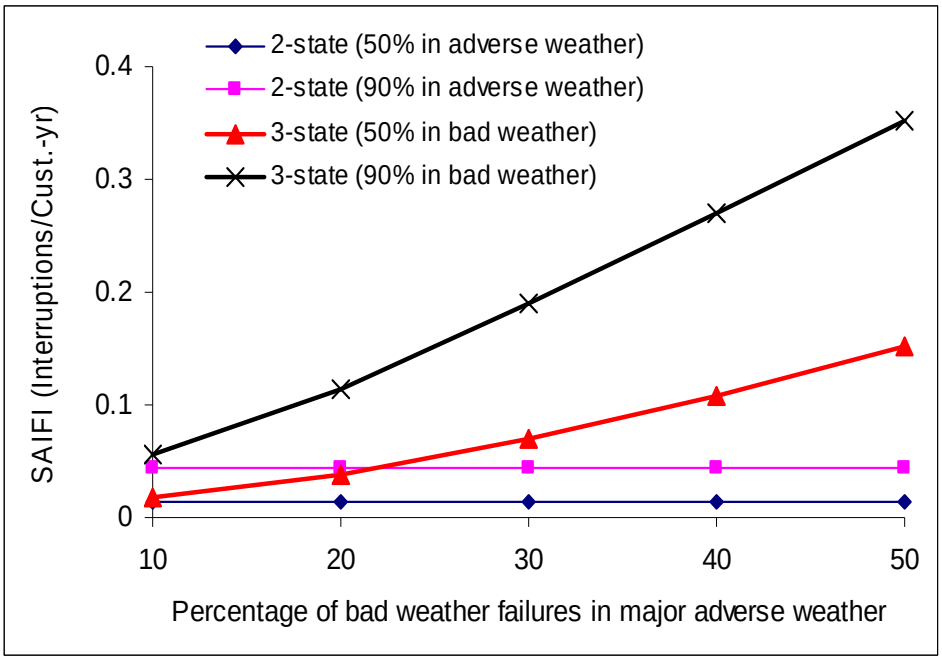

Figure 4.2 SAIFI using the two and three state weather models

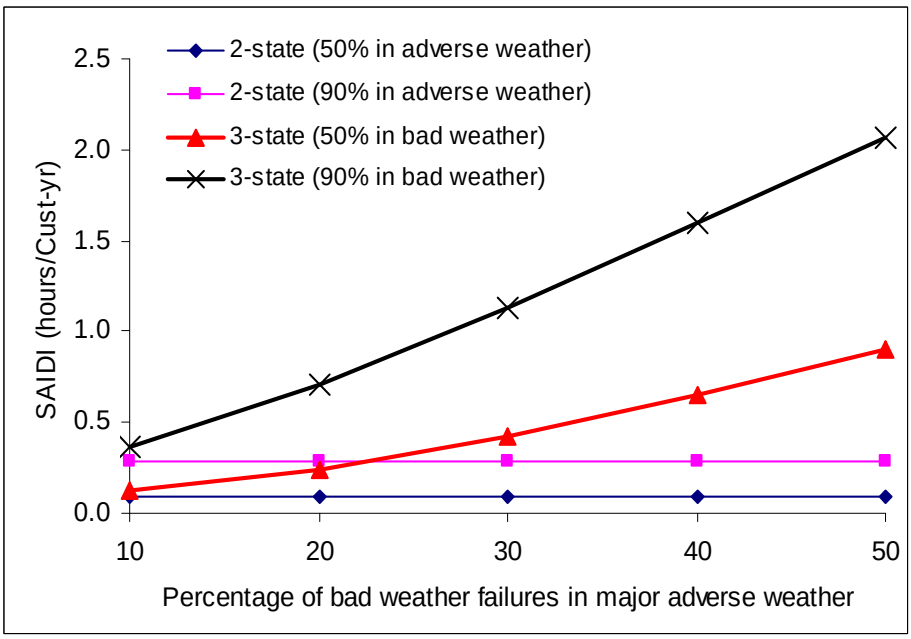

Figure 4.3 SAIDI using the two and three state weather models

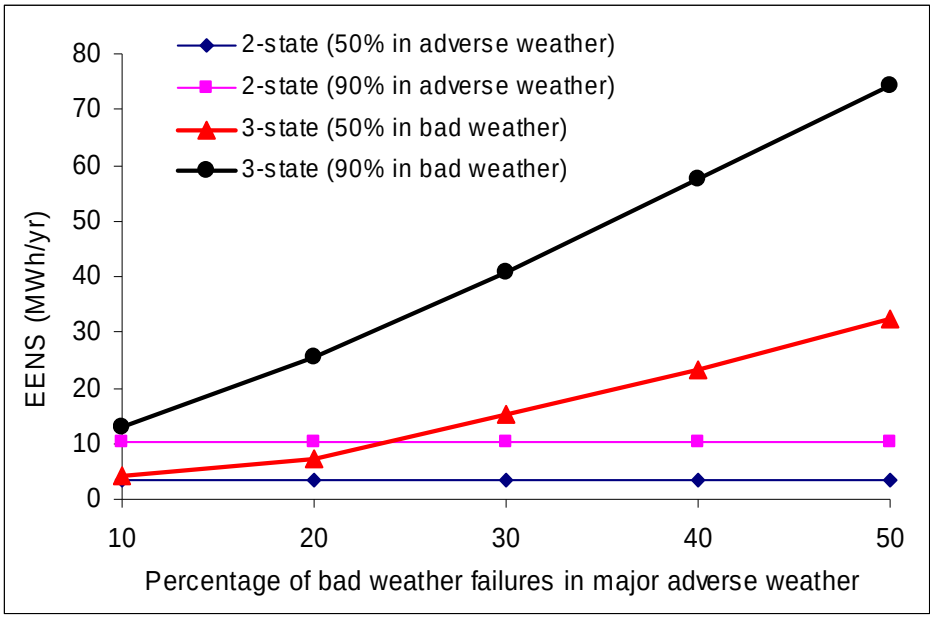

Figure 4.4 EENS using the two and three state weather models

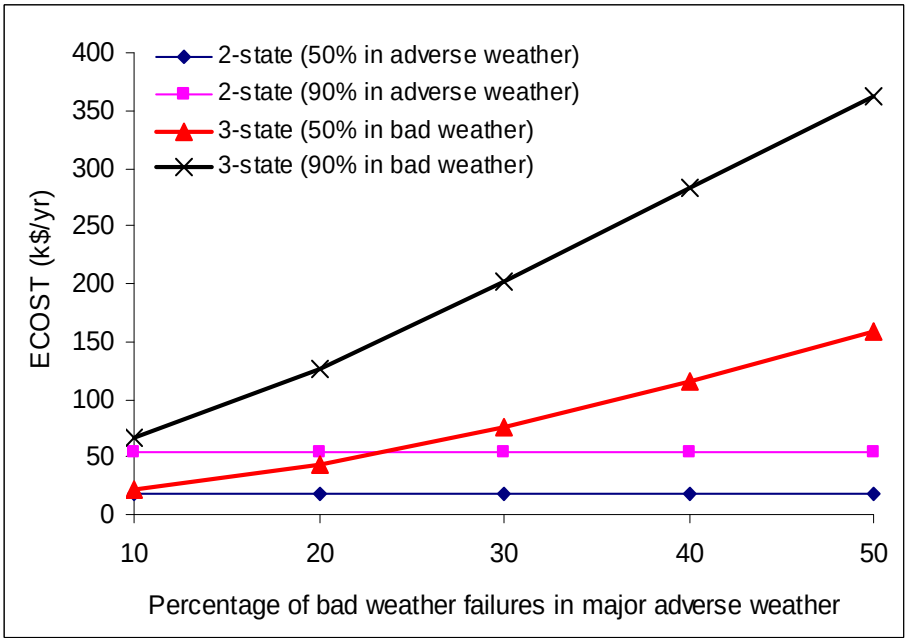

Figure 4.5 ECOST using the two and three state weather models

4.6 Summary

A simple practical system comprised of second order and third order minimal cuts was examined using the two different approaches. The first approach determines the system performance in a conventional way without considering the weather conditions, while the second approach employs the two different weather models to incorporate the effects of adverse and major adverse weather in the analysis. The load point indices and system indices were evaluated for varying percentages of line failures occurring in adverse weather and extreme weather periods. Load point indices show the actual adequacy at the customer connection points and the system indices provide an overall appraisal of the system adequacy. The significance of recognising the environmental stresses in the analysis is illustrated by comparing the estimated reliability indices in the different cases.

The load point adequacy studies clearly show the reliability benefits associated with increasing the level of redundancy in the system. This benefit, however, is severely affected when a large proportion of failures are attributable to extreme adverse weather. The analyses conducted in this chapter show that the reliability indices obtained using the two state weather model are significantly larger than those calculated using the conventional single weather state approach. The system indices increase further as a result of incorporating three weather states. A pictorial illustration of the differences between SAIIFI, SAIDI, EENS and ECOST determined using the two and three state weather models is presented in Figures 4.2-4.5. The influence of increasing the number of failures in major adverse weather is shown. These studies reveal that the application of the three weather state model becomes increasingly important as more failures occur in extreme weather periods.

Chapter 5

CONSIDERATION OF MULTI STATE WEATHER MODELS

5.1 Introduction

The influence of failure bunching due to fluctuating weather is illustrated in Chapter 2 using a two state weather model applied to two line and three line parallel systems. The three state weather model is developed and utilized in Chapter 3 in order to recognize the impacts of extreme weather periods. Weather is a continuous phenomenon that creates continuously varying stress on an associated system element. The failure rate of a component varies in accordance with the stress placed on that component. Transmission/distribution line failure rates are functions of weather conditions and increase with the weather intensity level.

In the three state weather model, a wide range of adverse weather conditions falling between normal and extreme weather is aggregated and generally termed as adverse weather. If the adverse weather state includes many relatively mild and non-destructive adverse weather periods, the failure bunching effect of more severe periods will be diluted. This suggests that only the weather periods that create a certain range of stress levels should be aggregated to form relevant weather states. This can be achieved by using a number of substates with different severity levels instead of using a single adverse weather state. A series of multi-state weather models are developed in this chapter and used to examine a two line parallel redundant configuration. The effects are illustrated using the basic reliability indices and the Error Factor. The basic techniques and processes underlying multi-state weather modeling are similar to those applied to a three state weather model. The number of actual states required to model the weather environment should be sufficient to represent the variable weather conditions and

minimize the potential error in the results. The objective of the work described in this chapter is to identify the number of weather states required to provide a reasonably accurate representation of the weather environment in a distribution system reliability study.

5.2 General methodology

The state space diagram for a general multi-state weather model is shown in Figure 5.1. In this model, the traditional classification [20] of the weather environment into three basic categories is maintained but the adverse weather state is represented by a number of substates in order to incorporate the variability in stress levels that occur due to the wide range of adverse weather. It can be seen in Figure 5.1 that the adverse weather is divided into S substates while the normal and extreme weather states retain their basic characteristics.

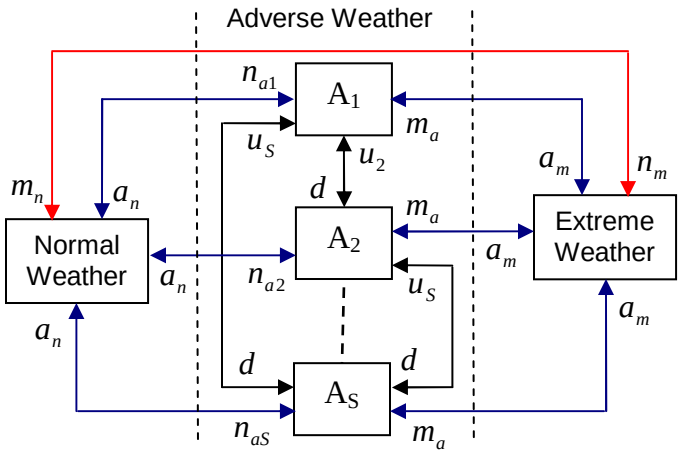

Figure 5.1 State space diagram for a general multi-state weather model

The weather statistics required in the multi-state weather modeling approach described in this chapter are not generally available. The following assumptions were made to illustrate the proposed approach. The average durations of normal, adverse and major adverse weather designated as N, A and M are approximately 200 hrs, 2 hrs, and 1 hr

respectively. The average duration of adverse weather substate A_1 is approximately 2 hours and that of A_2, A_3, …, A_S is 1 hour.

The assumed transition rates between the different weather states in occurrences per hour are as follows:

Any substate of adverse weather to normal weather, a_n = 1/A

Normal to major adverse weather, n_m = 1/8760

Major adverse to normal weather, m_n =1/2M

Any substate of adverse weather to major adverse weather, a_m = 1/8760

Major adverse to any substate of adverse weather, m_a = 1/(2SxM)

It is assumed that the frequency of encountering the less severe substates is higher than that of the more severe substates and that the occurrences of these periods are more likely following normal weather periods.

The transition rate from normal weather to the i^{th} adverse weather substate,

$$n_{ai} = \frac{(S+1)-i}{S(S+1)/2} \times \frac{1}{N} \qquad \text{(where, } i = 1,2,3....S \text{)}$$

The transition rate from a more severe adverse weather substate k to a less severe adverse weather substate i ($i < k$),

$$u_k = \frac{1}{(k-1)} \times \frac{1}{A}$$

The transition rate from a less severe adverse weather substate to a more severe adverse weather substate,

$$d = 1/8760$$

The frequency balance approach can be used to determine the steady state probabilities of each weather state.

5.3 Markov analysis

The complete system state space diagram becomes large and unmanageable with increase in the system states. Increasing the number of adverse weather substates can create a considerable number of system states. An n-component system with a m-state weather model results in $2^n \times m$ system states. A two component system with a ten state weather model generates 40 states and this increases to 80 states for a three component system. The stochastic transitional probability matrix can, however, be obtained without creating an exhaustive state space diagram, using the same concepts involved in creating the transitional probability matrix for a three state weather model. Equation 5.1 shows the generalized transitional probability matrix for the multi-state weather model with a two component system. The off-diagonal sub-matrices and their elements are easier to manipulate. Each of the diagonal sub-matrices is different in that the appropriate failure and repair rates are associated with the respective weather state.

$$[P] = \begin{bmatrix} M_N & n_{a1}[I] & n_{a2}[I] & \dots & n_{as}[I] & n_m[I] \\ a_n[I] & M_{A1} & d[I] & \dots & d[I] & a_m[I] \\ a_n[I] & u_2[I] & M_{A2} & \dots & d[I] & a_m[I] \\ \dots & \dots & \dots & \dots & \dots & \dots \\ a_n[I] & u_S[I] & u_S[I] & \dots & M_{AS} & a_m[I] \\ m_n[I] & m_a[I] & m_a[I] & \dots & m_a[I] & M_M \end{bmatrix} \qquad (5.1)$$

where, [I] is the identity matrix.

The matrix M_N is associated with normal weather. The failure rates and repair rates in this matrix are the component parameters in normal weather.

$$M_N = \begin{bmatrix} 1-\lambda_1^n-\lambda_2^n-X_n & \lambda_1^n & \lambda_2^n & 0 \\ \mu_2 & 1-\lambda_1^n-\mu_2-X_n & 0 & \lambda_1^n \\ \mu_1 & 0 & 1-\mu_1-\lambda_1^n-X_n & \lambda_2^n \\ 0 & \mu_2 & \mu_1 & 1-\mu_1-\mu_2-X_n \end{bmatrix}$$

where, $X_n = \sum_{i=1}^{S} n_{ai} + n_m$ is the sum of the departure rates from normal weather.

The matrix M_{Ai} is associated with the i^{th} adverse weather substate and X_{ai} is the sum of the departure rates from the i^{th} adverse weather substate. The component failure rates in this case are those for the corresponding weather state. It should be noted that all the elements below the diagonal are zero when no repair is performed in adverse weather.

$$M_{A1} = \begin{bmatrix} 1-\lambda_1^{a1}-\lambda_2^{a1}-X_{a1} & \lambda_1^{a1} & \lambda_2^{a1} & 0 \\ 0 & 1-\lambda_1^{a1}-X_{a1} & 0 & \lambda_1^{a1} \\ 0 & 0 & 1-\lambda_2^{a1}-X_{a1} & \lambda_2^{a1} \\ 0 & 0 & 0 & 1-X_{a1} \end{bmatrix}$$

where, $X_{a1} = a_n + (s-1)d + a_m$

$$M_{A2} = \begin{bmatrix} 1-\lambda_1^{a2}-\lambda_2^{a2}-X_{a2} & \lambda_1^{a2} & \lambda_2^{a2} & 0 \\ 0 & 1-\lambda_1^{a2}-X_{a2} & 0 & \lambda_1^{a2} \\ 0 & 0 & 1-\lambda_2^{a2}-X_{a2} & \lambda_2^{a2} \\ 0 & 0 & 0 & 1-X_{a2} \end{bmatrix}$$

where, $X_{a2} = a_n + u_2 + (s-2)d + a_m$

$$M_{AS} = \begin{bmatrix} 1-\lambda_1^{as}-\lambda_2^{as}-X_{as} & \lambda_1^{as} & \lambda_2^{as} & 0 \\ 0 & 1-\lambda_1^{as}-X_{as} & 0 & \lambda_1^{as} \\ 0 & 0 & 1-\lambda_2^{as}-X_{as} & \lambda_2^{as} \\ 0 & 0 & 0 & 1-X_{as} \end{bmatrix}$$

where, $X_{as} = a_n + (s-1)u_S + a_m$

$$M_M = \begin{bmatrix} 1-\lambda_1^{m}-\lambda_2^{m}-X_{m} & \lambda_1^{m} & \lambda_2^{m} & 0 \\ 0 & 1-\lambda_1^{m}-X_{m} & 0 & \lambda_1^{m} \\ 0 & 0 & 1-\lambda_2^{m}-X_{m} & \lambda_2^{m} \\ 0 & 0 & 0 & 1-X_{m} \end{bmatrix}$$

where, $X_m = m_n + m_a s$

The matrix M_M represents the condition when the system resides in major adverse weather. The term X_m which is subtracted from each diagonal element is the sum of the departure rates from the major adverse or extreme weather.

The stochastic transitional probability matrix can be used to calculate the steady state probabilities of each system state. The system failure rate is obtained using the process described in Chapter 2. Equation 5.2 is a generalized form of Equation 2.11.

$$\text{MTTF} = \sum_{i=1}^{D} N_{1,i} \tag{5.2}$$

where, D is the dimension of the square matrix [N].

The average system failure rate is the reciprocal of the MTTF. The average system outage duration can be obtained by dividing the sum of the failure state probabilities by the frequency of occurrence of the combined failure state. Equation 5.3 is used to evaluate the outage duration and Equation 5.4 gives the average system unavailability.

$$r_W = \frac{\sum P_{dn(i)}}{P_4\ (\mu_1 + \mu_2)} \tag{5.3}$$

$$U_W = \sum P_{dn(i)} \tag{5.4}$$

where,

$P_{dn(i)}$ is the probability of the i^{th} failure state.

5.4 Failure rate considerations

As noted in Chapters 2 and 3, there are virtually no available historical data on weather related failure rates. The average component failure rate can, however, be utilized to estimate the required parameters. Equation 5.5 is an extension of Equations 2.1 and 3.1 and indicates the contributions of the individual weather related failure rates to the total

average failure rate. The individual weather related failure rates can be estimated using Equation 5.6.

$$\lambda_{avg} = \sum_{k=1}^{WS} \lambda_k P_k \tag{5.5}$$

$$\lambda_k = \lambda_{avg} F_k / P_k \tag{5.6}$$

where,

λ_{avg} = average component failure rate per calendar year

λ_k = average component failure rate per year of the kth weather state

WS = total number of weather states

F_k = fraction of total failures occurring in the kth weather state

P_k = steady state probability of the kth weather state

Figure 5.2 shows the variation of the component failure rates in the multi-state weather representation. The parameters on the x-axis represent the normal weather, the adverse weather substates, and major adverse weather conditions.

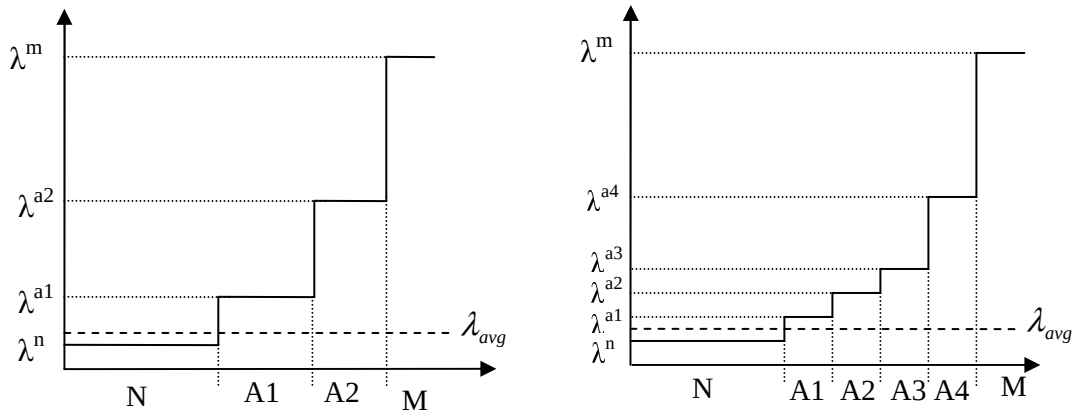

(a) (b)

Figure 5.2 Component failure rates as a function of the weather condition: (a) four-state weather model, (b) six-state weather model

Tables 5.1-5.5 show the component weather related failure rates and the weather state probabilities, durations and frequencies for selected weather state models obtained using the data assumed in the previous section. The total average component failure rate (λ_{avg}) is 1.0f/yr. The weather specific failure rates assume that 80% of the component failures are caused by bad weather and 20% of bad weather failures occur in major adverse weather.

Table 5.1 Weather parameters and component failure rates with a 3-state model

Weather state	Steady state probability	Average duration (hours)	Frequency of occurrence (occ/yr)	Component failure rate (f/yr)
Normal weather	0.989875	195.5357	44.35	0.202
Adverse weather	0.010011	1.9995	43.86	63.93
Extreme weather	0.000114	1	1	1401.76

Table 5.2 Weather parameters and component failure rates with a 4-state model

Weather state	Steady state probability	Average duration (hours)	Frequency of occurrence (occ/yr)	Component failure rate (f/yr)
Normal weather	0.989875	195.5357	44.35	0.202
Adverse weather, A1	0.008332	1.9991	36.51	38.41
Adverse weather, A2	0.001679	0.9999	14.71	190.58
Extreme weather	0.000114	1	1	1401.76

Table 5.3 Weather parameters and component failure rates with a 5-state model

Weather state	Steady state probability	Average duration (hours)	Frequency of occurrence (occ/yr)	Component failure rate (f/yr)
Normal weather	0.989875	195.5357	44.35	0.202
Adverse weather, A1	0.007285	1.9986	31.93	29.28
Adverse weather, A2	0.001880	0.9998	16.48	113.45
Adverse weather, A3	0.000845	0.9999	7.40	252.50
Extreme weather	0.000114	1	1	1401.76

Table 5.4 Weather parameters and component failure rates with a 6-state model

Weather state	Steady state probability	Average duration (hours)	Frequency of occurrence (occ/yr)	Component failure rate (f/yr)
Normal weather	0.989875	195.5357	44.35	0.202
Adverse weather, A1	0.006554	1.9982	28.73	24.41
Adverse weather, A2	0.001857	0.9997	16.27	86.17
Adverse weather, A3	0.001090	0.9998	9.55	146.80
Adverse weather, A4	0.000510	0.9999	4.47	313.58
Extreme weather	0.000114	1	1	1401.76

Table 5.5 Weather parameters and component failure rates with a 10-state model

Weather state	Steady state probability	Average duration (hours)	Frequency of occurrence (occ/yr)	Component failure rate (f/yr)
Normal weather	0.989875	195.5357	44.35	0.202
Adverse weather, A1	0.004933	1.9964	21.65	16.22
Adverse weather, A2	0.001555	0.9992	13.63	51.44
Adverse weather, A3	0.001135	0.9993	9.95	70.50
Adverse weather, A4	0.000855	0.9994	7.49	93.56
Adverse weather, A5	0.000638	0.9995	5.59	125.36
Adverse weather, A6	0.000455	0.9997	3.99	175.69
Adverse weather, A7	0.000294	0.9998	2.57	272.54
Adverse weather, A8	0.000146	0.9999	1.28	548.97
Extreme weather	0.000114	1	1	1401.76

The parameters presented in Table 5.1 can be compared with those shown in Tables 5.2-5.5 where adverse weather is divided into a number of substates. In each case, the sum of the probabilities of the adverse weather substates is equal to the probability of the aggregated adverse weather state in the three state weather model. The expected number of adverse weather occurrences are distributed among its substates. The last columns in Tables 5.1-5.5 are the component failure rates in the different weather states. The failure rate increases more rapidly as the adverse weather severity increases.

5.5 Sensitivity analysis

As noted earlier, the state space diagram expands rapidly as the number of weather states increases. The following analysis was done using a computer program "*RETADS* – Reliability Evaluation of Transmission and Distribution Systems" developed in Visual C++ during this research work. This is a general program that can consider two line and three line parallel redundant systems. The number of weather states in these studies is limited to 10, which is sufficient for reasonable accuracy. It can be upgraded relatively easily, however, if needed. The data required are the intended number of weather states to be included; the average durations of normal, adverse and extreme weather; and the average component failure rates and repair times. This program effectively generates the stochastic transitional probability matrix and successively computes the average system failure rate, outage duration, unavailability and the Error Factor. The results are directly exported to an Excel output file.

In the following sensitivity studies, four cases are considered in which 10%, 20%, 30% and 40% of bad weather failures are attributed to major adverse weather. The percentage of failures credited to bad weather is allowed to vary from 0% to 100% in steps of 10%. The percentage of failures attributed to adverse weather is assumed to be equally divided between the adverse weather substates. The notations F_b and F_m stand for the percentage of failures assigned to bad weather and the percentage of bad weather failures occurring in major adverse weather respectively. The basic system reliability indices and the Error Factor are evaluated and compared to examine the applicability of the weather models. It is assumed that repair cannot be performed during bad weather situations.

Case I: 10% of bad weather failures occurring in major adverse weather

Table 5.6 shows the Error Factor for the weather models created by varying the number of states from 3-10 assuming that 10% of bad weather failures occur in extreme weather.

The Error Factor obtained using the two weather state model is also shown in the second column of Table 5.6 for comparison purposes. Table 5.6 shows that the Error Factor increases as the number of adverse weather substates increases. The increase becomes smaller as the number of states in the weather model increases. This is illustrated pictorially in Figure 5.3.

Table 5.6 Error Factor using the different weather models, (F_m = 10%)

F_b (%)	Two state	Three state	Four State	Five state	Six state	Seven State	Eight state	Nine state	Ten state
0	1.01	1.01	1.01	1.01	1.01	1.01	1.01	1.01	1.01
10	1.27	1.35	1.39	1.42	1.43	1.45	1.46	1.47	1.48
20	2.06	2.34	2.51	2.61	2.69	2.75	2.80	2.84	2.88
30	3.37	3.96	4.34	4.56	4.72	4.85	4.96	5.05	5.13
40	5.18	6.18	6.84	7.22	7.50	7.73	7.91	8.06	8.20
50	7.48	8.98	9.99	10.57	11.00	11.33	11.60	11.83	12.03
60	10.27	12.34	13.75	14.57	15.17	15.63	16.00	16.32	16.59
70	13.52	16.22	18.11	19.20	19.98	20.58	21.08	21.48	21.83
80	17.25	20.62	23.04	24.42	25.41	26.17	26.78	27.29	27.72
90	21.42	25.51	28.51	30.22	31.43	32.35	33.10	33.71	34.23
100	26.05	30.88	34.51	36.56	38.01	39.11	39.99	40.71	41.32

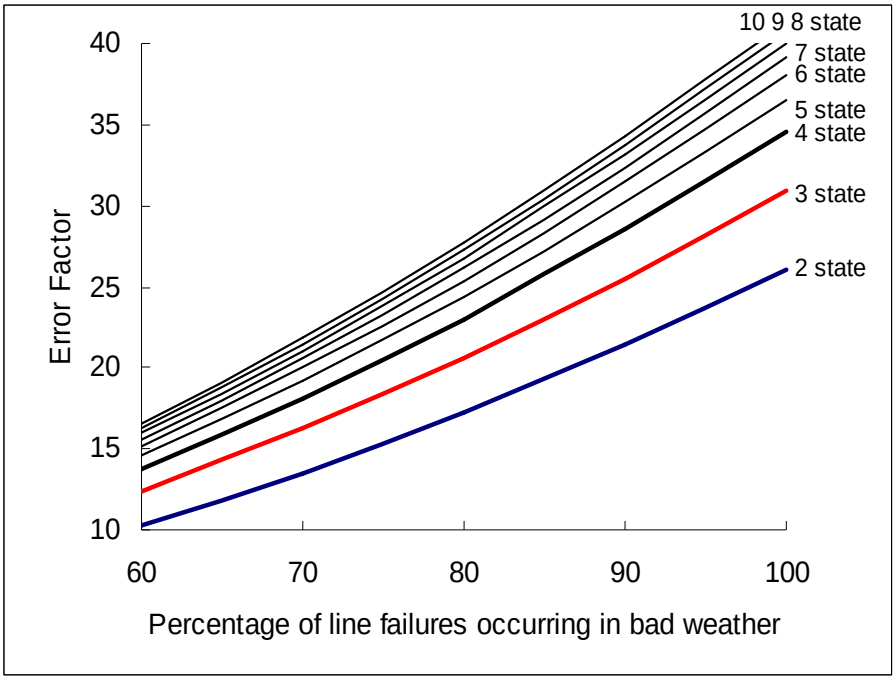

Figure 5.3 Error Factor for Case I

Figure 5.3 illustrates that the Error Factor increases with the recognition of the three state weather model and that the influence of using more weather states is considerable. The two state and three state weather models underestimate the predicted system failure rate and higher state weather models provide better estimates.

Table 5.7 shows the system unavailability and Table 5.8 shows the average outage duration for Case I.

Table 5.7 System unavailability, (F_m = 10%)

F_b (%)	Two state	Three state	Four State	Five state	Six state	Seven state	Eight state	Nine state	Ten state
0	0.007	0.007	0.007	0.007	0.007	0.007	0.007	0.007	0.007
10	0.009	0.010	0.011	0.011	0.011	0.011	0.011	0.012	0.012
20	0.018	0.020	0.022	0.023	0.024	0.024	0.025	0.025	0.026
30	0.031	0.037	0.041	0.043	0.044	0.046	0.047	0.048	0.048
40	0.049	0.059	0.066	0.070	0.072	0.075	0.076	0.078	0.079
50	0.072	0.087	0.097	0.103	0.107	0.111	0.113	0.116	0.118
60	0.100	0.121	0.135	0.143	0.149	0.154	0.157	0.161	0.163
70	0.132	0.160	0.179	0.189	0.197	0.203	0.208	0.212	0.216
80	0.169	0.204	0.228	0.242	0.251	0.259	0.265	0.270	0.274
90	0.210	0.253	0.282	0.299	0.311	0.321	0.328	0.334	0.339
100	0.256	0.306	0.342	0.363	0.377	0.388	0.397	0.404	0.410

Table 5.8 Average system outage duration, (F_m = 10%)

F_b (%)	Two state	Three state	Four State	Five state	Six state	Seven State	Eight state	Nine state	Ten state
0	3.79	3.79	3.79	3.79	3.79	3.79	3.79	3.79	3.79
10	4.36	4.44	4.48	4.51	4.53	4.54	4.55	4.56	4.57
20	5.00	5.10	5.15	5.17	5.19	5.20	5.21	5.22	5.23
30	5.37	5.43	5.46	5.48	5.49	5.50	5.51	5.51	5.52
40	5.55	5.59	5.61	5.62	5.63	5.63	5.64	5.64	5.64
50	5.65	5.68	5.69	5.69	5.70	5.70	5.70	5.70	5.71
60	5.71	5.72	5.73	5.73	5.74	5.74	5.74	5.74	5.74
70	5.74	5.75	5.76	5.76	5.76	5.76	5.76	5.76	5.76
80	5.77	5.77	5.77	5.77	5.77	5.77	5.77	5.77	5.77
90	5.78	5.78	5.78	5.78	5.78	5.78	5.78	5.78	5.78
100	5.79	5.79	5.79	5.79	5.79	5.79	5.79	5.79	5.79

As shown in Table 5.7, the unavailability increases with the percentage of failures occurring in bad weather. The utilization of a three state weather model increases the estimated system unavailability when a large portion of failures are attributed to bad weather. The unavailability increases further as the weather model includes more states, but the difference reduces with utilization of an increasing number of states. Table 5.8 shows that the average outage duration increases initially but does not progress in the same manner, as the percentage of failures in bad weather increases. The change in average outage duration as a result of incorporating multi-state weather models is negligible.

Case II: 20% of bad weather failures occurring in major adverse weather

The Error Factor for Case II is shown in Table 5.9. Figure 5.4 provides a pictorial illustration of the effects on the Error Factor of using a multi-state weather model.

Table 5.9 Error Factor using the different weather models, (F_m = 20%)

F_b (%)	Two state	Three state	Four State	Five state	Six state	Seven State	Eight state	Nine state	Ten state
0	1.01	1.01	1.01	1.01	1.01	1.01	1.01	1.01	1.01
10	1.27	1.63	1.67	1.69	1.71	1.72	1.73	1.74	1.75
20	2.06	3.41	3.55	3.64	3.70	3.75	3.79	3.83	3.86
30	3.37	6.19	6.51	6.70	6.83	6.94	7.03	7.11	7.17
40	5.18	9.87	10.41	10.74	10.97	11.16	11.31	11.44	11.56
50	7.48	14.33	15.17	15.66	16.02	16.30	16.53	16.72	16.89
60	10.27	19.51	20.68	21.37	21.87	22.26	22.58	22.84	23.07
70	13.52	25.31	26.88	27.79	28.45	28.96	29.37	29.72	30.02
80	17.25	31.69	33.70	34.86	35.69	36.33	36.85	37.28	37.65
90	21.42	38.58	41.08	42.50	43.52	44.31	44.94	45.46	45.90
100	26.05	45.95	48.97	50.68	51.90	52.83	53.58	54.20	54.72

It can be seen from Figure 5.4 that the Error Factor increases significantly with the utilization of a three state weather model when 20% of the bad weather failures are attributed to major adverse weather. The Error Factor increases further with increase in the number of weather states until the change becomes relatively insignificant. The two state weather model severely underestimates the expected failure rate. The use of a three

state weather model significantly reduces the potential error in the estimated failure rate. In this case, a four state weather model may provide a reasonably accurate assessment.

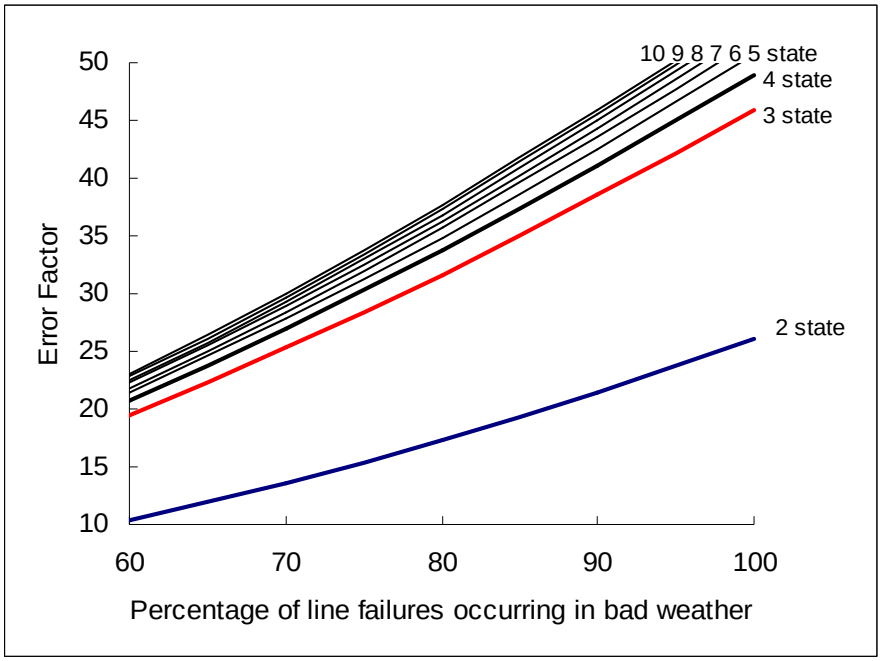

Figure 5.4 Error Factor for Case II

The system unavailability and average outage duration for this case are shown in Tables 5.10-5.11.

Table 5.10 System unavailability, (F_m = 20%)

F_b (%)	Two state	Three state	Four State	Five state	Six state	Seven State	Eight state	Nine state	Ten state
0	0.007	0.007	0.007	0.007	0.007	0.007	0.007	0.007	0.007
10	0.009	0.013	0.013	0.014	0.014	0.014	0.014	0.014	0.014
20	0.018	0.031	0.032	0.033	0.034	0.034	0.035	0.035	0.036
30	0.031	0.059	0.062	0.064	0.065	0.066	0.067	0.068	0.069
40	0.049	0.096	0.101	0.104	0.107	0.109	0.110	0.111	0.113
50	0.072	0.141	0.149	0.154	0.157	0.160	0.162	0.164	0.166
60	0.100	0.192	0.204	0.211	0.216	0.219	0.223	0.225	0.228
70	0.132	0.250	0.266	0.275	0.281	0.286	0.290	0.294	0.297
80	0.169	0.314	0.334	0.345	0.353	0.360	0.365	0.369	0.373
90	0.210	0.382	0.407	0.421	0.431	0.439	0.445	0.451	0.455
100	0.256	0.456	0.486	0.503	0.515	0.524	0.531	0.538	0.543

Table 5.11 Average system outage duration, (F_m = 20%)

F_b (%)	Two state	Three state	Four State	Five state	Six state	Seven State	Eight state	Nine state	Ten state
0	3.79	3.79	3.79	3.79	3.79	3.79	3.79	3.79	3.79
10	4.36	4.68	4.70	4.72	4.73	4.74	4.74	4.75	4.75
20	5.00	5.32	5.34	5.35	5.35	5.36	5.37	5.37	5.37
30	5.37	5.56	5.57	5.58	5.58	5.59	5.59	5.59	5.59
40	5.55	5.67	5.67	5.68	5.68	5.68	5.68	5.68	5.69
50	5.65	5.72	5.72	5.73	5.73	5.73	5.73	5.73	5.73
60	5.71	5.75	5.75	5.75	5.75	5.75	5.75	5.75	5.75
70	5.74	5.77	5.77	5.77	5.77	5.77	5.77	5.77	5.77
80	5.77	5.78	5.78	5.78	5.78	5.78	5.78	5.78	5.78
90	5.78	5.78	5.78	5.78	5.78	5.78	5.78	5.78	5.78
100	5.79	5.79	5.79	5.79	5.79	5.79	5.79	5.79	5.79

Case III: 30% of bad weather failures occurring in major adverse weather

Table 5.12 shows the Error Factor for Case III. As in Case II, the largest increase in Error Factor occurs when going from a two state to a three state weather model. The variation in Error Factor is presented graphically in Figure 5.5. It can be seen from Figure 5.5 that the difference between the Error Factors obtained using the two state and three state weather models is more than that in Figures 5.3 and 5.4.

Table 5.12 Error Factor using the different weather models, (F_m = 30%)

F_b (%)	Two state	Three state	Four State	Five state	Six state	Seven State	Eight state	Nine state	Ten state
0	1.01	1.01	1.01	1.01	1.01	1.01	1.01	1.01	1.01
10	1.27	2.12	2.15	2.17	2.18	2.19	2.20	2.21	2.22
20	2.06	5.14	5.26	5.33	5.38	5.42	5.45	5.48	5.51
30	3.37	9.67	9.93	10.08	10.19	10.28	10.36	10.42	10.47
40	5.18	15.41	15.86	16.12	16.31	16.46	16.59	16.69	16.79
50	7.48	22.12	22.80	23.20	23.49	23.72	23.90	24.06	24.20
60	10.27	29.62	30.57	31.13	31.53	31.85	32.11	32.33	32.51
70	13.52	37.76	39.02	39.76	40.29	40.71	41.04	41.33	41.57
80	17.25	46.42	48.03	48.97	49.64	50.16	50.59	50.94	51.25
90	21.42	55.50	57.50	58.66	59.48	60.12	60.64	61.07	61.44
100	26.05	64.95	67.36	68.75	69.74	70.50	71.12	71.63	72.06

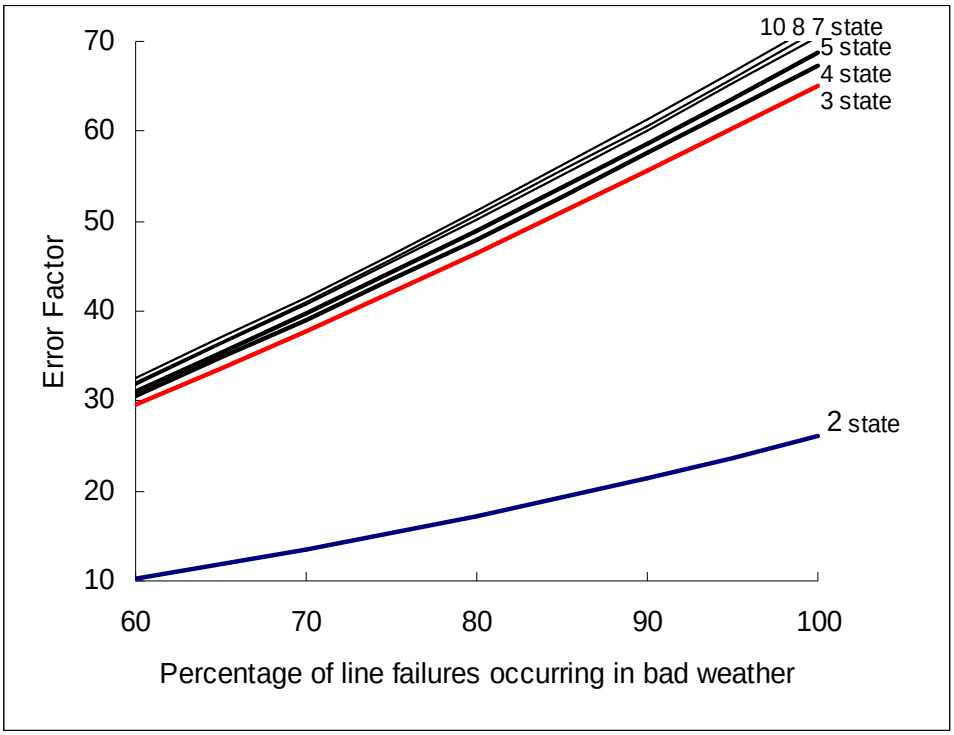

Figure 5.5 Error Factor for Case III

Table 5.13 and Table 5.14 present the system unavailability and average outage duration for Case III respectively.

Table 5.13 System unavailability, (F_m = 30%)

F_b (%)	Two state	Three state	Four State	Five state	Six state	Seven State	Eight state	Nine state	Ten state
0	0.007	0.007	0.007	0.007	0.007	0.007	0.007	0.007	0.007
10	0.009	0.018	0.018	0.018	0.019	0.019	0.019	0.019	0.019
20	0.018	0.048	0.049	0.050	0.051	0.051	0.051	0.052	0.052
30	0.031	0.094	0.096	0.098	0.099	0.100	0.100	0.101	0.102
40	0.049	0.151	0.155	0.158	0.160	0.161	0.163	0.164	0.165
50	0.072	0.218	0.225	0.228	0.231	0.234	0.235	0.237	0.238
60	0.100	0.293	0.302	0.307	0.311	0.315	0.317	0.319	0.321
70	0.132	0.374	0.386	0.393	0.399	0.403	0.406	0.409	0.411
80	0.169	0.460	0.476	0.485	0.492	0.497	0.501	0.505	0.508
90	0.210	0.550	0.570	0.581	0.590	0.596	0.601	0.605	0.609
100	0.256	0.644	0.668	0.682	0.692	0.699	0.705	0.710	0.715

Table 5.14 Average system outage duration, (F_m = 30%)

F_b (%)	Two state	Three state	Four State	Five state	Six state	Seven State	Eight state	Nine state	Ten state
0	3.79	3.79	3.79	3.79	3.79	3.79	3.79	3.79	3.79
10	4.36	4.93	4.95	4.95	4.96	4.96	4.97	4.97	4.97
20	5.00	5.48	5.48	5.49	5.49	5.49	5.50	5.50	5.50
30	5.37	5.64	5.65	5.65	5.65	5.65	5.65	5.66	5.66
40	5.55	5.71	5.71	5.72	5.72	5.72	5.72	5.72	5.72
50	5.65	5.74	5.75	5.75	5.75	5.75	5.75	5.75	5.75
60	5.71	5.76	5.76	5.76	5.76	5.76	5.76	5.77	5.77
70	5.74	5.77	5.77	5.77	5.77	5.77	5.77	5.77	5.78
80	5.77	5.78	5.78	5.78	5.78	5.78	5.78	5.78	5.78
90	5.78	5.79	5.79	5.79	5.79	5.79	5.79	5.79	5.79
100	5.79	5.79	5.79	5.79	5.79	5.79	5.79	5.79	5.79

Case IV: 40% of bad weather failures occurring in major adverse weather

The results for Case IV are shown in Tables 5.15-5.17. Table 5.15 shows that the increase in Error Factor when the three state weather model is applied is even greater than that in the previous cases and this effect diminishes with the utilization of higher state weather models. The variation in the Error Factor is shown in Figure 5.6.

Table 5.15 Error Factor using the different weather models, (F_m = 40%)

F_b (%)	Two state	Three state	Four State	Five state	Six state	Seven State	Eight state	Nine state	Ten state
0	1.01	1.01	1.01	1.01	1.01	1.01	1.01	1.01	1.01
10	1.27	2.79	2.81	2.83	2.84	2.84	2.85	2.86	2.86
20	2.06	7.42	7.52	7.57	7.61	7.65	7.67	7.70	7.72
30	3.37	14.11	14.31	14.43	14.52	14.59	14.65	14.70	14.74
40	5.18	22.26	22.61	22.82	22.97	23.09	23.19	23.27	23.34
50	7.48	31.47	32.00	32.31	32.54	32.72	32.86	32.99	33.10
60	10.27	41.43	42.17	42.60	42.92	43.17	43.37	43.55	43.69
70	13.52	51.93	52.90	53.47	53.89	54.22	54.48	54.71	54.90
80	17.25	62.78	64.03	64.75	65.28	65.69	66.02	66.30	66.54
90	21.42	73.88	75.42	76.32	76.96	77.46	77.87	78.21	78.50
100	26.05	85.14	87.00	88.08	88.85	89.44	89.93	90.33	90.67

Table 5.16 System unavailability, (F_m = 40%)

F_b (%)	Two state	Three state	Four State	Five state	Six state	Seven State	Eight state	Nine state	Ten state
0	0.007	0.007	0.007	0.007	0.007	0.007	0.007	0.007	0.007
10	0.009	0.025	0.025	0.025	0.025	0.025	0.025	0.025	0.025
20	0.018	0.071	0.072	0.072	0.073	0.073	0.073	0.074	0.074
30	0.031	0.138	0.140	0.141	0.142	0.142	0.143	0.143	0.144
40	0.049	0.219	0.222	0.224	0.226	0.227	0.228	0.229	0.230
50	0.072	0.311	0.316	0.319	0.321	0.323	0.324	0.326	0.327
60	0.100	0.410	0.417	0.421	0.424	0.427	0.429	0.431	0.432
70	0.132	0.514	0.524	0.529	0.534	0.537	0.539	0.542	0.544
80	0.169	0.622	0.634	0.642	0.647	0.651	0.654	0.657	0.659
90	0.210	0.732	0.748	0.757	0.763	0.768	0.772	0.775	0.778
100	0.256	0.844	0.863	0.873	0.881	0.887	0.892	0.896	0.899

Table 5.17 Average system outage duration, (F_m = 40%)

F_b (%)	Two state	Three state	Four State	Five state	Six state	Seven State	Eight state	Nine state	Ten state
0	3.79	3.79	3.79	3.79	3.79	3.79	3.79	3.79	3.79
10	4.36	5.14	5.15	5.15	5.15	5.15	5.15	5.16	5.16
20	5.00	5.57	5.58	5.58	5.58	5.58	5.58	5.58	5.58
30	5.37	5.69	5.69	5.69	5.69	5.69	5.69	5.69	5.70
40	5.55	5.74	5.74	5.74	5.74	5.74	5.74	5.74	5.74
50	5.65	5.76	5.76	5.76	5.76	5.76	5.76	5.76	5.76
60	5.71	5.77	5.77	5.77	5.77	5.77	5.77	5.77	5.77
70	5.74	5.78	5.78	5.78	5.78	5.78	5.78	5.78	5.78
80	5.77	5.78	5.78	5.78	5.78	5.78	5.78	5.78	5.78
90	5.78	5.79	5.79	5.79	5.79	5.79	5.79	5.79	5.79
100	5.79	5.79	5.79	5.79	5.79	5.79	5.79	5.79	5.79

Figure 5.6 clearly shows that the influence of using the three state weather model in this case is even higher than that in Figures 5.4 and 5.5. In this case, the effects of utilizing an increasing number of weather states diminish. The profiles associated with some of the weather models are not shown in Figures 5.5 and 5.6 to avoid overlapping profiles. It becomes clear that a three state representation is sufficient to achieve reasonably accurate results when a considerably large portion of failures are caused by extreme weather.

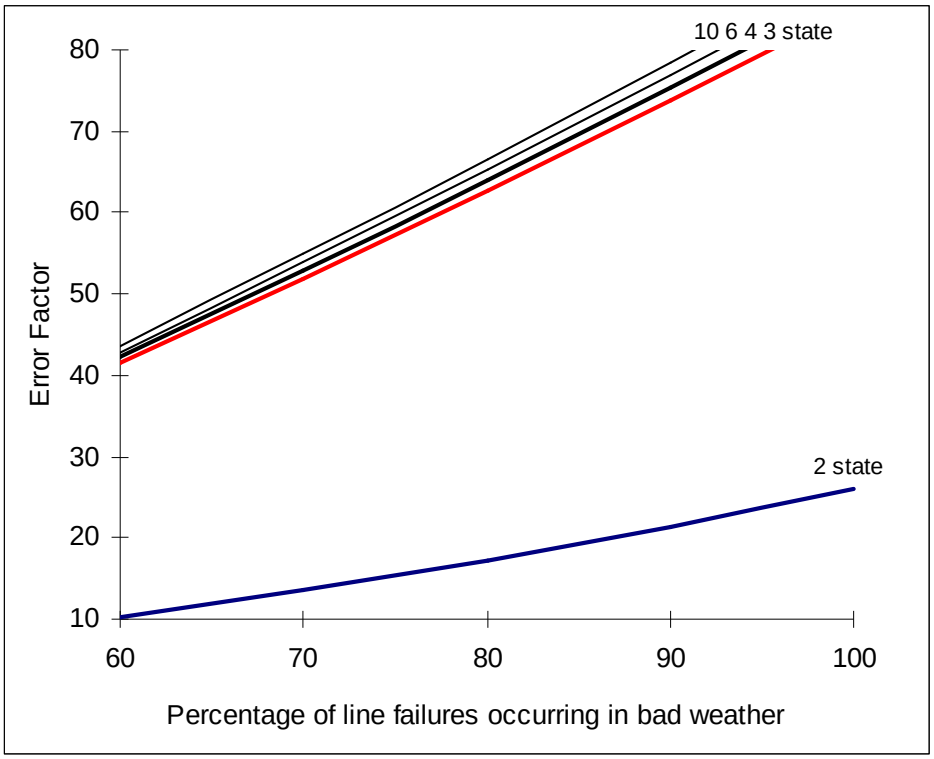

Figure 5.6 Error Factor for Case IV

Figures 5.3-5.6 illustrate that the inclusion of extreme weather conditions dominates the effect of considering multiple adverse weather substates. The influence on the predicted indices of incorporating multiple substates can be considerable when small percentages of bad weather failures are attributed to major adverse weather and the percentages of line failures in bad weather are relatively large.

The analysis indicates that the number of states in a weather model have different impacts when the percentage of failures occurring in major adverse weather varies. The profiles shown in Figure 5.3 are quite different from those in Figure 5.6 and the number of states selected depends on the percentage of failures occurring in extreme weather. All the Error Factor profiles, however, clearly show that at least three weather states should be utilized in a reliability assessment.

5.6 Summary

This chapter introduces the concept of multi-state weather modeling in the reliability assessment of a system exposed to a great deal of weather variation. A series of weather models are developed and examined by application to a two line parallel redundant system. The basic reliability indices of average system failure rate, average outage duration and unavailability are presented. The effects of using a particular weather model are illustrated by comparisons of the Error Factor obtained using the various weather models.

The studies show that the three state weather model can be used to accurately predict the system indices in some situations and that in other situations additional states should be included in the weather model to improve the accuracy. The analysis shows that the three state weather model provides acceptable results when the percentage of bad weather failures is significant and the percentage of failures caused by extreme weather is relatively high. The results also show that in virtually all situations a three state weather model provides a substantial improvement in reliability estimation than the utilization of a single or two state weather model.

It should be appreciated that it is much easier to collect the required weather and failure statistics for the three state weather model than for the higher state weather models. The calculations in this chapter are based on the assumption that the component failures are uniformly distributed in the whole adverse weather period regardless of the severity level in the individual substate. There are virtually no available data on specific weather related failures. The results shown, however, clearly indicate that the effects of incorporating adverse weather in reliability prediction are important and that data should be collected for at least one or more adverse weather severity levels.

Chapter 6

SEGMENTED RELIABILITY INDICES

6.1 Introduction

The weather environment is a vital element that severely impacts an electric utility's operational ability and system reliability in overhead transmission and distribution systems. Outdoor electrical networks are vulnerable to extreme weather conditions such as ice storms, hurricanes, lightning etc. Although extreme events have relatively low probabilities of occurring, when they do occur, they can cause considerable physical destruction resulting in large numbers of customers being interrupted for long periods of time. The impacts can vary depending on the nature of the weather event and the system topology. It is important to identify the weather specific contribution to the total system indices. This can provide a quantitative insight into the potential risk due to failures in the various weather conditions. The recognition of the risk contributed by a particular weather category can be valuable information in working to minimize the anticipated impact.

A distribution system usually occupies a small geographic area and therefore it is liable to be affected by prevailing weather situations. It is noted in Chapter 1, that the majority of power supply outages occur mainly in distribution systems and that most of these interruptions are due to bad weather conditions. The adequacy performance of a utility is measured using a wide range of reliability indices. The System Average Interruption Frequency Index (SAIFI) and the System Average Interruption Duration Index (SAIDI) are commonly used reliability indices throughout the world. Canadian statistics on outage causes are published annually by the Canadian Electricity Association (CEA). Figure 1.2 and Figure 1.3 in Chapter 1 show the individual cause contributions to the

SAIFI and SAIDI respectively. It is relatively easy to quantify such contributions from past performance. There has, however, been relatively little work done in estimating the reliability indices associated with weather specific failures in predictive assessment.

The studies described in this chapter focus on dividing the system risk indices into the three main segments related to the weather conditions. An approach to determine the weather specific indices is proposed and illustrated using a practical test distribution system. The effect of utilizing more repair resources is examined using a series of sensitivity studies. The analyses also illustrate the impact of more frequently occurring weather events. The load point indices are provided in the form of expected failure rate, average outage duration and unavailability. The feeder indices and the system indices of SAIFI and SAIDI are presented as index segments attributable to the three weather states.

6.2 RBTS distribution system analysis

The example system shown in Figure 6.1 is used to illustrate the proposed methodology. It is a part of the Roy Billinton Test System (RBTS) [23] and represents a typical urban distribution system. Detailed reliability data associated with this system are presented in [23]. Tables 6.1-6.3 show the data used in the subsequent analyses. The customer types include residential, commercial, institution/government and small users. The transformers on Feeders 1, 3 and 4 are utility property and are included in the analysis. The transformers that supply the small users on Feeder 2 are customer owned and are not incorporated in the study. Although the feeders can be meshed through normally open points, they are normally operated as radial feeders. The feeder is sectionalized by disconnect switches. This permits isolation of the faulted sections and service to be restored to the customers on the healthy feeder sections.

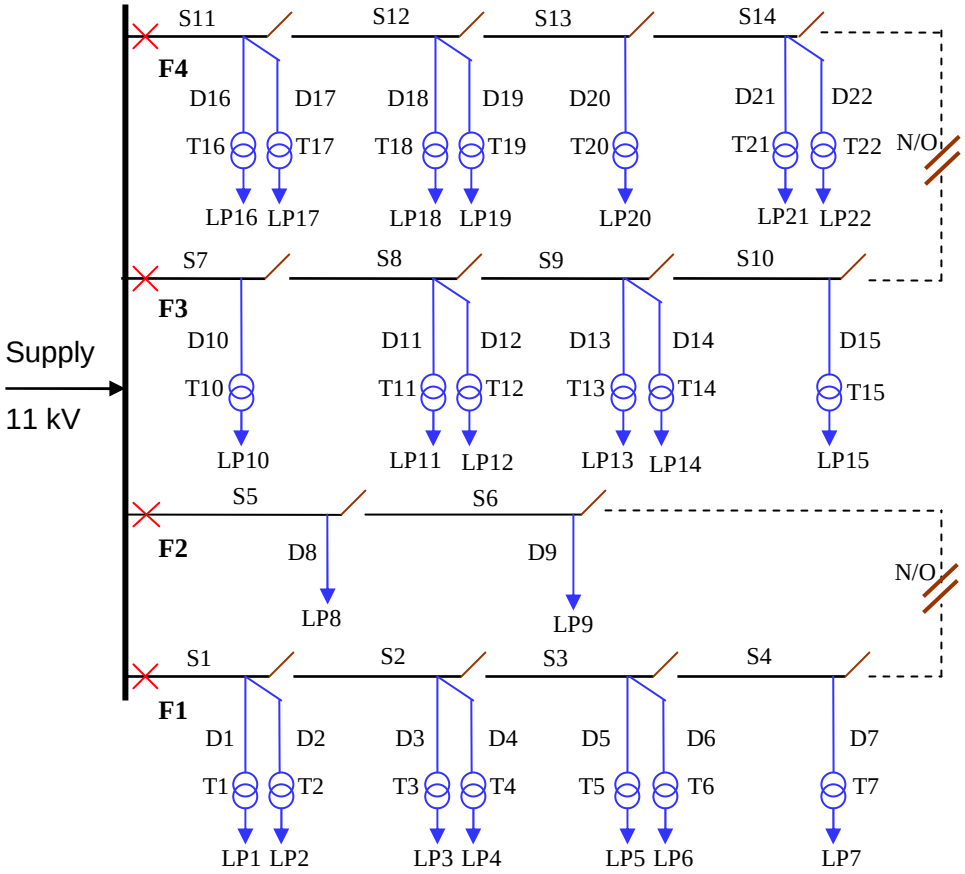

Symbols : T – Transformer, D – Distributor, S – Section, F – Feeder, Lp – Load point

Figure 6.1 Representative urban distribution system

The reliability parameters are as follows:

Average failure rate for each section and distributor = 0.065 failures/yr-km

Average repair time for each section and distributor = 5 hours

Average failure rate for a transformer = 0.015 failures/year

Average replacement time for a transformer = 10 hours

Average switching time = 1 hour

The fuses located on the lateral distributors are not shown in Figure 6.1. The circuit breakers and fuses are assumed to be 100% reliable. The failure rate of a transformer is

considered to be unaffected by the weather conditions. A faulted transformer is replaced by a mobile transformer rather than repairing it.

Table 6.1 Feeder section and lateral distributor lengths

Length	Feeder sections	Lateral distributors
0.60 km	S4, S6, S9, S14	D1, D4, D10, D15, D17, D18
0.75 km	S1, S2, S3, S5, S7, S10, S12, S13	D6, D11, D13, D16, D21
0.80 km	S8, S11	D2, D3, D5, D7, D8, D9, D12,D14, D19, D20, D22

Table 6.2 Load point data

Load point	Average load (MW)	Peak load (MW)	Number of customers	Customer type
1, 2, 3, 10, 11	0.535	0.8668	210	Residential
12, 17, 18, 19	0.450	0.7291	200	Residential
8	1.000	1.6279	1	Small user
9	1.150	1.8721	1	Small user
4, 5, 13, 14, 20, 21	0.566	0.9167	1	Institutional
6, 7, 15, 16, 22	0.454	0.7500	10	Commercial

Table 6.3 Feeder data

Feeder	Load points	Average load (MW)	Peak load (MW)	Number of customers
F1	1−7	3.645	5.934	652
F2	8−9	2.150	3.500	2
F3	10−15	3.106	5.057	632
F4	16−22	3.390	5.509	622
Total	22	12.291	20.00	1908

6.2.1 Conventional approach

Failure events at the specified load point can be identified by a visual inspection of the system topology. A faulted distributor is isolated automatically by a 100% reliable fuse; therefore, the fault on any distributor does not interrupt other loads on the same feeder. A load point on a feeder experiences an outage due to failure of the transformer on the load point, the distributor and any segment of the feeder. The approximate equation method [17] is used to calculate the primary indices. The fundamental reliability indices of load point k are given by Equation 6.1. For load points 8 and 9, the parameters λ_T and r_T are not applicable. The outage duration depends on the applicable restoration process. The value of r_{Si} is 5 hours when it is necessary to repair the faulted line element to restore the service and 1 hour if the supply can be simply restored by switching action.

$$\lambda_k = \lambda_T + \lambda_{Dk} + \sum \lambda_{Si} \tag{6.1a}$$

$$U_k = \lambda_T r_T + \lambda_{Dk} r_{Dk} + \sum \lambda_{Si} r_{Si} \tag{6.1b}$$

$$R_k = U_k / \lambda_k \tag{6.1c}$$

where, λ_T = average failure rate of a transformer

λ_{Dk} = average failure rate of distributor k

λ_{Si} = average failure rate of feeder section i

r_T = average repair time of a transformer

r_{Dk} = average repair time of distributor k

r_{Si} = average repair time of feeder section i

The load point indices (λ_k, U_k) computed using Equation 6.1 are used to obtain the feeder or system indices (SAIFI, SAIDI) given by Equation 6.2.

$$SAIFI = \sum_{k=1}^{lp} \lambda_k N_k \Big/ N \tag{6.2a}$$

$$SAIDI = \sum_{k=1}^{lp} U_k N_k \Big/ N \tag{6.2b}$$

where, *lp* denotes the number of load points connected to the feeder/system and N_k is the number of customers at load point k, and N is the total number of customers in the system.

The load point indices of average failure rate, average annual outage time (unavailability) and average outage duration obtained without considering weather conditions using Equation 6.1 are shown in Table 6.4.

Table 6.4 Load point indices for conventional approach

Load point	Failure rate (failures/year)	Unavailability (hours/year)	Outage duration (hours)
1	0.239	0.73	3.03
2	0.252	0.79	3.13
3	0.252	0.79	3.13
4	0.239	0.73	3.03
5	0.252	0.79	3.13
6	0.249	0.77	3.11
7	0.252	0.75	2.98
8	0.140	0.54	3.88
9	0.140	0.50	3.60
10	0.243	0.73	3.00
11	0.252	0.79	3.13
12	0.256	0.81	3.16
13	0.252	0.74	2.93
14	0.256	0.75	2.95
15	0.243	0.73	3.00
16	0.252	0.79	3.13
17	0.242	0.74	3.06
18	0.242	0.73	3.00
19	0.256	0.79	3.11
20	0.256	0.79	3.11
21	0.252	0.74	2.93
22	0.256	0.75	2.95

The primary indices for the different load points given in Table 6.4 differ marginally from each other. A significant difference can be seen in the case of load points 8 and 9. These load points are inherently more reliable as Feeder 2 is a relatively short feeder and the transformers are not included.

The indices, SAIFI and SAIDI, can be determined for different levels in the system. A single feeder or the combination of feeders can be considered. The load points connected to the common feeder are aggregated to determine the system indices at the feeder level. The indices for the four feeders are denoted by *F1-F4*. The evaluation of indices for the whole system considers all 22 load points and is designated as *SYSTEM* in Table 6.5 and in the subsequent analyses. The system indices for the feeders and the whole system are given in Table 6.5.

Table 6.5 SAIFI and SAIDI for conventional method

Feeder	*SAIFI*	*SAIDI*
F1	0.248	0.770
F2	0.140	0.540
F3	0.250	0.770
F4	0.247	0.760
SYSTEM	0.248	0.770

It can be seen from Table 6.5 that Feeder 2 has better indices. It should be noted that the indices for the entire system cannot be obtained by simply summing the indices of the four feeders. Table 6.5 shows that the overall system indices are dominated by the less reliable feeders.

6.2.2 Weather considerations

The following studies incorporate the effects of weather on the component failure rates and repair times. The process used to determine the component failure rates in various weather conditions is the same as that illustrated in Chapter 3. In this process, the weather steady state probabilities are first evaluated and the failure rate in each individual weather state is calculated by allocating a portion of the total line failures to each weather state. The average annual failure rate and weather related failure rates are related to each other. For convenience, Equation 3.1 from Chapter 3 is shown as Equation 6.3.

$$\lambda_{avg} = P_n \lambda^n + P_a \lambda^a + P_m \lambda^m \qquad (6.3)$$

The P_n, P_a, P_m are the steady state probabilities of normal, adverse and major adverse weather, respectively, and λ^n, λ^a, λ^m are the failure rates in normal, adverse and major adverse weather expressed in failures per year of the respective weather state. As discussed in Chapter 3, these failure rates can be deduced using Equation 3.2 by assigning the percentage of failures occurring in bad weather (F_b), and the portion of bad weather failures that occur in major adverse weather (F_m).

Using the line failure rates and repair times for normal weather, the load point indices of failure rate, average outage duration and unavailability in the normal weather condition can be obtained. The fundamental reliability indices of load point k in normal weather are given by Equation 6.4.

$$\lambda_k^n = \lambda_T + \lambda_{Dk}^n + \sum \lambda_{Si}^n \tag{6.4a}$$

$$U_k^n = \lambda_T r_T^n + \lambda_{Dk}^n r_{Dk}^n + \sum \lambda_{Si}^n r_{Si}^n \tag{6.4b}$$

$$R_k^n = U_k^n / \lambda_k^n \tag{6.4c}$$

The indices for the feeders and for the entire system in the normal weather condition, i.e. $SAIFI^n$ and $SAIDI^n$, can be evaluated using the load point indices given in Equation 6.5.

$$SAIFI^n = \sum_{k=1}^{lp} \lambda_k^n N_k \Big/ N \tag{6.5a}$$

$$SAIDI^n = \sum_{k=1}^{lp} U_k^n N_k \Big/ N \tag{6.5b}$$

The line failure rates and repair times in adverse weather can be used to find the load point indices in the adverse weather state. The load point indices obtained in adverse weather subsequently provide the feeder and system indices. The indices corresponding to major adverse weather can be determined in a similar manner.

The equations for the calculation of adverse and major adverse weather related indices are shown in Equations 6.6-6.9.

Adverse weather:

$$\lambda_k^a = \lambda_T + \lambda_{Dk}^a + \sum \lambda_{Si}^a \tag{6.6a}$$

$$U_k^a = \lambda_T r_T^a + \lambda_{Dk}^a r_{Dk}^a + \sum \lambda_{Si}^a r_{Si}^a \tag{6.6b}$$

$$R_k^a = U_k^a / \lambda_k^a \tag{6.6c}$$

$$SAIFI^a = \sum_{k=1}^{lp} \lambda_k^a N_k / N \tag{6.7a}$$

$$SAIDI^a = \sum_{k=1}^{lp} U_k^a N_k / N \tag{6.7b}$$

Major adverse weather:

$$\lambda_k^m = \lambda_T + \lambda_{Dk}^m + \sum \lambda_{Si}^m \tag{6.8a}$$

$$U_k^m = \lambda_T r_T^m + \lambda_{Dk}^m r_{Dk}^m + \sum \lambda_{Si}^m r_{Si}^m \tag{6.8b}$$

$$R_k^m = U_k^m / \lambda_k^m \tag{6.8c}$$

$$SAIFI^m = \sum_{k=1}^{lp} \lambda_k^m N_k / N \tag{6.9a}$$

$$SAIDI^m = \sum_{k=1}^{lp} U_k^m N_k / N \tag{6.9b}$$

The load point and feeder/system indices in the different weather conditions obtained using Equations 6.4-6.9 are not actual values. These indices can, however, be weighted by the respective weather probability and summed to obtain the expected values.

The expected indices of the k^{th} load point are given by Equation 6.10.

$$\lambda_k = P_n \lambda_k^n + P_a \lambda_k^a + P_m \lambda_k^m \tag{6.10a}$$

$$U_k = P_n U_k^n + P_a U_k^a + P_m U_k^m \tag{6.10b}$$

$$R_k = U_k / \lambda_k \tag{6.10c}$$

The expected values of SAIFI and SAIDI considering the weather effects are obtained using Equation 6.11.

$$SAIFI_W = P_n SAIFI^n + P_a SAIFI^a + P_m SAIFI^m \quad (6.11a)$$

$$SAIDI_W = P_n SAIDI^n + P_a SAIDI^a + P_m SAIDI^m \quad (6.11b)$$

In order to illustrate the procedure described above, consider the line and transformer data shown in Table 6.6 and Feeder 2 of the system shown in Figure 6.1. The analysis assumes that the unavailability of the breakers and fuses is negligible.

Table 6.6 Basic reliability data

Circuit element	Failure rate (failures/year)	Average restoration time (hours)		
		Normal weather	Adverse weather	Extreme weather
Line	0.065 per km	5	10	100
Transformer	0.015	10	20	100

The repair times for failures that occur in adverse and extreme weather are extended in Table 6.6. Difficulties due to adverse weather can delay component repair or replacement activities and extreme weather can create considerable damage and require a long time to restore service.

The resulting steady state weather probabilities using the three state weather model and weather statistics shown in Section 3.2 are given below. The average durations of normal, adverse and major adverse weather are approximately 200 hours, 2 hours and 1 hour, respectively, and major adverse weather occurs once per year.

$$P_n = 0.989875 \qquad P_a = 0.010011 \qquad P_m = 0.000114$$

The line failure rates under the various weather conditions can be illustrated using distributor D8, which is 0.8km long. The average failure rate for this line is 0.052 f/yr. Assume that 40% of the line failures occur in bad weather and 40% of the bad weather failures occur in major adverse weather. In this case, the failure rates under the various weather conditions are as follows:

λ^n = 0.032 f/yr of normal weather

λ^a = 1.247 f/yr of adverse weather

λ^m = 72.98 f/yr of major adverse weather

The unweighted load point indices for Feeder 2 in the three different weather states are shown in Table 6.7 for the purpose of illustration. The unadjusted system indices for Feeder 2 are shown in Table 6.8. These results represent the intermediate stage of the calculation procedure.

Table 6.7 Unadjusted load point indices in the three different weather conditions

Load point index	Load point 8			Load point 9		
	Normal weather	Adverse weather	Extreme weather	Normal weather	Adverse weather	Extreme weather
Failure rate	0.085	3.350	195.89	0.085	3.350	195.89
Unavailability	0.330	25.09	14177.4	0.310	22.99	12824.4
Outage duration	3.88	7.49	72.37	3.60	6.86	65.47

Table 6.8 Unadjusted system indices for Feeder 2 in the three weather conditions

Index	Normal weather	Adverse weather	Extreme weather
SAIFI	0.085	3.35	195.89
SAIDI	0.330	25.09	14177.4

In order to obtain the actual reliability indices, the results shown in Tables 6.7-6.8 are weighted by the appropriate weather probabilities using Equation 6.10 and Equation 6.11. The resulting load point indices are shown in Table 6.9 and the system indices are shown in Table 6.10. Table 6.10 also shows the individual weather state contributions to the total system indices.

Table 6.9 Load point indices for Feeder 2

Load point	Failure rate (failure/year)	Unavailability (hours/yr)	Average outage duration (hours)
8	0.140	2.194	15.671
9	0.140	1.999	14.278

Table 6.10 System indices for Feeder 2

Index	Normal weather	Adverse weather	Extreme weather	Expected value Sum(C2:C4*)
SAIFI	0.084	0.034	0.022	0.140
SAIDI	0.327	0.251	0.811	1.389

*C2, C4 – Column 2, Column 4

As expected, the load point failure rate and the SAIFI shown in Tables 6.9-6.10 are the initial values shown in Tables 6.4-6.5 calculated using the conventional approach. The unavailability and SAIDI differ from the values obtained using the conventional method because of the changes in the restoration time for failures in the various weather states.

The analysis can be extended to examine a larger system. The next section presents a series of case studies for the test distribution system.

6.3 Case studies

The following analyses examine the distribution system shown in Figure 6.1 in order to illustrate the influence of weather conditions on the basic reliability indices and on the system indices of SAIFI and SAIDI. The alternative supply available through a normally open point is assumed to be 100% reliable and the switching time is 1.0 hour regardless of the weather condition.

The cases considered involve different combinations of the percentages of failures occurring in bad weather and in major adverse weather and are designated as Case I-Case IV as follows:

- Case I: 40% of line failures in bad weather and 10% of bad weather failures in extreme weather, i.e. F_b = 40% and F_m = 10%

- Case II: 40% of line failures in bad weather and 40% of bad weather failures in extreme weather, i.e. F_b = 40% and F_m = 40%
- Case III: 80% of line failures in bad weather and 10% of bad weather failures in extreme weather, i.e. F_b = 80% and F_m = 10%
- Case IV: 80% of line failures in bad weather and 40% of bad weather failures in extreme weather, i.e. F_b = 80% and F_m = 40%

Table 6.11 shows the load point indices for Case I obtained using Equation 6.11. It can be seen from Table 6.11 that the average load point failure rates are equal to those shown in Table 6.4 obtained using the conventional approach. Unlike the failure rates, the unavailabilities and the average outage durations increase significantly when weather is included in the calculation.

Table 6.11 Load point indices considering weather effects, Case I

Load point	Failure rate (failures/year)	Unavailability (hours/year)	Outage duration (hours)
1	0.239	1.219	5.095
2	0.252	1.358	5.378
3	0.252	1.358	5.378
4	0.239	1.219	5.095
5	0.252	1.358	5.378
6	0.249	1.323	5.310
7	0.252	1.258	4.982
8	0.140	1.107	7.908
9	0.140	1.018	7.266
10	0.243	1.220	5.031
11	0.252	1.358	5.378
12	0.256	1.392	5.444
13	0.252	1.234	4.889
14	0.256	1.269	4.962
15	0.243	1.220	5.031
16	0.252	1.358	5.378
17	0.243	1.254	5.168
18	0.243	1.220	5.031
19	0.256	1.359	5.314
20	0.256	1.359	5.314
21	0.252	1.234	4.889
22	0.256	1.269	4.962

The load point unavailabilities for all the cases are collectively shown in Table 6.12. Table 6.13 presents the load point average outage durations for the cases considered. Figures 6.2-6.3 further illustrate these indices. It is clear from Figure 6.2 that the load point unavailabilities increase significantly when going from Case I to Case II. The difference is even larger when going from Case III to Case IV. The unavailability for Case III is smaller than that for Case II because the percentage of bad weather failures assigned to major adverse weather is smaller in Case III than in Case II. The failures that occur in extreme weather drive these changes. The variations in the load point average outage durations for the various cases are shown in Figure 6.3.

Table 6.12 Load point unavailabilities for Cases I-IV

Load point	Conventional	Case I	Case II	Case III	Case IV
1	0.725	1.219	2.166	1.713	3.605
2	0.790	1.358	2.444	1.920	4.093
3	0.790	1.358	2.444	1.920	4.093
4	0.725	1.219	2.166	1.713	3.605
5	0.790	1.358	2.444	1.920	4.093
6	0.774	1.323	2.374	1.871	3.974
7	0.751	1.258	2.239	1.770	3.733
8	0.543	1.107	2.194	1.671	3.844
9	0.504	1.018	1.999	1.520	3.483
10	0.729	1.220	2.167	1.715	3.608
11	0.790	1.358	2.444	1.920	4.093
12	0.806	1.392	2.514	1.969	4.213
13	0.738	1.234	2.181	1.723	3.616
14	0.755	1.269	2.250	1.772	3.735
15	0.729	1.220	2.167	1.715	3.608
16	0.790	1.358	2.444	1.920	4.093
17	0.742	1.254	2.235	1.762	3.725
18	0.729	1.220	2.167	1.715	3.608
19	0.794	1.359	2.445	1.923	4.096
20	0.794	1.359	2.445	1.923	4.096
21	0.738	1.234	2.181	1.723	3.616
22	0.755	1.269	2.250	1.772	3.735

Table 6.13 Load point average outage durations for Cases I-IV

Load point	Conventional	Case I	Case II	Case III	Case IV
1	3.031	5.095	9.050	7.168	15.094
2	3.133	5.378	9.684	7.610	16.228
3	3.133	5.378	9.684	7.610	16.228
4	3.031	5.095	9.050	7.168	15.094
5	3.133	5.378	9.684	7.610	16.228
6	3.108	5.310	9.532	7.521	15.982
7	2.978	4.982	8.871	7.015	14.799
8	3.884	7.908	15.671	11.975	27.560
9	3.605	7.266	14.278	10.898	24.975
10	3.004	5.031	8.933	7.072	14.882
11	3.133	5.378	9.684	7.610	16.228
12	3.157	5.444	9.832	7.696	16.467
13	2.927	4.889	8.640	6.829	14.335
14	2.953	4.962	8.801	6.926	14.601
15	3.004	5.031	8.933	7.072	14.882
16	3.133	5.378	9.684	7.610	16.228
17	3.058	5.168	9.215	7.265	15.364
18	3.004	5.031	8.933	7.072	14.882
19	3.106	5.314	9.564	7.513	16.010
20	3.106	5.314	9.564	7.513	16.010
21	2.927	4.889	8.640	6.829	14.335
22	2.953	4.962	8.801	6.926	14.601

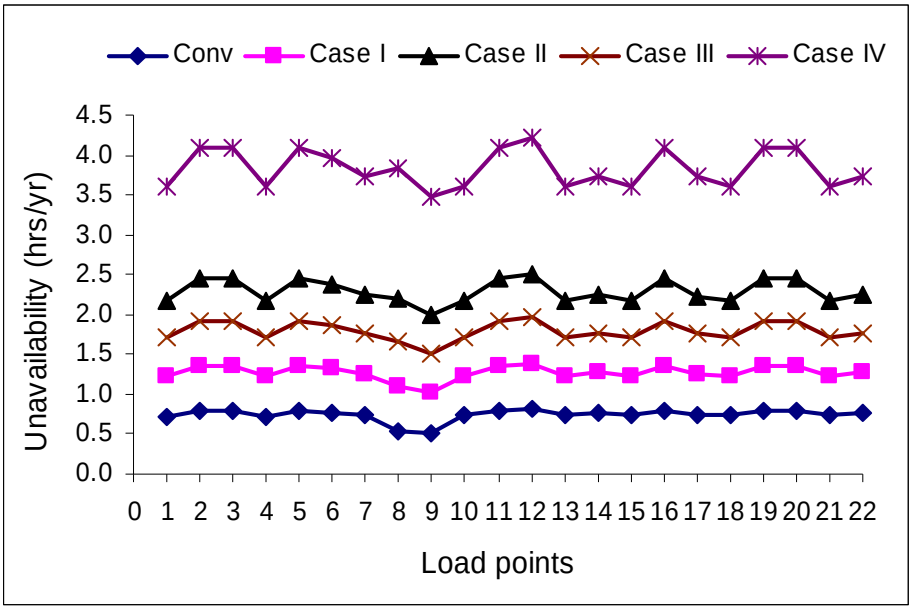

Figure 6.2 Load point unavailabilities for Cases I-IV

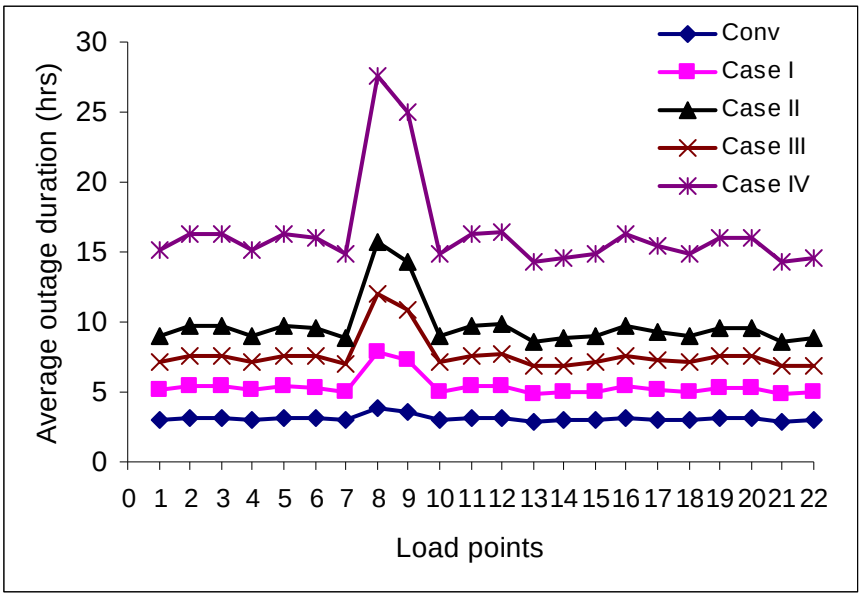

Figure 6.3 Load point average outage durations for Cases I-IV

The segmented SAIFI and SAIDI and the total values ($SAIFI_w$ and $SAIDI_w$) are shown in Tables 6.14-6.21. The last columns are evaluated using Equation 6.11. Tables 6.14-6.15 present the system SAIFI and SAIDI for Case I. The results for Case II are shown in Tables 6.16-6.17. Tables 6.18-6.19 apply to Case III. Tables 6.20-6.21 show the results for Case IV.

The study shows that the expected SAIFI, i.e $SAIFI_w$, obtained from weather related failures and the SAIFI from a conventional calculation are the same. A large contribution to the expected SAIFI, however, comes from bad weather situations. The SAIFI in normal weather in Cases I and II are the same because the portion of failures in normal weather is constant. The contribution of adverse weather decreases and that of major adverse weather increases when going from Case I to Case II. The SAIFI in extreme weather is even higher in Case III and Case IV.

The expected SAIDI, i.e. $SAIDI_w$, however, is largely influenced by the bad weather conditions. Table 6.15 shows that the SAIDI incorporating weather effects differs significantly from that obtained using the conventional method shown in Table 6.5 and that the pronounced effect is dictated by the adverse and major adverse weather. The results shown in Tables 6.14-6.21 indicate that the extreme weather contribution to the system indices increases significantly as more failures are assigned to extreme weather.

Table 6.14 SAIFI, Case I, (F_b = 40% and F_m = 10%)

Feeder	$P_n \times SAIFI^n$	$P_a \times SAIFI^a$	$P_m \times SAIFI^m$	$SAIFI_W$
F1	0.154	0.084	0.009	0.248
F2	0.084	0.050	0.006	0.140
F3	0.155	0.085	0.009	0.250
F4	0.154	0.084	0.009	0.247
SYSTEM	0.154	0.084	0.009	0.248

Table 6.15 SAIDI, Case I, (F_b = 40% and F_m = 10%)

Feeder	$P_n \times SAIDI^n$	$P_a \times SAIDI^a$	$P_m \times SAIDI^m$	$SAIDI_W$
F1	0.515	0.399	0.391	1.305
F2	0.327	0.377	0.405	1.108
F3	0.525	0.403	0.395	1.322
F4	0.515	0.389	0.379	1.282
SYSTEM	0.515	0.397	0.388	1.300

Table 6.16 SAIFI, Case II, (F_b = 40% and F_m = 40%)

Feeder	$P_n \times SAIFI^n$	$P_a \times SAIFI^a$	$P_m \times SAIFI^m$	$SAIFI_W$
F1	0.154	0.056	0.037	0.248
F2	0.084	0.034	0.022	0.140
F3	0.155	0.057	0.038	0.250
F4	0.154	0.056	0.037	0.247
SYSTEM	0.154	0.056	0.037	0.248

Table 6.17 SAIDI, Case II, (F_b = 40% and F_m = 40%)

Feeder	$P_n \times SAIDI^n$	$P_a \times SAIDI^a$	$P_m \times SAIDI^m$	$SAIDI_W$
F1	0.515	0.267	1.564	2.345
F2	0.327	0.251	1.618	2.196
F3	0.525	0.269	1.578	2.372
F4	0.515	0.260	1.514	2.289
SYSTEM	0.515	0.265	1.552	2.332

Table 6.18 SAIFI, Case III, (F_b = 80% and F_m = 10%)

Feeder	$P_n \times SAIFI^n$	$P_a \times SAIFI^a$	$P_m \times SAIFI^m$	$SAIFI_W$
F1	0.061	0.168	0.019	0.248
F2	0.028	0.101	0.011	0.140
F3	0.061	0.169	0.019	0.249
F4	0.061	0.167	0.019	0.247
SYSTEM	0.061	0.168	0.019	0.248

Table 6.19 SAIDI, Case III, (F_b = 80% and F_m = 10%)

Feeder	$P_n \times SAIDI^n$	$P_a \times SAIDI^a$	$P_m \times SAIDI^m$	$SAIDI_W$
F1	0.267	0.795	0.782	1.844
F2	0.109	0.753	0.809	1.671
F3	0.277	0.802	0.789	1.868
F4	0.267	0.774	0.757	1.799
SYSTEM	0.267	0.791	0.776	1.834

Table 6.20 SAIFI, Case IV, (F_b = 80% and F_m = 40%)

Feeder	$P_n \times SAIFI^n$	$P_a \times SAIFI^a$	$P_m \times SAIFI^m$	$SAIFI_W$
F1	0.061	0.112	0.075	0.248
F2	0.028	0.067	0.045	0.140
F3	0.061	0.113	0.075	0.249
F4	0.061	0.112	0.074	0.247
SYSTEM	0.061	0.112	0.075	0.248

Table 6.21 SAIDI, Case IV, (F_b = 80% and F_m = 40%)

Feeder	$P_n \times SAIDI^n$	$P_a \times SAIDI^a$	$P_m \times SAIDI^m$	$SAIDI_W$
F1	0.267	0.531	3.127	3.925
F2	0.109	0.502	3.236	3.848
F3	0.277	0.536	3.155	3.968
F4	0.267	0.517	3.029	3.813
SYSTEM	0.267	0.528	3.104	3.900

6.4 The effect of restoration time

Major storms can cause lengthy customer interruptions, resulting in huge monetary losses. The EEI's survey on Utility Storm Restoration Response [6] found that the average time required to restore service after a major storm strikes the system is 5.6 days. This statistic is based on the survey results of 44 responses from six participating utilities over a period of 14 years. Outage durations increase considerably when more damage occurs due to exceeding the system design level. A system with a low design level suffers more damage than a system that can tolerate more severe stress when exposed to the same storm. In order to examine the effects, the repair time is reduced from the 100 hours considered in the previous section to 50 hours following system failures due to storms.

Table 6.22 and Table 6.23 show the load point unavailabilities and average outage durations respectively for the four cases studied. The load point failure rates are found to be the same as for the repair time of 100 hours.

The variation in unavailabilities for the different percentages of failures occurring in bad weather and major adverse weather is shown in Figure 6.4. This figure can be compared with Figure 6.2. The quantitative differences between the various cases in Figure 6.2 and in Figure 6.4 are similar. It is important to note that the unavailability values in Figure 6.4 are considerably smaller. The load point average outage durations are illustrated in Figure 6.5.

Table 6.22 Load point unavailabilities for restoration time = 50 hours (hours/year)

Load point	Conventional	Case I	Case II	Case III	Case IV
1	0.725	1.044	1.464	1.362	2.203
2	0.790	1.156	1.639	1.517	2.483
3	0.790	1.156	1.639	1.517	2.483
4	0.725	1.044	1.464	1.362	2.203
5	0.790	1.156	1.639	1.517	2.483
6	0.774	1.128	1.595	1.481	2.416
7	0.751	1.076	1.512	1.406	2.278
8	0.543	0.906	1.389	1.268	2.234
9	0.504	0.836	1.272	1.157	2.029
10	0.729	1.045	1.466	1.364	2.206
11	0.790	1.156	1.639	1.517	2.483
12	0.806	1.184	1.683	1.554	2.551
13	0.738	1.059	1.479	1.372	2.213
14	0.755	1.087	1.523	1.409	2.281
15	0.729	1.045	1.466	1.364	2.206
16	0.790	1.156	1.639	1.517	2.483
17	0.742	1.072	1.508	1.398	2.271
18	0.729	1.045	1.466	1.364	2.206
19	0.794	1.158	1.640	1.520	2.486
20	0.794	1.158	1.640	1.520	2.486
21	0.738	1.059	1.479	1.372	2.213
22	0.755	1.087	1.523	1.409	2.281

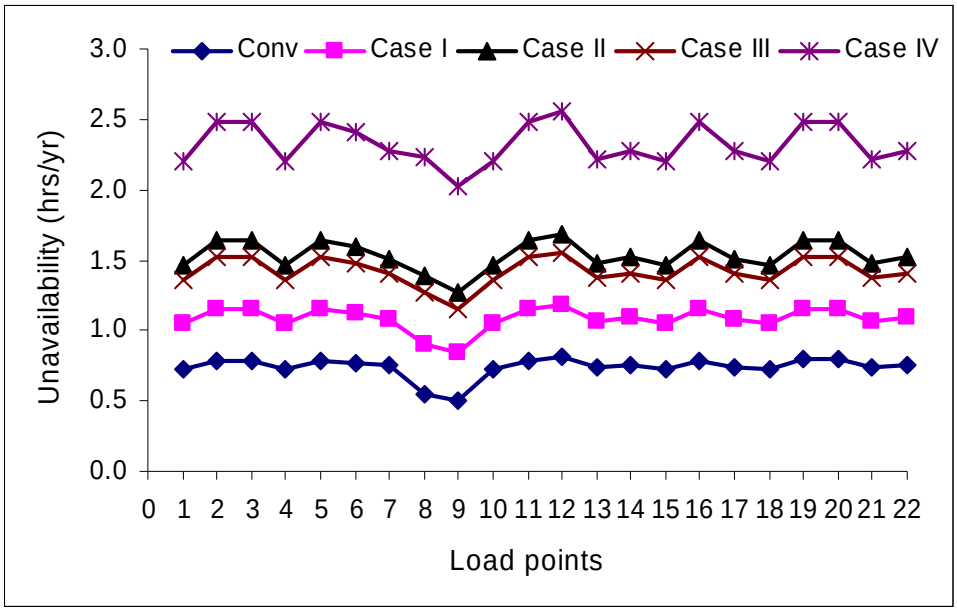

Figure 6.4 Load point unavailabilities for restoration time = 50 hours

Table 6.23 Load point average outage durations for restoration time = 50 hours (hours)

Load point	Conventional	Case I	Case II	Case III	Case IV
1	3.031	4.362	6.120	5.700	9.223
2	3.133	4.580	6.494	6.014	9.844
3	3.133	4.580	6.494	6.014	9.844
4	3.031	4.362	6.120	5.700	9.223
5	3.133	4.580	6.494	6.014	9.844
6	3.108	4.528	6.404	5.955	9.715
7	2.978	4.262	5.990	5.573	9.033
8	3.884	6.471	9.921	9.090	16.016
9	3.605	5.968	9.084	8.292	14.548
10	3.004	4.308	6.042	5.626	9.097
11	3.133	4.580	6.494	6.014	9.844
12	3.157	4.631	6.581	6.072	9.970
13	2.927	4.195	5.861	5.439	8.775
14	2.953	4.251	5.957	5.505	8.916
15	3.004	4.308	6.042	5.626	9.097
16	3.133	4.580	6.494	6.014	9.844
17	3.058	4.418	6.217	5.766	9.365
18	3.004	4.308	6.042	5.626	9.097
19	3.106	4.527	6.415	5.940	9.716
20	3.106	4.527	6.415	5.940	9.716
21	2.927	4.195	5.861	5.439	8.775
22	2.953	4.251	5.957	5.505	8.916

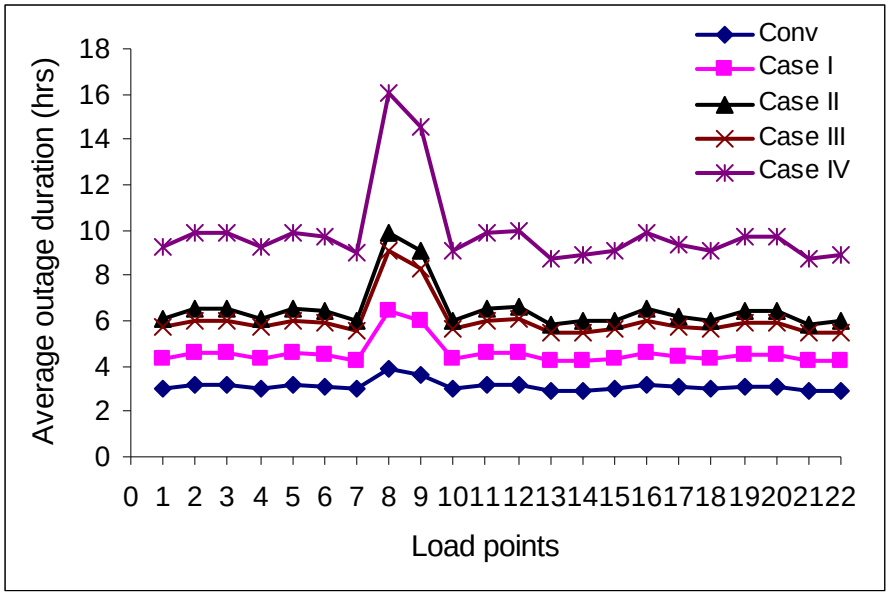

Figure 6.5 Load point average outage durations for restoration time = 50 hours

The average outage durations shown in Figure 6.3 where the repair time is 100 hours and those in Figure 6.5 where the repair time is 50 hours can be compared. The variations in the average outage durations are similar and the effect of a fast repair strategy can be seen.

The SAIFI contributions for three different weather classes and the total SAIFI under the conditions that 40% of the total line failures occur in bad weather and 10% of the bad weather failures are attributed to major adverse weather are given in Table 6.24. The SAIDI for this case is given in Table 6.25. The results for the rest of the case studies are shown in Tables 6.26-6.31.

Table 6.24 SAIFI, Case I, (F_b = 40% and F_m = 10%)

Feeder	$P_n \times SAIFI^n$	$P_a \times SAIFI^a$	$P_m \times SAIFI^m$	$SAIFI_W$
F1	0.154	0.084	0.009	0.248
F2	0.084	0.050	0.006	0.140
F3	0.155	0.085	0.009	0.250
F4	0.154	0.084	0.009	0.247
SYSTEM	0.154	0.084	0.009	0.248

Table 6.25 SAIDI, Case I, (F_b = 40% and F_m = 10%)

Feeder	$P_n \times SAIDI^n$	$P_a \times SAIDI^a$	$P_m \times SAIDI^m$	$SAIDI_W$
F1	0.515	0.399	0.198	1.112
F2	0.327	0.377	0.203	0.906
F3	0.525	0.403	0.200	1.127
F4	0.515	0.389	0.192	1.095
SYSTEM	0.515	0.397	0.197	1.108

Table 6.26 SAIFI, Case II, (F_b = 40% and F_m = 40%)

Feeder	$P_n \times SAIFI^n$	$P_a \times SAIFI^a$	$P_m \times SAIFI^m$	$SAIFI_W$
F1	0.154	0.056	0.037	0.248
F2	0.084	0.034	0.022	0.140
F3	0.155	0.057	0.038	0.249
F4	0.154	0.056	0.037	0.247
SYSTEM	0.154	0.056	0.037	0.248

Table 6.27 SAIDI, Case II, (F_b = 40% and F_m = 40%)

Feeder	$P_n \times SAIDI^n$	$P_a \times SAIDI^a$	$P_m \times SAIDI^m$	$SAIDI_W$
F1	0.515	0.267	0.792	1.573
F2	0.327	0.251	0.811	1.389
F3	0.525	0.269	0.799	1.593
F4	0.515	0.260	0.767	1.542
SYSTEM	0.515	0.265	0.786	1.566

Table 6.28 SAIFI, Case III, (F_b = 80% and F_m = 10%)

Feeder	$P_n \times SAIFI^n$	$P_a \times SAIFI^a$	$P_m \times SAIFI^m$	$SAIFI_W$
F1	0.061	0.168	0.019	0.248
F2	0.028	0.101	0.011	0.140
F3	0.061	0.169	0.019	0.249
F4	0.061	0.167	0.019	0.247
SYSTEM	0.061	0.168	0.019	0.248

Table 6.29 SAIDI, Case III, (F_b = 80% and F_m = 10%)

Feeder	$P_n \times SAIDI^n$	$P_a \times SAIDI^a$	$P_m \times SAIDI^m$	$SAIDI_W$
F1	0.267	0.795	0.396	1.458
F2	0.109	0.754	0.406	1.268
F3	0.277	0.802	0.399	1.479
F4	0.267	0.774	0.384	1.425
SYSTEM	0.267	0.791	0.393	1.451

Table 6.30 SAIFI, Case IV, (F_b = 80% and F_m = 40%)

Feeder	$P_n \times SAIFI^n$	$P_a \times SAIFI^a$	$P_m \times SAIFI^m$	$SAIFI_W$
F1	0.061	0.112	0.074	0.248
F2	0.028	0.067	0.045	0.139
F3	0.061	0.113	0.075	0.249
F4	0.061	0.112	0.074	0.247
SYSTEM	0.061	0.112	0.075	0.248

Table 6.31 SAIDI, Case IV, (F_b = 80% and F_m = 40%)

Feeder	$P_n \times SAIDI^n$	$P_a \times SAIDI^a$	$P_m \times SAIDI^m$	$SAIDI_W$
F1	0.267	0.531	1.583	2.382
F2	0.109	0.502	1.622	2.234
F3	0.277	0.536	1.598	2.411
F4	0.267	0.517	1.535	2.319
SYSTEM	0.267	0.528	1.572	2.368

The SAIFI values calculated in this section compare with those of the preceding section, regardless of the variation in repair time. The case-to-case comparisons show that the variation in the percentage of failures assigned to bad weather or major adverse weather does not have any influence on the total SAIFI.

The ability to conduct repairs in a short period when failures occur in extreme weather has a very positive effect on SAIDI. The contributions due to extreme weather failures decrease proportionately as the repair time is reduced. This reduction is more pronounced when a large percentage of failures occur in major adverse weather than when the percentage of failures in this weather is small. In the former case, the major adverse weather contribution dominates the total effect while in the latter case the contribution of major adverse weather is relatively close to that of adverse weather.

6.5 Extreme weather severity analysis

The occurrence of major storms can vary from region to region and from year to year. Weather scientists claim that extreme weather conditions are becoming more frequent and severe. This section considers the impact of increases in the frequency of major adverse or extreme weather. It is assumed that the number of major storms varies from one event per year to three events per year. The case of a major adverse weather event occurring once a year was illustrated in the previous section. The following analysis is performed under the conditions that the major adverse weather occurs two and three times per year.

The line failure rates under the various weather conditions are held constant for the different frequencies of encountering major adverse weather. As an example, for a total average failure rate of 1.0 f/yr, the weather related failure rates for 40% of the line failures occurring in bad weather and 10% of the bad weather failures occurring in major adverse weather are as follows.

λ^n = 0.606 failures per year of normal weather

λ^a = 35.96 failures per year of adverse weather

λ^m = 350.88 failures per year of major adverse weather

The steady state probabilities of normal, adverse and major adverse weather are 0.989875, 0.010011 and 0.000114 respectively for major adverse weather occurring once a year. These probabilities change when the frequency of major adverse weather changes. The steady state probabilities of the three weather states are determined using the state space diagram shown in Figure 3.1 in Chapter 3 and the following weather transition rates:

$a_m = f_m/8760$ occ/hr $\qquad$ $n_m = f_m/8760$ occ/hr

$n_a = 1/195.54 - n_m$ occ/hr $\qquad$ $a_n = 1/2 - a_m$ occ/hr

$m_a = 1/2$ occ/hr $\qquad$ $m_n = 1/2$ occ/hr

The parameter f_m is the frequency of occurrence of major adverse weather. The normal weather average duration using the transition rates shown in Section 3.2 is 195.54 hours.

The resulting steady state probabilities for major adverse weather occurring two times per year are P_n = 0.989871, P_a = 0.009901 and P_m = 0.000228 and for three times per year are P_n = 0.989869, P_a = 0.009789 and P_m = 0.000342.

The two cases, designated as Case (a) and Case (b), are examined to investigate the impact of the variation in the frequency of extreme weather occurrence.

Case (a): 40% of failures occur in bad weather and 10% of bad weather failures in extreme weather

The load point indices are shown in Tables D.1-D.3 in Appendix D. The system indices SAIFI and SAIDI are presented in Tables 6.24-6.35.

- *Major adverse weather occurring two times per year*

Table 6.32 SAIFI, Case (a), (F_b = 40% and F_m = 10%), f_m = 2

Feeder	$P_n \times SAIFI^n$	$P_a \times SAIFI^a$	$P_m \times SAIFI^m$	$SAIFI_W$
F1	0.154	0.083	0.019	0.256
F2	0.084	0.050	0.011	0.145
F3	0.155	0.084	0.019	0.258
F4	0.154	0.083	0.019	0.256
SYSTEM	0.154	0.083	0.019	0.256

Table 6.33 SAIDI, Case (a), (F_b = 40% and F_m = 10%), f_m = 2

Feeder	$P_n \times SAIDI^n$	$P_a \times SAIDI^a$	$P_m \times SAIDI^m$	$SAIDI_W$
F1	0.515	0.395	0.781	1.690
F2	0.327	0.373	0.808	1.507
F3	0.525	0.398	0.788	1.711
F4	0.515	0.384	0.757	1.656
SYSTEM	0.515	0.392	0.775	1.683

- *Major adverse weather occurring three times per year*

Table 6.34 SAIFI, Case (a), (F_b = 40% and F_m = 10%), f_m = 3

Feeder	$P_n \times SAIFI^n$	$P_a \times SAIFI^a$	$P_m \times SAIFI^m$	$SAIFI_W$
F1	0.154	0.082	0.028	0.265
F2	0.084	0.049	0.017	0.150
F3	0.155	0.083	0.028	0.266
F4	0.154	0.082	0.028	0.264
SYSTEM	0.154	0.082	0.028	0.265

Table 6.35 SAIDI, Case (a), (F_b = 40% and F_m = 10%), f_m = 3

Feeder	$P_n \times SAIDI^n$	$P_a \times SAIDI^a$	$P_m \times SAIDI^m$	$SAIDI_W$
F1	0.515	0.390	1.172	2.076
F2	0.327	0.368	1.212	1.907
F3	0.525	0.394	1.182	2.100
F4	0.515	0.380	1.135	2.030
SYSTEM	0.515	0.388	1.163	2.066

It can be seen from Tables 6.32-6.35 that both the SAIFI and SAIDI increase when extreme weather hits the system more frequently and that the increase is basically due to the increase in the index segment associated with extreme weather.

The effect on the failure rate is illustrated in Figure 6.6. The label 'Fr' represents the frequency of extreme weather occurrence.

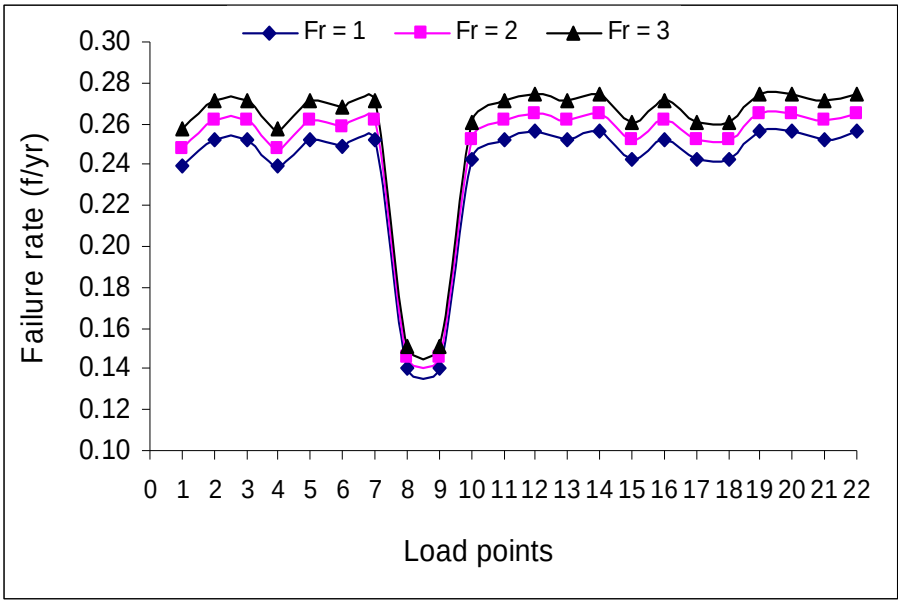

Figure 6.6 Load point failure rates, Case (a)

Case (b): 80% of failures occur in bad weather and 40% of bad weather failures in extreme weather

Tables D.1-D.3 in Appendix D show the load point indices in Case (b). The system indices SAIFI and SAIDI are shown in Table 6.36-6.39. The system indices increase more in Case (b) than in Case (a) when the frequency increases. This relatively large increase arises due to the fact that the contribution of extreme weather increases considerably when more failures occur during extreme weather.

The failure rate is shown graphically in Figure 6.7. This figure, when compared with Figure 6.5, clearly illustrates that the increase in failure rate with the frequency of extreme weather in Case (b) is larger than that in Case (a).

- *Major adverse weather occurring two times per year*

Table 6.36 SAIFI, Case (b), (F_b = 80% and F_m = 40%), f_m = 2

Feeder	$P_n \times SAIFI^n$	$P_a \times SAIFI^a$	$P_m \times SAIFI^m$	$SAIFI_W$
F1	0.061	0.111	0.149	0.321
F2	0.028	0.066	0.089	0.183
F3	0.061	0.112	0.150	0.323
F4	0.061	0.110	0.148	0.320
SYSTEM	0.061	0.111	0.149	0.321

Table 6.37 SAIDI, Case (b), (F_b = 80% and F_m = 40%), f_m = 2

Feeder	$P_n \times SAIDI^n$	$P_a \times SAIDI^a$	$P_m \times SAIDI^m$	$SAIDI_W$
F1	0.267	0.525	6.246	7.039
F2	0.109	0.497	6.465	7.071
F3	0.277	0.530	6.302	7.110
F4	0.267	0.512	6.050	6.829
SYSTEM	0.267	0.522	6.201	6.990

- *Major adverse weather occurring three times per year*

Table 6.38 SAIFI, Case (b), (F_b = 80% and F_m = 40%), f_m = 3

Feeder	$P_n \times SAIFI^n$	$P_a \times SAIFI^a$	$P_m \times SAIFI^m$	$SAIFI_W$
F1	0.061	0.110	0.223	0.394
F2	0.028	0.066	0.134	0.227
F3	0.061	0.110	0.225	0.397
F4	0.061	0.109	0.223	0.393
SYSTEM	0.061	0.110	0.224	0.395

Table 6.39 SAIDI, Case (b), (F_b = 80% and F_m = 40%), f_m = 3

Feeder	$P_n \times SAIDI^n$	$P_a \times SAIDI^a$	$P_m \times SAIDI^m$	$SAIDI_W$
F1	0.267	0.519	9.369	10.156
F2	0.109	0.491	9.697	10.297
F3	0.277	0.524	9.454	10.255
F4	0.267	0.506	9.075	9.848
SYSTEM	0.267	0.516	9.301	10.085

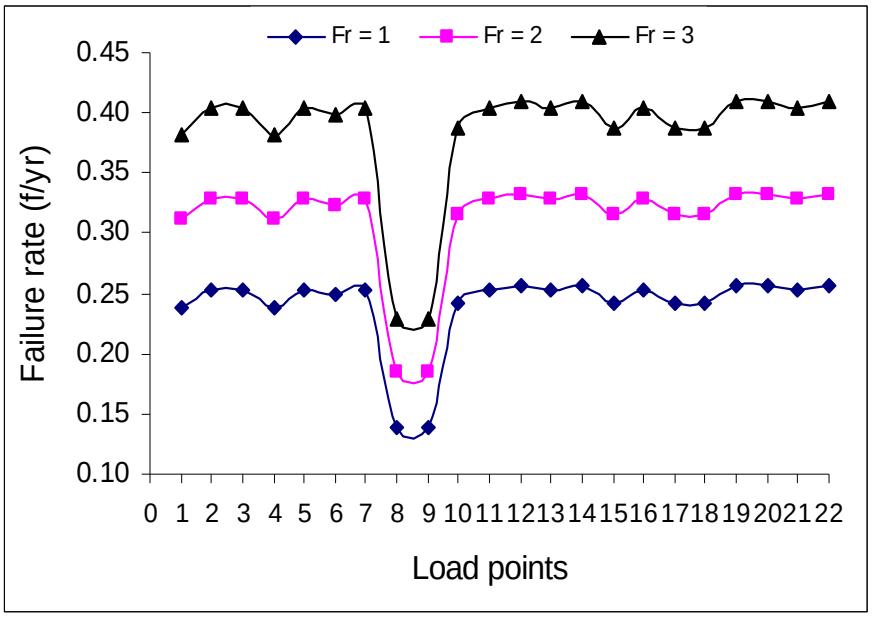

Figure 6.7 Load point failure rates, Case (b)

The load point unavailabilities and average outage durations for both Cases (a) and (b) are shown in Figure 6.8 and Figure 6.9 respectively.

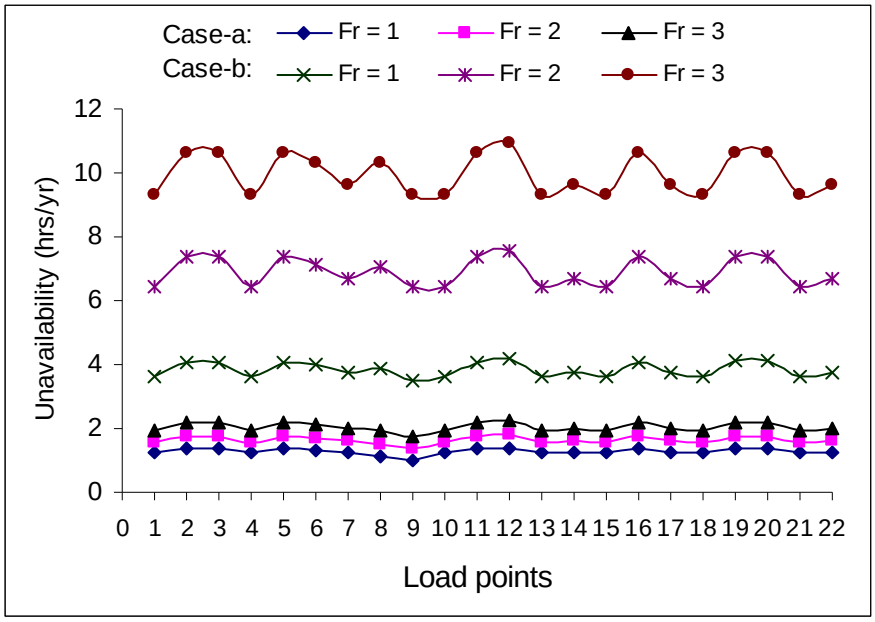

Figure 6.8 Load point unavailabilities, Case (a) and Case (b)

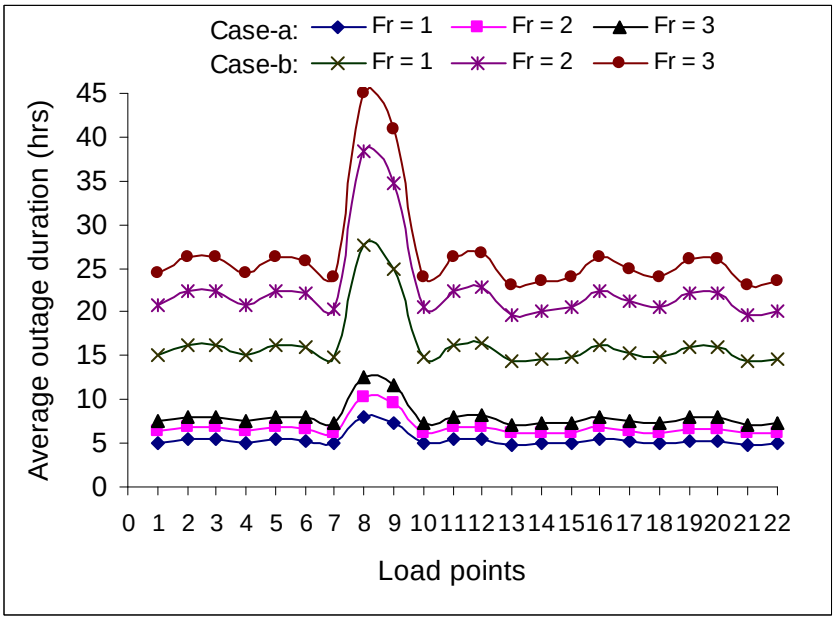

Figure 6.9 Load point average outage durations, Case (a) and Case (b)

It is clear from Figures 6.8-6.9 that the influence on the unavailability and the average outage duration as a result of an increasing number of extreme weather events is significant. The impact increases further when the percentage of failures in extreme weather increases. The unavailabilities and average outage durations in Case (b) increase more rapidly than in Case (a) when extreme weather occurs more frequently.

6.6 Failure bunching analysis of radial feeders

Although many distribution systems are designed and constructed as loop or mesh circuits, they are operated as single radial feeders using normally open points. As noted earlier, a normally open point basically reduces the amount of component exposed to failure. In the event of a system failure, a normally open point can be closed and another opened in order to minimize the total disconnected load. Most studies do not consider the overlapping failure of two radial feeders based on the reasoning that the likelihood of multiple failures is negligible. This may not be the case when a severe storm occurs, as a storm can impact two or more radial feeders in the same area. The storm can create failure bunching of the radial feeders. Under these conditions, no alternative supply will be available and service restoration will involve repair rather than switching actions.

In order to illustrate the failure bunching of two radial feeders, consider the system shown in Figure 6.10. The system has been simplified to make the problem amenable by avoiding a large possible combination of failure events and therefore there are no sectionalizing points on the feeder. The lateral distributors and transformers are not included in this analysis. The attention in this study is on failure bunching of multiple feeders. In Figure 6.10, when both Feeder 3 and Feeder 4 are on outage, the entire system experiences failure. This is a second order failure event and can be considered as a second order mincut. The system shown in Figure 6.11 is used to investigate failure bunching of three feeders. The basic reliability data for the feeders are shown in Table 6.40.

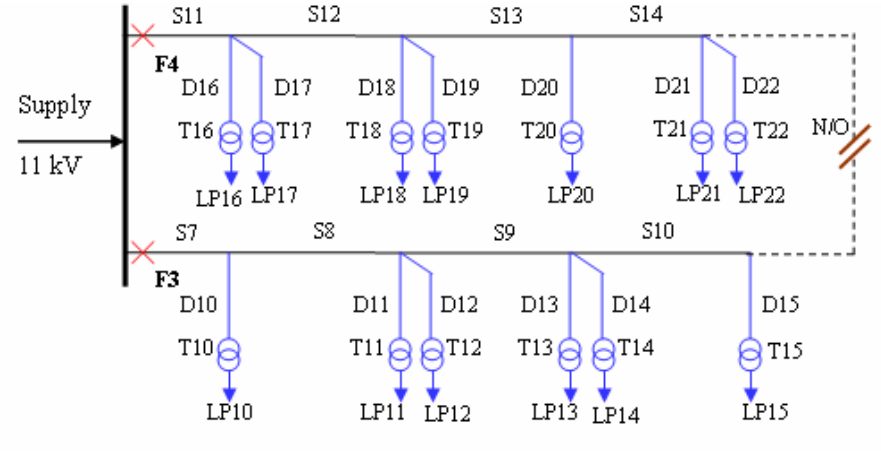

Figure 6.10 Distribution system with two feeders

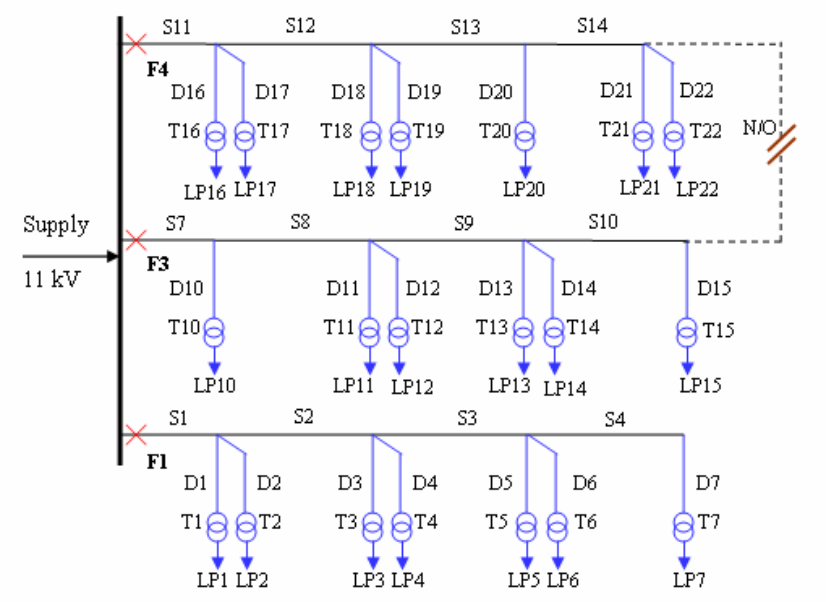

Figure 6.11 Distribution system with three feeders

Table 6.40 Basic feeder reliability data

Feeder	Length (km)	Average failure rate (f/yr)	Average repair time (hrs)
F1	2.85	0.18525	5
F3	2.90	0.18850	5
F4	2.90	0.18850	5

The Markov approach described in Section 3.4 and Section 3.5 can be used to determine the basic reliability indices of the second order mincut (Figure 6.10) and the third order mincut (Figure 6.11), respectively. Repair is conducted only in normal weather.

The overlapping failure of both primary circuits will impact all the load points on Feeder 3 and Feeder 4 in Figure 3.10. The load point failure rates are therefore equal. The SAIFI can be deduced from Equation 6.2a. Since the load point failure rate (λ) in Equation 6.2a is equal for each load point, the SAIFI is equal to the load point failure rate. The SAIDI is determined using Equation 6.2b and is equal to the unavailability.

Table 6.41 shows the reliability indices for coincident failures of the radial feeders. The two cases of 40% and 80% of failures occurring in bad weather are considered. The percentage of bad weather failures occurring in major adverse weather is held at 40%.

Table 6.41 Reliability indices for the second order and the third order failures

Reliability indices	System in Figure 6.10		System in Figure 6.11	
	F_b = 40% F_m = 40%	F_b = 80% F_m = 40%	F_b = 40% F_m = 40%	F_b = 80% F_m = 40%
Failure rate (f/yr)	0.00183	0.0066	0.00014	0.00094
Unavailability(hrs/yr)	0.00820	0.0300	0.00514	0.00348
Outage duration (hrs)	4.48	4.54	3.67	3.70
SAIFI (int/cust-yr)	0.00183	0.0066	0.00014	0.00094
SAIDI (hrs/cust-yr)	0.00820	0.0300	0.00514	0.00348

The results shown in Table 6.41 indicate that the concurrent failure of multiple feeders is relatively rare and its expected contribution to the average reliability indices over a long period is small. It should be appreciated, however, that when the actual event does occur it will have a major impact on the system indices during that year. The method applied in this study has some limitations as it deals with probability and expected values. It does not provide a simulation of actual outage events. Other rigorous methods such as sequential Monte Carlo simulation can be used if this information is desired.

6.7 Summary

This chapter introduces an approach to divide the overall reliability index into segments relevant to the weather conditions. The approach is illustrated using a practical distribution configuration representing an urban system. A series of case studies are performed to examine the effect of failures that occur in bad weather. This chapter also illustrates how reliability is affected when repair can be performed in a relatively short period following a major storm. Sensitivity studies are conducted to quantify the implication of more frequently occurring extreme weather conditions and a failure bunching effect analysis of multiple radial feeders is presented.

The numerical results show that the major portion of the system indices comes from the bad weather failures. The load point failure rates are immune to variations in the percentages of failures occurring in bad weather. The load point unavailabilites and average outage durations, however, are directly influenced. The SAIFI therefore remains constant but the SAIDI is largely affected. Sensitivity analysis shows that the major adverse weather contribution increases significantly when a majority of failures are attributed to major adverse weather.

The reduction in repair time following the system damage caused by storms has a positive impact on the SAIDI. The SAIFI, however, does not change. On the other hand, the variation in the frequency of major adverse weather significantly impacts both SAIFI and SAIDI. Extreme weather events occur relatively infrequently but when they do occur, they can have a big impact on the system reliability indices as the likelihood of multiple feeder failures increases significantly.

The weather specific reliability evaluation procedure described in this chapter gives considerably more information than is provided by a single aggregated index. This knowledge can be useful in deducing those areas in which investment may provide the greatest reliability improvement.

Chapter 7

MAJOR EVENT DAY ANALYSIS

7.1 Introduction

Electric power systems are designed to withstand a certain level of stress. They cannot, however, be constructed to resist excessive physical disturbances. It is not feasible for utilities to build power systems that provide their customers with reliable and economical power under all possible conditions. The system reliability should reflect the ability of the system to meet the stress levels for which it was planned, designed, maintained and operated. Electric utilities have significant control over internal causes such as switching procedures, maintenance schedules, etc., but their control over external factors is limited. Severe weather conditions such as high winds, extreme precipitation, hurricanes, etc., often exceed the system design and operational limits. The occurrence of these events significantly affects the overall performance of a power system.

The utilization of a range of reliability indices to measure the performance of a utility is a common practice throughout the world. Many utilities use reliability indices to track the performance of a utility, region or a part of a circuit. Reliability indices are also used for quantitative comparison of the performance between various utilities. The regulatory trend appears to be moving to performance-based rates, where performance is rewarded or penalized based on service continuity quantified by reliability indices. In the modern electricity market, customers have options to purchase electricity from their suppliers. Some commercial and industrial customers ask utilities for their reliability indices before locating a facility within the utility's service territory.

In some circumstances, external interferences significantly impact the daily operational ability of a utility and the reliability indices increase dramatically. The extraordinary days in which such events occur are generally referred to as “major event days” [19]. It is important that utilities evaluate their actual performance for normal day operations that exclude the significant abnormal days. This policy seems to favour the utility and some people believe that if utilities are allowed to exclude major events, the utility may diminish its ability to assure reliable service. The argument of whether or not utilities should be permitted to exclude major events is not within the scope of this research. The attention in this chapter is on major event day identification.

There is no completely uniform method that is equitable to all utilities for separating a particular abnormal event from normal day operations. In the past, relatively simple methods have been used to define a major event day [19]. An IEEE Working Group has recently [19] developed a statistically based approach called the “Beta Method” based on using the log-normal distribution. This chapter briefly discusses the traditional and the new statistical ways to classify a major event. A wide range of possible reliability distributions are presented for randomly generated data samples. The histograms and corresponding correlation between utility performance data and lognormal distributions are examined.

7.2 Major Event Day classification

As noted earlier, there are two general approaches to classify a major event, or major event day. These approaches are described in the following sections.

7.2.1 Traditional approach

A major event was classified in IEEE Standard 1366-1998 [24] as follows:

"Designates a catastrophic event which exceeds reasonable design or operational limits of the electric power system and during which at least 10% of the customers within an operational area experience a sustained interruption during a 24-hour period".

The magnitude of physical destruction and the number of customers on outage depends largely on the intensity of the disastrous events and the service territory. Storms, hurricanes, earthquakes, etc. are intuitively declared as disasters. There are no physical measures that permit a comparison of the severity associated with a catastrophic event with the system design and operational limits. No two ice storms are the same; no two hurricanes are the same; nor are two earthquakes. The "outage of 10% of the customers" criterion is easy to understand, but the number of customers interrupted can vary widely due to the utility service area. For instance, a storm striking an area causes relatively fewer customers on outage in a rural distribution system than in an urban distribution system. The traditional classification of a major event is therefore inconsistent when applied to distribution utilities with different sizes and operating in various geographic areas.

7.2.2 New statistical approach

A statistically based approach designated as the "Beta Method" has been developed by the IEEE Working Group on System Design. This approach is anticipated to be fair to all utilities regardless of their size, and facilitates removal of abnormal events from normal days [25]. The blanket assumption made in creating the Beta Method is that the natural logarithm of the daily reliability index, preferably the SAIDI, is normally distributed.

The following is the basic procedure used to segment the major event days in the Beta Method [25]:

- Sort the SAIDI/day in descending order
- Calculate the natural log of each value, ignore zero values if any
- Evaluate the mean (α) and standard deviation (β) of the log values

- Determine the threshold using Equation 7.1

$$T_{MED} = e^{\alpha+2.5\beta} \tag{7.1}$$

- Each day which exceeds the threshold is designated as a Major Event Day

The total SAIDI after removing the major event days represents the SAIDI over only the period of normal days. This index should be adjusted to account for the disregarded days. Theoretically, a major event day that is omitted would have had an average normal index if the major event had not occurred. Equation 7.2 [26], can be used to determine the adjusted SAIDI.

$$SAIDI_{adj} = \frac{D_{Total}}{D_{Total} - D_{MED}} SAIDI_{raw} \tag{7.2}$$

where,

$SAIDI_{adj}$ = adjusted index

$SAIDI_{raw}$ = the index over the period omitting the major events

D_{Total} = the total days including major event days (days)

D_{MED} = the major event days over the reporting period (days)

The beta methodology has been approved in IEEE Standard 1366-2003 and many utilities are implementing it. There are, however, two major problems in regard to approximating the index (SAIDI) by a log normal distribution. If the reliability index is not really log normally distributed, the process will be inconsistent. The lognormal distribution also does not account for the days which experience no interruptions because the natural log of zero is undefined. This will distort the reliability distribution. It has been reported by a number of small utilities that they have a significantly large number of days without any outages [25]. The IEEE Working Group has proposed several alternatives to address this problem, but there is no unique conclusion as yet.

The applicability of the lognormal distribution is examined in the following studies.

7.3 Reliability distributions

As discussed in the previous section, the Beta Method depends entirely on the log normality of the reliability index. Recent research shows that reliability indices can have a wide variety of distributions [27]. The reliability distributions differ due to topological changes, operational policies, maintenance practices and sizes of systems. For instance, rural and urban electric distribution systems can have quite different reliability index distributions, including normal, log-normal, exponential, etc.

The focus in this section is on the possible shapes of reliability index distributions. A range of probability distributions including lognormal, and Weibull distributions with different shape and scale parameters are illustrated. The resulting distributions when Weibull samples are subjected to a natural logarithm transformation are displayed.

7.3.1 The lognormal distribution

The lognormal distribution is an important tool in reliability studies. A random variable X is said to be log-normally distributed if ln$X$ is normally distributed. The probability density function of the lognormal distribution can be defined by Equation 7.3 [17].

$$f(x) = \frac{1}{X\beta\sqrt{2\pi}} Exp\left[-\frac{(\ln X - \alpha)^2}{2\beta^2}\right] \tag{7.3}$$

where, $X > 0$

β = standard deviation of ln$X$

α = mean of ln$X$

One million log-normally distributed samples were randomly generated using the *MATLAB* function $lognrnd(\mu,\sigma,V)$, where, μ and σ are the mean and standard deviation of the random variable X, respectively, and V is the row vector. The resulting relative frequency distribution is shown in Figure 7.1. The number of bins is considered

to be equal to the nearest integer of the square root of the number of samples [28]. The distribution of the natural log of the log-normal samples is shown in Figure 7.2.

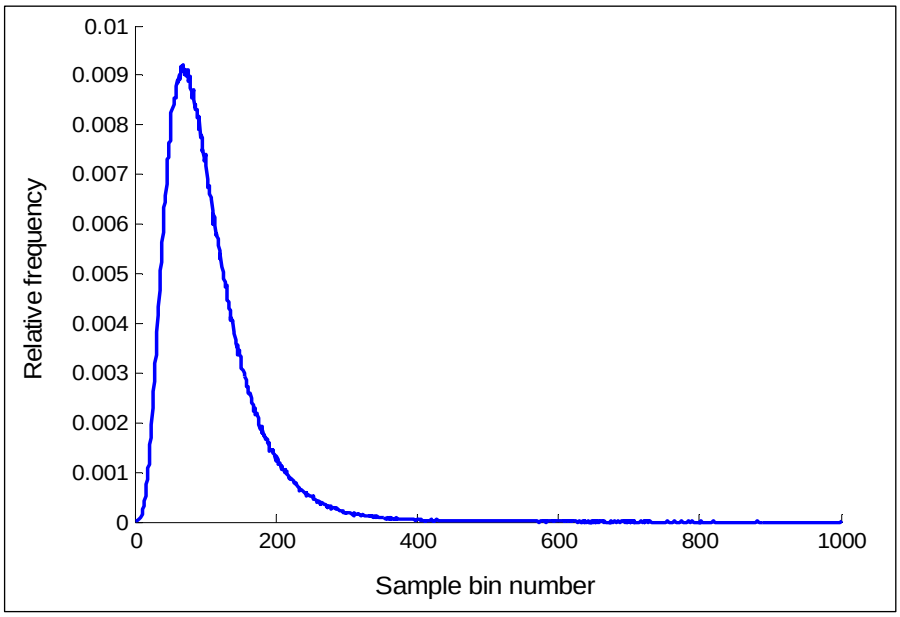

Figure 7.1 A typical lognormal distribution

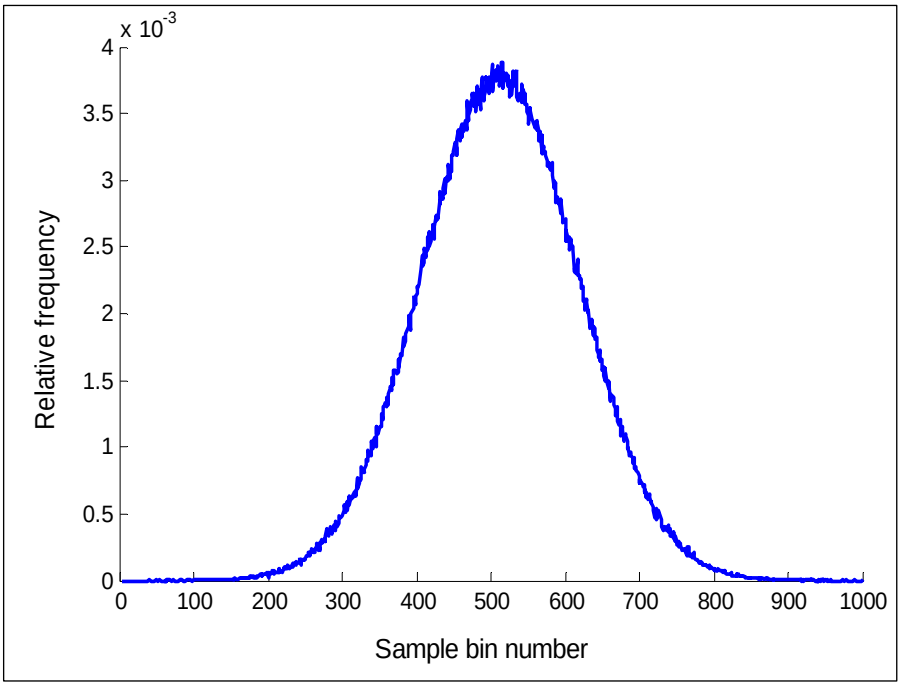

Figure 7.2 Distribution of the natural-log of the lognormal samples

It can be seen from Figure 7.2 that the distribution is a good fit to the normal distribution. This process was used to examine other possible reliability index distributions.

7.3.2 The Weibull distribution

The Weibull distribution is an important distribution in general statistical analysis and reliability evaluation due to its flexible nature. It has one very special feature; the distribution has no fixed shape. The shape is characterised by the values of the parameters in the function. The general Weibull probability density function is given by Equation 7.4 [17].

$$f(x) = \frac{\gamma}{\omega}\left(\frac{x-\mu}{\omega}\right)^{\gamma-1} Exp\left[-\left(\frac{x-\mu}{\omega}\right)^{\gamma}\right] \qquad (7.4)$$

where,

$x \geq \mu$

$\gamma, \alpha > 0$

γ = shape parameter

μ = location parameter

ω = scale parameter

The resulting distribution when $\mu = 0$ and $\omega = 1$ is known as the standard Weibull distribution, and the case where $\mu = 0$ is called the two parameter Weibull distribution.

The *MATLAB* function $wblrnd(\omega, \gamma, V)$ can be used to produce the Weibull random samples. The parameter V is the row vector of random numbers. Table 7.1 presents the basic parameter values associated with one million randomly generated samples.

Table 7.1 Parameter values for the random samples

Statistic	γ = 0.5	γ = 1.0	γ = 1.5	γ = 2.0	γ = 3.0
Sample mean	0.502109	0.500053	0.496362	0.496523	0.517766
Standard deviation	1.129639	0.49934	0.337376	0.259152	0.188028
Minimum value	0	0	0.00003	0.00064	0.0059
Maximum value	46.34944	6.74502	3.11945	2.05546	1.38162
Log mean, α	-2.53959	-1.26993	-0.98354	-0.86742	-0.73719
Log standard dev., β	2.56792	1.28243	0.85635	0.63994	0.42654

Figure 7.3 shows the probability distributions for various shape parameters (γ). The number of bins is the closest integer of the square root of the number of samples. The distributions of the natural-log of the same samples are displayed in Figure 7.4. The shapes of the distributions are similar to that of the standard normal distribution, but are not completely symmetrical. This is illustrated by comparing the cumulative probabilities of each distribution with that of the standard normal distribution.

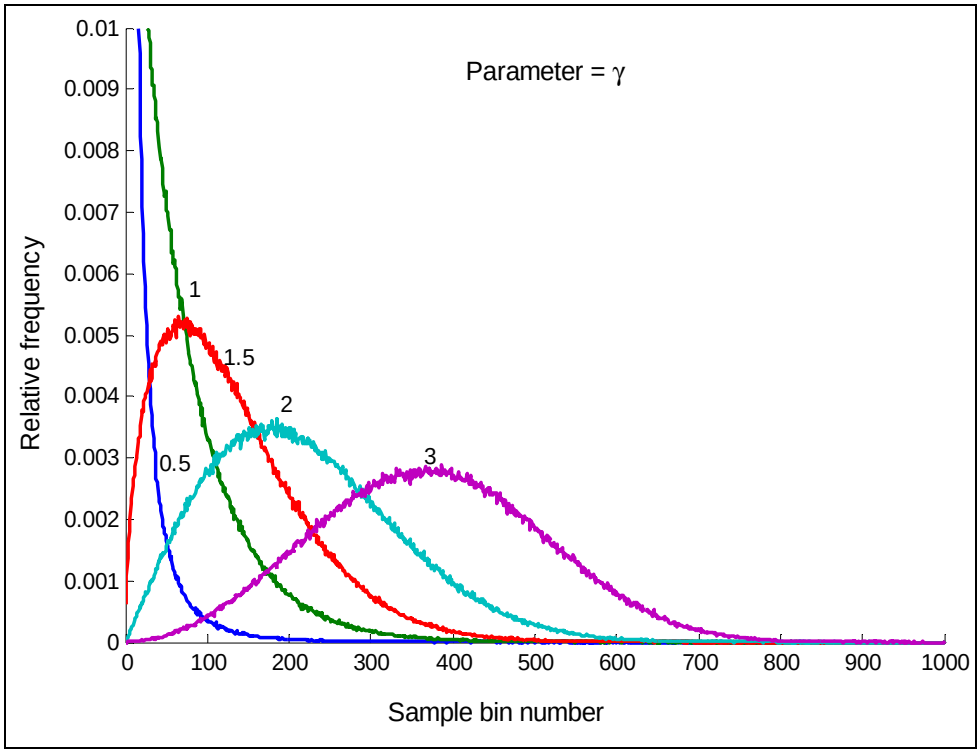

Figure 7.3 Distribution of the Weibull samples

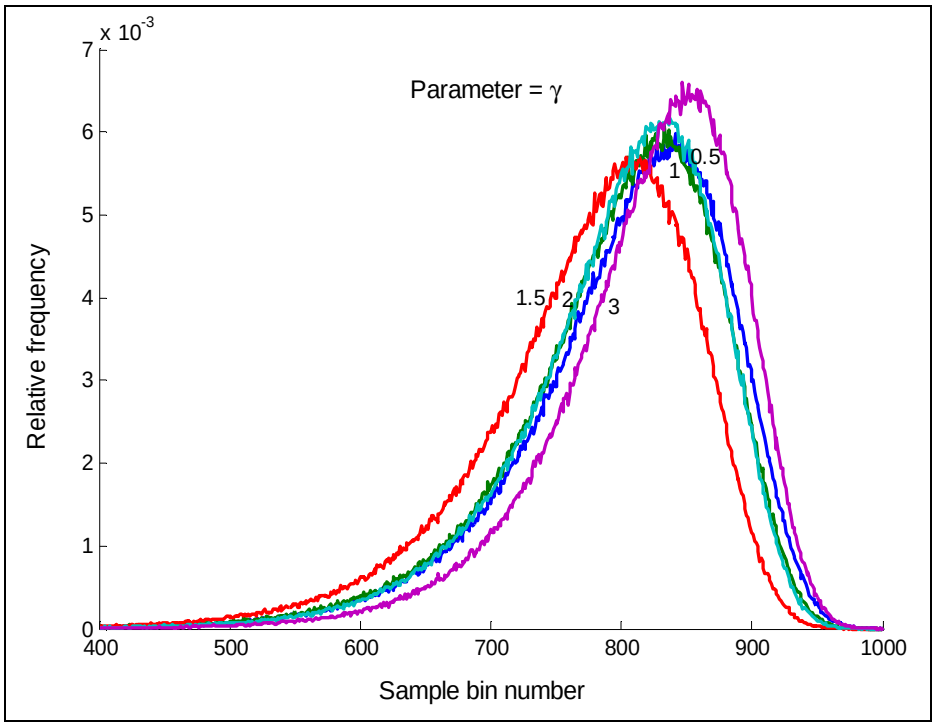

Figure 7.4 Distribution of natural-log of the Weibull samples

Table 7.2 shows the respective cumulative probability values associated with each distribution shown in Figure 7.4. The parameters μ and σ given in the first column refer to the mean and standard deviation of the corresponding distributions. Table 7.2 shows that the probability of a value exceeding a specified level i.e. $\mu + 0.5\sigma$, is different for each distribution and that all the Weibull generated values are different from the normally distributed values.

Table 7.2 Comparison of the cumulative probabilities for the different distributions

Sample value being greater than	Standard normal distribution	Weibull data distributions				
		γ = 0.5	γ = 1.0	γ = 1.5	γ = 2.0	γ = 3.0
$\mu + 0.0\sigma$	0.5000	0.5702	0.5703	0.5704	0.5706	0.5706
$\mu + 0.5\sigma$	0.3085	0.3442	0.3445	0.3440	0.3446	0.3444
$\mu + 1.0\sigma$	0.1587	0.1324	0.1323	0.1322	0.1324	0.1321
$\mu + 1.5\sigma$	0.0668	0.0214	0.0213	0.0212	0.0215	0.0216
$\mu + 2.0\sigma$	0.0227	0.0007	0.0007	0.0007	0.0007	0.0007
$\mu + 2.5\sigma$	0.0062	0.0000	0.0000	0.0000	0.0000	0.0000

Table 7.3 shows the number of standard deviations that yield the same probability value for all the associated distributions. This factor has the same meaning as the β coefficient in Equation 7.1.

Table 7.3 Number of standard deviation from the mean of the respective distribution

Multiplier of the standard deviation for a normal distribution	Probability from the normal distribution	Multiplying factor for the other distributions				
		γ = 0.5	γ = 1.0	γ = 1.5	γ = 2.0	γ = 3.0
0.0	0.5000	0.1631	0.1644	0.1645	0.1650	0.1648
0.5	0.3085	0.5776	0.5767	0.5762	0.5765	0.5763
1.0	0.1587	0.9267	0.9264	0.9267	0.9266	0.9255
1.5	0.0668	1.2261	1.2259	1.2258	1.2260	1.2262
2.0	0.0228	1.4887	1.4872	1.4892	1.4863	1.4864
2.5	0.0062	1.7200	1.7248	1.7169	1.7180	1.7210

The coefficients given in the first column give the probabilities in the second column for the pure normal distribution. The remaining columns show the multiplying factors, or the coefficients of β, in order to provide the same probability.

The results shown in Table 7.3 indicate that the utilization of the same multiplying factor for different kinds of distributions will result in different numbers of major event days. In other words, the number of segmented major event days will be more in the case of a normal distribution than for the rest of the distributions if the same β coefficient is implemented. In conclusion, the beta methodology will allot different numbers of major event days for utilities operating under the same conditions but having different performance index distributions.

7.4 Utility performance index distributions

The probability plot method can be used to provide a visual inspection as to whether a given random variable belongs to a particular distribution. The normal probability plot of the natural-log of the reliability index provides the visual indication for the fitness of

the data to the log normal distribution. If the log values do come from the normal distribution, the plot will appear linear.

The following analysis examines the data for an unknown utility over different numbers of years [29]. The histograms and the corresponding probability plots are presented. The number of bins in the following analyses is approximately the square root of the sample size. Figure 7.5 shows the histogram of the one year (1998) of data and its probability plot is shown in Figure 7.6. Figures 7.7-7.8 show the histogram and probability plot for two years of data respectively. The histograms for three years (1998-2000), four years (unknown) and seven years (1995-2001) of data are shown in Figures 7.9, 7.11 and 7.13, respectively. Their respective probability plots are illustrated in Figures 7.10, 7.12 and 7.14.

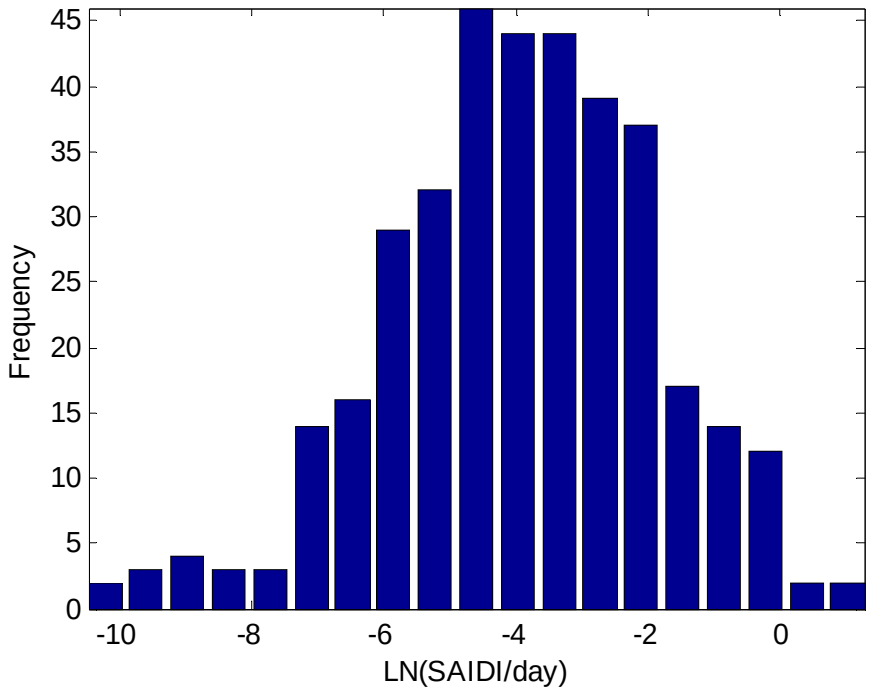

Figure 7.5 Histogram of one year data

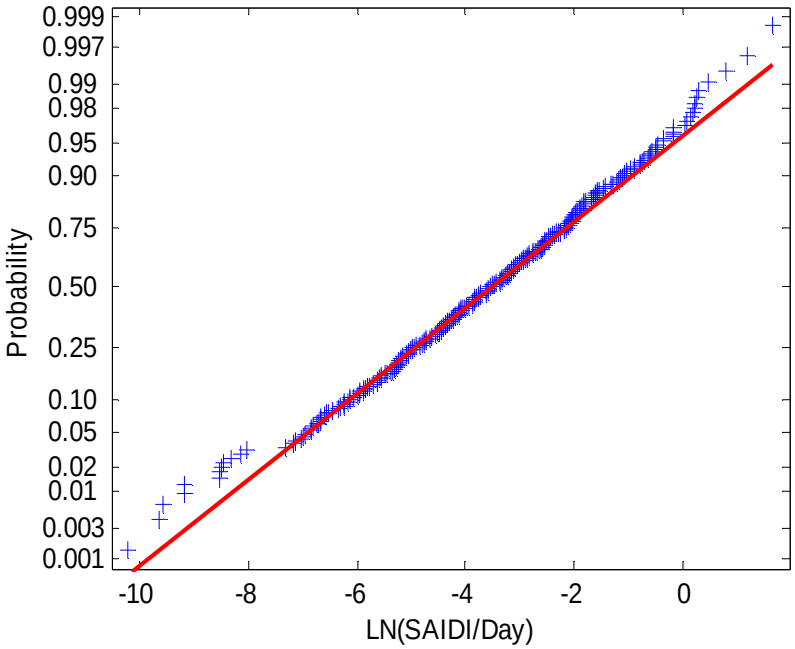

Figure 7.6 Normal probability plot of one year data

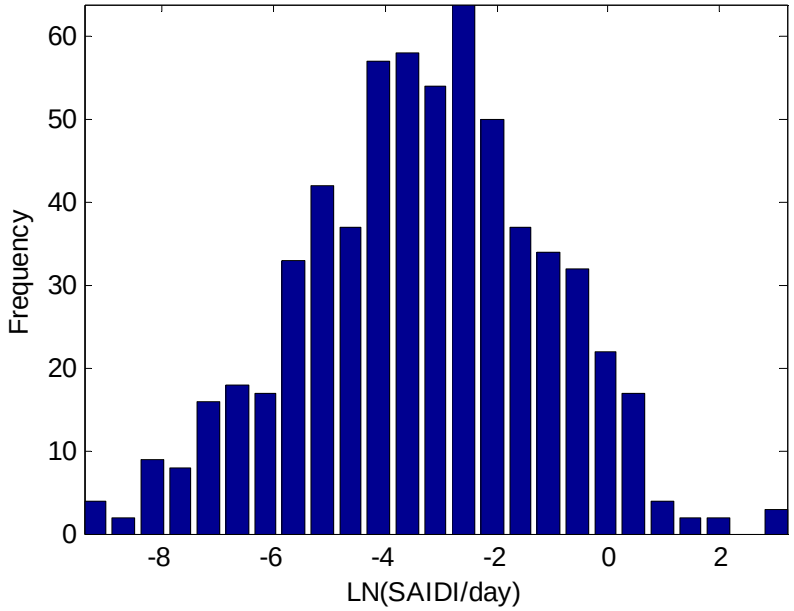

Figure 7.7 Histogram of two year data

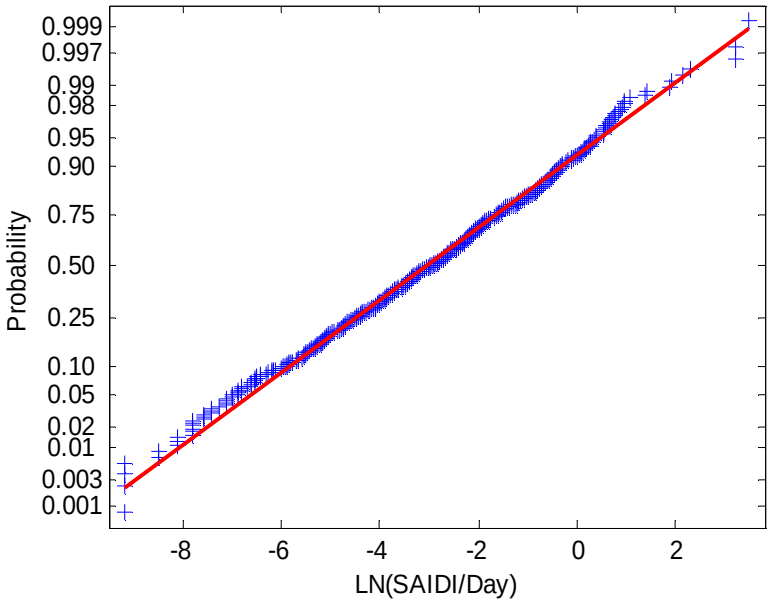

Figure 7.8 Normal probability plot of two year data

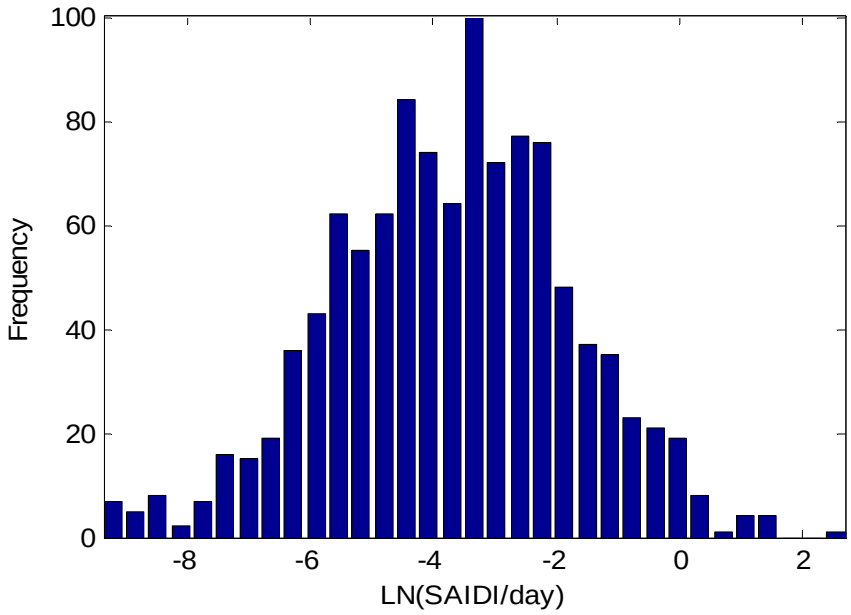

Figure 7.9 Histogram of three year data

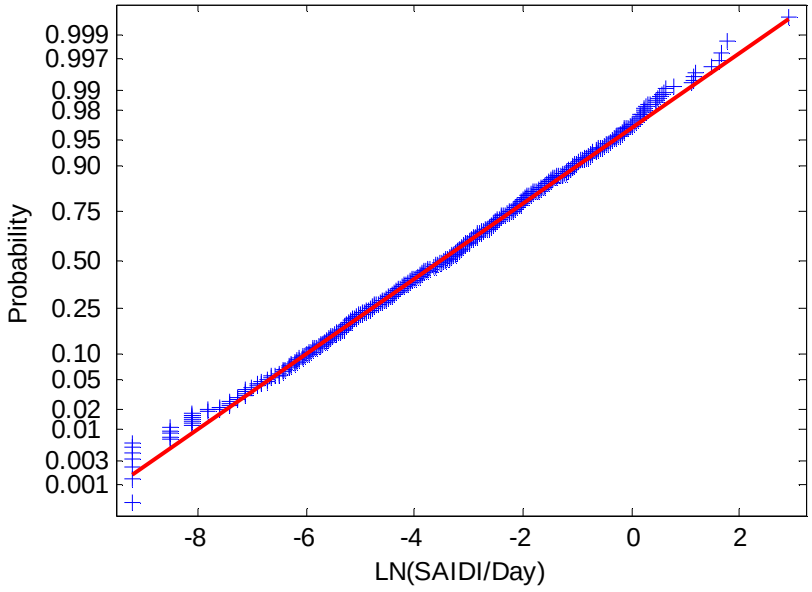

Figure 7.10 Normal probability plot of three year data

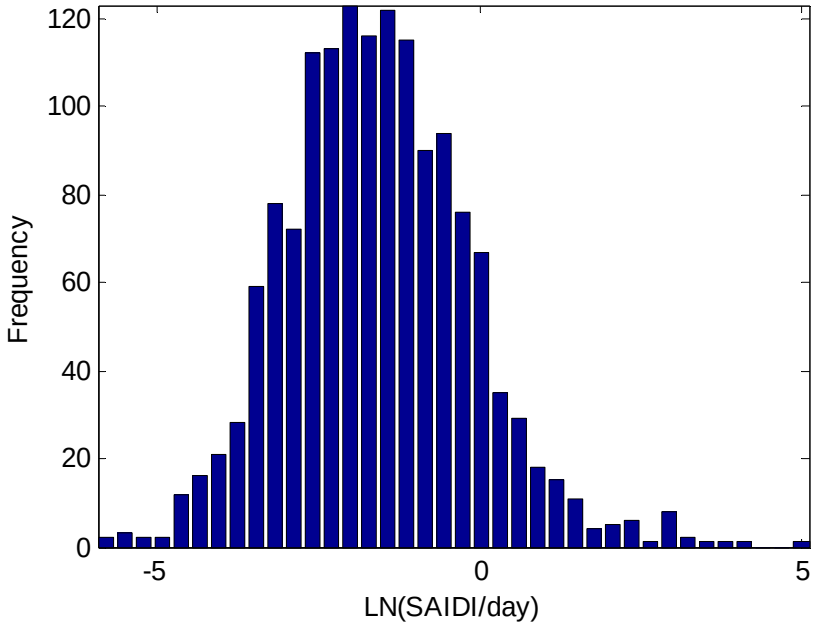

Figure 7.11 Histogram of four year data

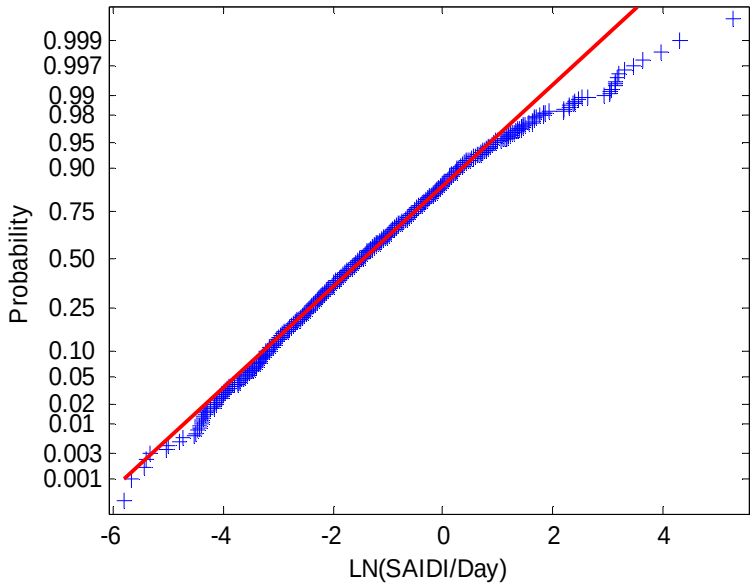

Figure 7.12 Normal probability plot of four year data

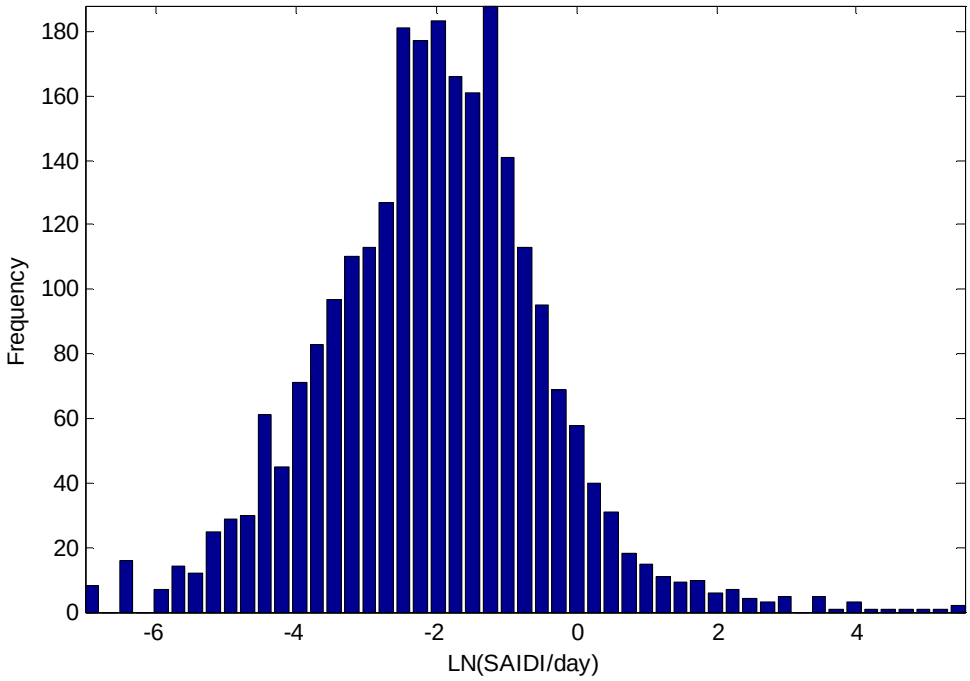

Figure 7.13 Histogram of seven year data

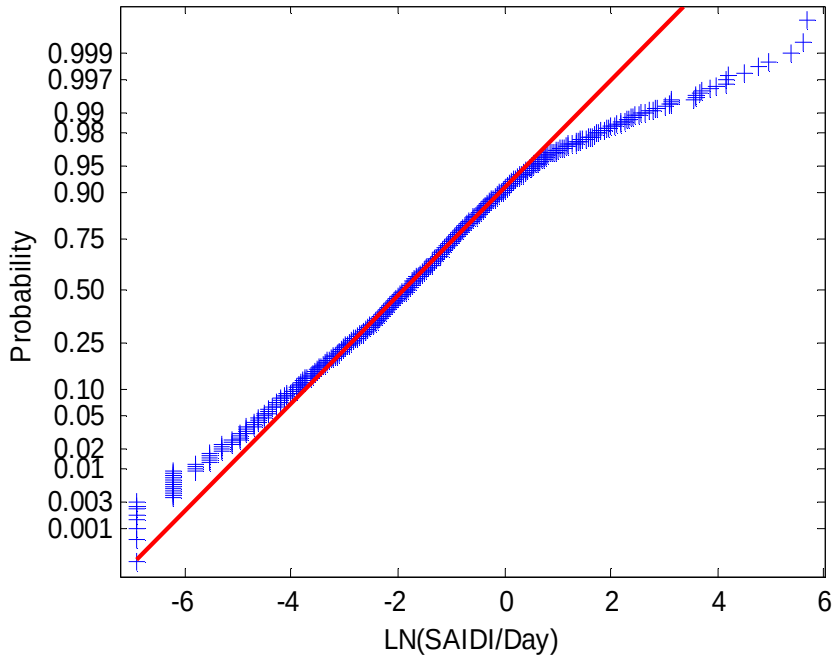

Figure 7.14 Normal probability plot of seven year data

It can be seen from the displays on the preceding pages that the distribution shapes are dissimilar for different amounts of data used. For example, the histogram in Figure 7.5 obtained for one year of data shows a scooped left tail and a relatively short right tail whereas Figure 7.11 shows a comparatively peaky histogram with a relatively long tail to the right, when four years of data is employed. It is clear from the displays that the right tail tends to be longer when more data are used in the analysis.

Normal probability plots in conjunction with histograms can be used to examine the historical data. Figure 7.6 illustrates that a large number of observations fall in the linear zone, but the data on the two extreme ends depart from the extrapolated line. It is clear from Figures 7.8 and 7.10 that the highest values of the given samples reasonably reside in a straight line. This indicates the upper end extreme values fit a log normal distribution. There are, however, some outliers associated with the left tail of these histograms. This is not the case with the plot of the four year data shown in Figure 7.12.

The upper end extreme values of the given samples do not reasonably fit a lognormal distribution. This is even more pronounced in Figure 7.14 for the seven year data. It is important to appreciate that decisions regarding major event day determination are based on the probabilities associated with the tail of the assumed distribution.

The analysis shows that the shape of the distribution is sensitive to the number of years during which the performance data is collected. It appears from the data set that the reliability index can be represented by a log normal distribution in some cases but not in others. In some cases, the transformed histogram of the performance data differs significantly from a normal distribution. The peak values, which are the candidate major event days, do not satisfy the log normal distribution and in this case the log normal distribution may not be a valid representation of the reliability index. As a consequence, a major day will be classified improperly. The study of a relatively small amount of historical data from one utility, however, makes it difficult to reach specific conclusions regarding the inconsistencies that may exist between utilities of different sizes, in various environments and with dissimilar operating philosophies.

7.5 Summary

Exceptional abnormal events that cause a significantly large number of customers on outage for an extended time are generally categorised as major events. Some of the reliability data reported to regulators by electric power utilities exclude storm or major event interruptions. Major events considerably impact the reliability indices. Many regulators allow exclusions based on the reasoning that the capability of a utility during storms does not reflect the true everyday performance. There is, however, no specific boundary value which segments a major event day from the normal days.

This chapter describes approaches for segmenting major event days. The recently published statistically based “Beta Method” and the more traditional classification for the definition of a major event day are briefly reviewed. A series of reliability

distributions including the lognormal distribution and a number of Weibull distributions with varying shape parameters are observed. The differences in shape are illustrated using the cumulative probability values of the distribution function. This chapter graphically presents some performance data, in the form of SAIDI/day, for an unknown utility and illustrates the inconsistency associated with the automatic assumption that the reliability index is log-normally distributed.

The analysis of different candidate reliability distributions shows that the variations in the shapes of distributions affect the resulting probabilities of a major event days. This can create inconsistencies between utility applications when the same metric is enforced. The study of normal probability plots reveal that the lognormal distribution does not always provide the best representation of the reliability performance index.

Chapter 8

SUMMARY AND CONCLUSIONS

Electric power delivery systems usually exist in open weather environments. The weather creates varying degrees of physical stresses on the system elements, sometimes to the extent that the stress exceeds the system design and operational limits. The failure rate of a component is greatly enhanced by bad weather situations. The likelihood of multiple line failures is much higher in bad weather than in normal weather. The phenomenon of coincident failures of two or more circuits as a result of excessive stress imposed by weather conditions is designated as failure bunching. The reliability of electrical transmission or distribution systems is normally improved by parallel operation of lines and therefore multiple circuit failures severely deteriorate the system reliability. As noted in Chapter 1, problems that arise in distribution systems are responsible for most customer interruptions and a large number of supply outages occur during unfavourable weather situations.

The research described in this thesis is focused on weather modeling in the reliability evaluation of parallel redundant systems. A series of weather models are developed and used to illustrate the impacts on the predicted reliability indices. An approach to divide the reliability indices into normal, adverse and extreme weather conditions is introduced and illustrated using a practical distribution system. The methods associated with classifying extraordinary events that can have immense impacts on the overall system performance are discussed.

The fundamental concepts of weather modeling in reliability evaluation of transmission and distribution systems are introduced in Chapter 2 where the weather environment is divided into the two states of normal and adverse weather. The application of the two state weather model is illustrated using two simple systems, a second order mincut and a

third order mincut. The Error Factor curves and the basic reliability indices of average system failure rate, average outage duration and unavailability clearly show the importance of incorporating adverse weather in reliability assessments. The results show that the recognition of failure bunching effects becomes more significant as the level of redundancy increases. The creation of a two state weather model [8,10] was a significant improvement over the single state weather representation. The basic weakness of the two state model, however, is that it aggregates extreme weather periods with other relatively mild adverse weather periods and consequently results in incorrect appraisals.

A three state weather model is introduced in Chapter 3 in order to incorporate extremely adverse weather conditions. The systems studied in Chapter 2, using the two state weather model, are re-examined to investigate the impacts due to including extreme weather in the analysis. The results show that the reliability estimates obtained using the two state weather model are highly optimistic and the error increases as more failures occur in major adverse weather. The three state weather model should therefore be applied in these assessments. The Error Factor curves presented in Figure 3.10 with the variation in component parameters illustrate that systems with relatively low reliability experience lower impacts compared to those with better reliability. The studies show that higher frequency weather events with short durations and lower frequency weather events with longer durations have similar impacts on the average system failure rates.

The significance of weather modeling in transmission and distribution system reliability evaluation is illustrated in Chapter 4, using a simple practical system consisting of second order and third order mincuts. The load point and system indices are evaluated with varying percentages of failures occurring in bad weather and in extreme weather. Three line parallel systems are relatively more reliable than two line parallel systems. The reliability benefits, however, diminish when more failures occur in bad weather. Figures 4.2-4.5 accentuate the differences between the system indices of SAIFI, SAIDI, AENS and ECOST obtained utilizing the two state and three state weather models. This illustrates how the two state weather model underestimates the potential risk when more failures occur in extreme weather. The utilization of a three state weather model provides better appraisals in practical situations.

The stress created by weather is a continuous function of the weather intensity which directly correlates with the failure rate of an overhead circuit. Chapter 5 attempts to reflect the continuous phenomenon of weather conditions by using a large number of discrete states to represent the weather severity. The applicability of various multi-state weather models is illustrated in Figures 5.3-5.6 by a comparison of the respective Error Factor curves. It is clearly shown that a particular weather model does not provide accurate results in all conditions. The number of weather states used should be in accordance with the relative combinations of line failures occurring in adverse and major adverse weather. A three state weather model can provide acceptable results when a large percentage of line failures occur in bad weather and more than 20% of the bad weather failures occur in major adverse weather. Additional states should be included in the weather model in other situations.

The reliability index segmenting approach introduced in Chapter 6 emphasizes the contribution of different weather conditions to the system indices of SAIFI and SAIDI. The analysis of a practical distribution configuration shows that bad weather conditions make significant contributions to the system indices when relatively more outages occur in bad weather and that the reliability index segment due to extreme weather increases sharply when more failures occur in this weather. The study shows that the SAIDI can be significantly improved by reducing the restoration time due to the damage caused by major storms. Sensitivity studies on the frequency of storm occurrence illustrate that the system reliability degrades with increase in the frequency of storms. The approach proposed in this research work permits these factors to be quantified and examined in attempts to optimize customer service reliability.

The metric established in IEEE Standard 1366 [19] for separating the major event days, i.e. the days in which exceptional events occur that are beyond the control of a utility, is discussed in Chapter 7. The statistical approach designated as the Beta Method is based on the assumption that the SAIDI/day statistic is log-normally distributed. This method is being increasingly adopted by many utilities. The analysis of candidate reliability distributions indicates that the utilization of a lognormal distribution does not

consistently classify a major event. Electric distribution systems of different sizes and operating in different environments can have a variety of reliability index distributions. The Beta Method is not consistent in this situation. In a purely statistical approach, some situations that are not major events may be designated as major events in the numerical evaluation. For example, a tree falling on a transmission circuit may cause a lengthy power interruption. The increased daily SAIDI in this case could result in this situation being classified as a major event.

The reliability models developed in this thesis by incorporating the continuously varying weather become physically compatible with actual weather situations and can provide reasonably accurate appraisals. A two state weather model is easy to implement and requires relatively fewer data. It should, however, be appreciated that disregarding extreme weather conditions and varying weather phenomenon results in highly inaccurate assessments. It therefore becomes important to include sufficient weather states in the analysis. Future work in multi-state weather modeling could represent a particular weather situation such as lightning, hurricane, tornadoes, ice storms, wind velocities etc. by relevant individual states and each state accompanied by corresponding weather and line failure statistics.

The recognition of different weather contributions to the system indices pinpoints the situations where maximum reliability improvement can be achieved. The discussions associated with major event day classification should provide valuable information to utilities/regulators that are increasingly scrutinising the exclusion of major events from reliability performance evaluation.

The research described in this thesis illustrates the increasing concerns regarding weather effects on power system reliability. The concepts presented are a step forward in the continuing development of accurate transmission and distribution system reliability evaluation techniques and clearly illustrate the need to collect data associated with weather conditions and line failures.

REFERENCES

[1] R. Billinton and R. N. Allan, "Reliability Evaluation of Power Systems" Second Edition, Plenum Press, New York, 1996.

[2] Canadian Electricity Association, "2003 Annual Service Continuity Report on Distribution System Performance in Electrical Utilities," June 2004.

[3] Canadian Electricity Association, "2000 Annual Service Continuity Report on Distribution System Performance in Electrical Utilities," 2001.

[4] D. V. Ford, "The British Electricity Board National Fault and Interruption Reporting Scheme- Objectives, Development and Operating Experience," IEEE Winter Power Meeting, 1972.

[5] A. A. Chowdhury and D. O. Koval, "Deregulated Transmission System Reliability Planning Criteria Based on Historical Equipment Performance Data," IEEE Trans. on Industry Applications, Vol. 37, No. 1, Jan/Feb. 2001.

[6] Edition Electric Institute (EEI), "Utility Storm Restoration Response," Jan 2004.

[7] R. Billinton and J. E. Billinton, "Distribution System Reliability Indices," IEEE Trans. on Power Delivery, Vol. 4, No.1, Jan.1989, pp. 561-568.

[8] D. P. Gaver, F. E. Montmeat, and A.D. Patton, "Power System Reliability I-Measures of Reliability and Methods of Calculation," IEEE Trans. on Power Apparatus and Systems, Vol. 83, No. 7, pp. 727-737, July 1964.

[9] R. Billinton and W. Li, "A Novel Method for Incorporating Weather Effects in Composite System Adequacy Evaluation," IEEE Trans. on Power Systems, Vol. 6, No. 3, 1991, pp. 1154-1160.

[10] R. Billinton and K.E. Bollinger, "Transmission System Reliability Evaluation Using Markov Processes," IEEE Trans. on Power Apparatus and Systems, Vol. PAS-87, No. 2, pp. 538-547, Feb. 1968.

[11] R. Billinton and M. S. Grover, "Reliability Assessment of Transmission and Distribution Systems," IEEE Trans. on PAS-94, No.3, pp. 724-732, May/June 1975.

[12] R. Billinton and M.S. Grover, "Quantitative Evaluation of Permanent Outages in Distribution Systems," IEEE Trans. on PAS-94, No.3, pp.733-741, May/June 1975.

[13] R. Billinton, G. Singh and J. Acharya, "Failure Bunching Phenomena in Electrical Power Transmission Systems," 16th Advances in Reliability Technology Symposium, UK, April 14-16, 2005.

[14] R. Billinton, C. Wu, and G. Singh, "Extreme Adverse Weather Modeling in Transmission and Distribution System Reliability Evaluation," Proceedings of Power Systems Computation Conference, Spain, June 2002.

[15] R. Billinton, and J. Acharya, "Consideration of Multi-state Weather Models in Reliability Evaluation of Transmission and Distribution Systems," Proceedings of CCECE, pp. 601-604, May 2005.

[16] Z. G. Todd, "A Probability Method for Transmission and Distribution Outage Calculations," IEEE Trans. on Power Apparatus and Systems, Vol. 33, No. 7, pp. 696-701, July 1964.

[17] R. Billinton and R.N. Allan, "Reliability Evaluation of Engineering Systems: Concepts and Techniques," Second Edition, Plenum Press, 1992.

[18] G. D. Singh, "Extreme Weather Modeling in Transmission and Distribution System Reliability Modeling Incorporating Extreme Adverse Weather Considerations," M. Sc. Thesis, University of Saskatchewan, 2003.

[19] IEEE Standard 1366-2003, "IEEE Guide for Electric Power Distribution System Reliability Indices," May 2004.

[20] IEEE Standard 346:1973, "Terms For Reporting and Analyzing Outages of Electrical Transmission and Distribution Facilities and Interruptions to Customer Service," 1973.

[21] Critical Infrastructure Protection and Emergency Preparedness Canada. [Online] Available: http://www.ocipep.gc.ca/disaster/default.asp

[22] S. A. Ali, "Application of Customer Interruption Costs in Distribution System Reliability Worth Evaluation," M.Sc. Thesis, University of Saskatchewan, 2000.

[23] R. N. Allan, R. Billinton, I. Sarief, L. Goel and K. S. So, "A Reliability Test System for Educational Purposes – Basic Distribution System Data and Results," IEEE Trans. on Power Systems, Vol. 6, No. 2, May 1991.

[24] IEEE Standards 1366-1998, "IEEE Guide for Electric Power Distribution System Reliability Indices," 1998.

[25] C. A. Warren and R. Saint, "IEEE Reliability Indices Standards, Major Event Day Calculations and How They Relate to Small Utilities," IEEE Industry Applications Magazine, Vol. 11, Issue 1, pp. 16-22, Jan/Feb. 2005.

[26] R. Christie, J. Bouford, J. McDaniel, D. Schepers and C. Warren, "P1366 Major Event Day Language Draft," [Online], Downloaded in March 2005, http://grouper.ieee.org/groups/td/dist/sd/doc/

[27] Z. Pan, "Distribution System Risk Assessment using Reliability Distributions," M. Sc. Thesis, University of Saskatchewan, Canada, 2003.

[28] N. T. Kottegoda and R. Rosso, "Statistics, Probability and Reliability for Civil and Environmental Engineers," McGraw-Hill, New York, 1997.

[29] IEEE Working Group on System Design, [Online], Downloaded in March, 2005, http://grouper.ieee.org/groups/td/dist/sd/doc/

Appendix A

STORM DATA

The following data are taken from Utility Storm Restoration Response report of the Edison Electric Institute (EEI) [6].

Table A.1 Effect of Ice Storms

Date (mm-yy)	Peak number of customers on outage	Outage duration (days)	Estimated physical damage			Comment
			Number of poles replaced	Number of transfor-mers replaced	Wire replaced (miles)	
Feb-94	224,000	16	15,565	828	1,037	Major ice storm
Jan-96	61,000	4	NA	NA	NA	
Feb-96	650,000	8	NA	NA	100	
Mar-97	160,000	5	420	420	100	
Oct-97	213,000	4	670	610	170	Snow & wind
Jan-98	83,400	2	NA	NA	NA	
Dec-98	167,700	5	525	276	NA	Christmas-98
Nov-98	160,000	3	860	780	130	Snow & wind
Jan-99	120,000	4	100	100	NA	
Jan-99	109,685	5	153	62	NA	New year-99
Jan-99	220,000	4	NA	250	38	
Jan-00	17,3000	5	NA	NA	NA	
Dec-00	226,139	8	1,917	174	547	Storm #1
Dec-00	212,508	8	1,383	123	772	Storm #2
Oct-01	99,000	3	580	620	120	Snow & wind
Mar-02	93,000	2	620	270	70	Snow & wind
Dec-02	464,000	6	1,322	2,196	85	
Dec-02	1,375,000	9	3,200	2,300	549	
Dec-02	41,951	5	463	64	NA	
Feb-03	350,000	5	NA	NA	NA	
Apr-03	196,000	6	600	580	160	

Table A.2 Effect of Hurricanes

Date (mm-yr)	Peak #of customers on outage	Outage duration (days)	Estimated physical damage			
			Poles replaced	Transformer replaced	Wire replaced	Name of Hurricane
Sep-89	696,000	18	8,800	6,308	700	Hugo
Sep-89	180,000	12	NA	2,300	286	Hugo
Aug-96	225,000	4	NA	NA	NA	Bertha
Sep-96	790,000	10	5,500	2,800	3,000	Fran
Sep-96	450,000	9	1,400	921	217	Fran
Sep-98	244,500	4	NA	NA	NA	Bonnie
Sep-98	260,000	3	644	328	118	Georges
Sep-99	537,000	6	1,160	586	680	Floyd
Sep-02	95,000	2	310	520	85	Isadora
Oct-02	243,000	2	1,800	920	202	Lily
Sep-03	320,000	2	212	307	70	Isabel

Table A.3 Effect of other weather conditions

Date (mm-yr)	Peak # of Customers on outage	Outage duration (days)	Estimated physical damage			Storm event
			Poles replaced	Tranfor-mers replaced	Wire replaced (miles)	
May-89	228,000	8	NA	NA	NA	Tornadoes
Mar-93	170,000	7	NA	NA	NA	Snow blizzard
Apr-97	80,000	2	790	340	80	Wind storm
May-98	442,000	8	1,540	1,210	470	Lightning & wind storm
July-98	106,000	2	570	820	90	Lightning & wind storm
May-99	99,000	2	680	570	110	Lightning & wind storm
Sep-99	322,494	8	350	210	85	Tropical storm Floyd
May-00	155,000	4	NA	NA	NA	Thunderstorm
May-03	142,000	1.5	NA	NA	NA	Thunderstorm
May-03	218,000	6	1,100	200	NA	Tornadoes
Jun-03	350,000	3	NA	NA	NA	Thunderstorm
Sep-03	480,883	8	444	306	103	Tropical storm Isabel

NA ─ data not available

Appendix B

STOCHASTIC TRANSITIONAL PROBABILITY MATRICES

B.1 Three component system with a two state weather model

The stochastic transitional probability matrix for the state space diagram shown in Figure 2.6 is given by Equation B.1.

$$[P] = \begin{bmatrix} A & B \\ C & D \end{bmatrix} \tag{B.1}$$

where, $[B] = n_a [I]_{8x8}$

$[D] = a_n [I]_{8x8}$

$[I]$ is the identity matrix and matrices [A] and [C] are given below.

[A] =

$$\begin{bmatrix}
1-\lambda_1-\lambda_2-\lambda_3-n_a & \lambda_1 & \lambda_2 & \lambda_3 & 0 & 0 & 0 & 0 \\
\mu_1 & 1-\mu_1-\lambda_2-\lambda_3-n_a & 0 & 0 & \lambda_2 & 0 & \lambda_3 & 0 \\
\mu_2 & 0 & 1-\mu_2-\lambda_1-\lambda_3-n_a & 0 & \lambda_1 & \lambda_3 & 0 & 0 \\
\mu_3 & 0 & 0 & 1-\mu_3-\lambda_1-\lambda_2-n_a & 0 & \lambda_2 & \lambda_1 & 0 \\
0 & \mu_2 & \mu_1 & 0 & 1-\mu_1-\mu_2-\lambda_3-n_a & 0 & 0 & \lambda_3 \\
0 & 0 & \mu_3 & \mu_2 & 0 & 1-\mu_2-\mu_3-\lambda_1-n_a & 0 & \lambda_1 \\
0 & \mu_3 & 0 & \mu_1 & 0 & 0 & 1-\mu_1-\mu_3-\lambda_2-n_a & \lambda_2 \\
0 & 0 & 0 & 0 & \mu_3 & \mu_1 & \mu_2 & 1-\mu_1-\mu_2-\mu_3-n_a
\end{bmatrix}$$

[C] =

$$\begin{bmatrix}
1-\lambda'_1-\lambda'_2-\lambda'_3-a_n & \lambda'_1 & \lambda'_2 & \lambda'_3 & 0 & 0 & 0 & 0 \\
0 & 1-\lambda'_2-\lambda'_3-a_n & 0 & 0 & \lambda'_2 & 0 & \lambda'_3 & 0 \\
0 & 0 & 1-\lambda'_1-\lambda'_3-a_n & 0 & \lambda'_1 & \lambda'_3 & 0 & 0 \\
0 & 0 & 0 & 1-\lambda'_1-\lambda'_2-a_n & 0 & \lambda'_2 & \lambda'_1 & 0 \\
0 & 0 & 0 & 0 & 1-\lambda'_3-a_n & 0 & 0 & \lambda'_3 \\
0 & 0 & 0 & 0 & 0 & 1-\lambda'_1-a_n & 0 & \lambda'_1 \\
0 & 0 & 0 & 0 & 0 & 0 & 1-\lambda'_2-a_n & \lambda'_2 \\
0 & 0 & 0 & 0 & 0 & 0 & 0 & 1-a_n
\end{bmatrix}$$

B.2 Three component system with a three state weather model

Equation B.2 gives the stochastic transitional probability matrix associated with the state space diagram shown in Figure 3.4.

$$[P]=\begin{bmatrix} A & B & C \\ D & E & F \\ G & H & J \end{bmatrix} \qquad \text{(B.2)}$$

where,

$$[B]=n_a[I]_{8x8} \qquad [C]=n_m[I]_{8x8}$$

$$[D]=a_n[I]_{8x8} \qquad [F]=a_m[I]_{8x8}$$

$$[G]=m_n[I]_{8x8} \qquad [H]=m_a[I]_{8x8}$$

$[I]$ is the identity matrix and matrices [A], [E] and [J] are given as follows.

$[A] =$

$$\begin{bmatrix}
1-\lambda_1-\lambda_2-\lambda_3-n_a-n_m & \lambda_1 & \lambda_2 & \lambda_3 & 0 & 0 & 0 & 0 \\
\mu_1 & 1-\mu_1-\lambda_2-\lambda_3-n_a-n_m & 0 & 0 & \lambda_2 & 0 & \lambda_3 & 0 \\
\mu_2 & 0 & 1-\mu_2-\lambda_1-\lambda_3-n_a-n_m & 0 & \lambda_1 & \lambda_3 & 0 & 0 \\
\mu_3 & 0 & 0 & 1-\mu_3-\lambda_1-\lambda_2-n_a-n_m & 0 & \lambda_2 & \lambda_1 & 0 \\
0 & \mu_2 & \mu_1 & 0 & 1-\mu_1-\mu_2-\lambda_3-n_a-n_m & 0 & 0 & \lambda_3 \\
0 & 0 & \mu_3 & \mu_2 & 0 & 1-\mu_2-\mu_3-\lambda_1-n_a-n_m & 0 & \lambda_1 \\
0 & \mu_3 & 0 & \mu_1 & 0 & 0 & 1-\mu_1-\mu_3-\lambda_2-n_a-n_m & \lambda_2 \\
0 & 0 & 0 & 0 & \mu_3 & \mu_1 & \mu_2 & 1-\mu_1-\mu_2-\mu_3-n_a-n_m
\end{bmatrix}$$

$[E] =$

$$\begin{bmatrix}
1-\lambda_1^a-\lambda_2^a-\lambda_3^a-a_n-a_m & \lambda_1^a & \lambda_2^a & \lambda_3^a & 0 & 0 & 0 & 0 \\
0 & 1-\lambda_2^a-\lambda_3^a-a_n-a_m & 0 & 0 & \lambda_2^a & 0 & \lambda_3^a & 0 \\
0 & 0 & 1-\lambda_1^a-\lambda_3^a-a_n-a_m & 0 & \lambda_1^a & \lambda_3^a & 0 & 0 \\
0 & 0 & 0 & 1-\lambda_1^a-\lambda_2^a-a_n-a_m & 0 & \lambda_2^a & \lambda_1^a & 0 \\
0 & 0 & 0 & 0 & 1-\lambda_3^a-a_n-a_m & 0 & 0 & \lambda_3^a \\
0 & 0 & 0 & 0 & 0 & 1-\lambda_1^a-a_n-a_m & 0 & \lambda_1^a \\
0 & 0 & 0 & 0 & 0 & 0 & 1-\lambda_2^a-a_n-a_m & \lambda_2^a \\
0 & 0 & 0 & 0 & 0 & 0 & 0 & 1-a_n-a_m
\end{bmatrix}$$

$$[J] =$$

$$\begin{bmatrix}
1-\lambda_1^m-\lambda_2^m-\lambda_3^m-m_n-m_a & \lambda_1^m & \lambda_2^m & \lambda_3^m & 0 & 0 & 0 & 0 \\
0 & 1-\lambda_2^m-\lambda_3^m-m_n-m_a & 0 & 0 & \lambda_2^m & 0 & \lambda_3^m & 0 \\
0 & 0 & 1-\lambda_1^m-\lambda_3^m-m_n-m_a & 0 & \lambda_1^m & \lambda_3^m & 0 & 0 \\
0 & 0 & 0 & 1-\lambda_1^m-\lambda_2^m-m_n-m_a & 0 & \lambda_2^m & \lambda_1^m & 0 \\
0 & 0 & 0 & 0 & 1-\lambda_3^m-m_n-m_a & 0 & 0 & \lambda_3^m \\
0 & 0 & 0 & 0 & 0 & 1-\lambda_1^m-m_n-m_a & 0 & \lambda_1^m \\
0 & 0 & 0 & 0 & 0 & 0 & 1-\lambda_2^m-m_n-m_a & \lambda_2^m \\
0 & 0 & 0 & 0 & 0 & 0 & 0 & 1-m_n-m_a
\end{bmatrix}$$

Appendix C

LOAD POINT INDICES AND INTERRUPTION COSTS

Table C.1-C.16 show the reliability indices for the system shown in Figure 4.1 when the percentage of failures occurring in bad weather and major adverse (extreme) weather is varied. Table C.17 provides the individual user sector interruption costs and the composite customer damage functions (CCDF) for the different outage durations.

Case I: Percentage of line failures occurring in bad weather = 50%

(a) 10% of bad weather failures occurring in major adverse weather

Table C.1 Reliability indices for load point L1 (F_b = 50% and F_m = 10%)

Minimal cut	Failure rate (f/yr)	Average outage duration (hrs)	Unavailability (hrs/yr)	ECOST ($/yr)	EENS (kWh/yr)
1-2-3	0.002047	5.34	0.0109	1006.31	218.78
1-2-4	0.003843	5.34	0.0205	1889.22	410.68
Total	0.005890	5.34	0.0314	2895.53	629.46

Table C.2 Reliability indices for load point L2 (F_b = 50% and F_m = 10%)

Minimal cut	Failure rate (f/yr)	Average outage duration (hrs)	Unavailability (hrs/yr)	ECOST ($/yr)	EENS (kWh/yr)
3-4	0.030864	6.91	0.2135	17841.86	3415.76
1-2-4	0.003843	5.34	0.0205	1574.09	328.54
Total	0.034707	6.74	0.2340	19415.95	3744.30

(b) 30% of line failures in bad weather occurring in major adverse weather

Table C.3 Reliability indices for load point L1 (F_b = 50% and F_m = 30%)

Minimal cut	Failure rate (f/yr)	Average outage duration (hrs)	Unavailability (hrs/yr)	ECOST ($/kW)	EENS (kWh/yr)
1-2-3	0.018005	5.36	0.0966	8898.07	1932
1-2-4	0.029600	5.36	0.1588	14628.32	3176
Total	0.047605	5.36	0.2554	23526.39	5108

Table C.4 Reliability indices for load point L2 (F_b = 50% and F_m = 30%)

Minimal cut	Failure rate (f/yr)	Average outage duration (hrs)	Unavailability (hrs/yr)	ECOST ($/kW)	EENS (kWh/yr)
3-4	0.066867	6.99	0.4679	39253.60	7486.40
1-2-4	0.029600	5.36	0.1588	12185.73	2540.80
Total	0.096467	6.50	0.6267	51439.33	10027.20

(c) 40% bad weather failures occurring in major adverse weather

Table C.5 Reliability indices for load point L1 (F_b = 50% and F_m = 40%)

Minimal cut	Failure rate (f/yr)	Average outage duration (hrs)	Unavailability (hrs/yr)	ECOST ($/kW)	EENS (kWh/yr)
1-2-3	0.032020	5.36	0.1719	15824.28	3438
1-2-4	0.050435	5.36	0.2707	24924.98	5414
Total	0.082455	5.36	0.4426	40749.26	8852

Table C.6 Reliability indices for load point L2 (F_b = 50% and F_m = 40%)

Minimal cut	Failure rate(f/yr)	Average outage duration (hrs)	Unavailability (hrs/yr)	ECOST ($/kW)	EENS (kWh/yr)
3-4	0.090257	7.00	0.6331	53085.56	10129.60
1-2-4	0.050435	5.36	0.2707	20763.08	4331.20
Total	0.140692	6.42	0.9038	73848.64	14460.80

(d) 50% of bad weather failures occurring in major adverse weather

Table C.7 Reliability indices for load point L1, (F_b = 50% and F_m = 50%)

Minimal cut	Failure rate (f/yr)	Average outage duration (hrs)	Unavailability (hrs/yr)	ECOST ($/kW)	EENS (kWh/yr)
1-2-3	0.048655	5.36	0.2612	24045.3	5224
1-2-4	0.074012	5.36	0.3973	36576.73	7946
Total	0.122667	5.37	0.6585	60622.03	13170

Table C.8 Reliability indices for load point L2, (F_b = 50% and F_m = 50%)

Minimal cut	Failure rate (f/yr)	Average outage duration (hrs)	Unavailability (hrs/yr)	ECOST ($/kW)	EENS (kWh/yr)
3-4	0.114802	7.02	0.8065	67779.10	129040
1-2-4	0.074012	5.36	0.3973	30469.26	6356.80
Total	0.188814	6.38	1.2038	98248.36	19260.8

Case II: Percentage of line failures occurring in bad weather = 90%

(a) 10% bad weather failures occurring in major adverse weather

Table C.9 Reliability indices for load point L1 (F_b = 90% and F_m = 10%)

Minimal cut	Failure rate (f/yr)	Average outage duration (hrs)	Unavailability (hrs/yr)	ECOST ($/yr)	EENS (kWh/yr)
1-2-3	0.009477	5.36	0.0509	4683.53	1017.60
1-2-4	0.017158	5.36	0.0921	8479.48	1842.56
Total	0.026635	5.36	0.1430	13163.01	2860.16

Table C.10 Reliability indices for load point L2 (F_b = 90% and F_m = 10%)

Minimal cut	Failure rate (f/yr)	Average outage duration (hrs)	Unavailability (hrs/yr)	ECOST ($/yr)	EENS (kWh/yr)
3-4	0.083628	7.04	0.5898	49561.30	9436.80
1-2-4	0.009477	5.36	0.0509	3901.49	814.40
Total	0.093105	6.88	0.6407	53462.79	10251.20

(b) 30% bad weather failures occurring in major adverse weather

Table C.11 Reliability indices for load point L1 (F_b = 90% and F_m = 30%)

Minimal cut	Failure rate (f/yr)	Average outage duration (hrs)	Unavailability (hrs/yr)	ECOST ($/yr)	EENS (kWh/yr)
1-2-3	0.058448	5.37	0.3139	28955.14	6278
1-2-4	0.088518	5.37	0.4755	43851.82	9510
Total	0.146966	5.37	0.7894	72806.96	15788

Table C.12 Reliability indices for load point L2 (F_b = 90% and F_m = 30%)

Minimal Cut	Failure rate (f/yr)	Average outage duration (hrs)	Unavailability (hrs/yr)	ECOST ($/yr)	EENS (kWh/yr)
3-4	0.155517	7.05	1.0972	92339.77	17555.20
1-2-4	0.088518	5.37	0.4755	36526.07	7608.00
Total	0.244035	6.44	1.5727	128865.84	25163.20

(c) 40% bad weather failures occurring in major adverse weather

Table C.13 Reliability indices for load point L1 (F_b = 90% and F_m = 40%)

Minimal cut	Failure rate (f/yr)	Average outage duration (hrs)	Unavailability (hrs/yr)	ECOST ($/yr)	EENS (kWh/yr)
1-2-3	0.092633	5.37	0.4975	45890.39	9950
1-2-4	0.13342	5.37	0.7166	66096.27	14332
Total	0.226053	5.370864	1.2141	111986.66	24282

Table C.14 Reliability indices for load point L2 (F_b = 90% and F_m = 40%)

Minimal cut	Failure rate (f/yr)	Average outage duration (hrs)	Unavailability (hrs/yr)	ECOST ($/yr)	EENS (kWh/yr)
3-4	0.194327	7.05	1.3710	115383.60	21936.00
1-2-4	0.13342	5.37	0.7166	55054.43	11465.60
Total	0.327747	6.37	2.0876	170438.03	33401.60

(d) 50% bad weather failures occurring in major adverse weather

Table C.15 Reliability indices for load point L1 (F_b = 90% and F_m = 50%)

Minimal cut	Failure rate (f/yr)	Average outage duration (hrs)	Unavailability (hrs/yr)	ECOST ($/yr)	EENS (kWh/yr)
1-2-3	0.128379	5.37	0.6894	63598.96	13788
1-2-4	0.177994	5.37	0.9559	88178.23	19118
Total	0.306373	5.37	1.6453	151777.19	32906

Table C.16 Reliability indices for load point L2 (F_b = 90% and F_m = 50%)

Minimal cut	Failure rate (f/yr)	Average outage duration (hrs)	Unavailability (hrs/yr)	ECOST ($/yr)	EENS (kWh/yr)
3-4	0.231402	7.05	1.6325	137397.25	26120.00
1-2-4	0.177994	5.37	0.9559	73447.44	15294.40
Total	0.409396	6.32	2.5884	210844.69	41414.40

Table C.17 Sector interruption costs and composite customer damage functions (CCDF)

Duration (hr)	User sector interruption cost ($/kW)				CCDF ($/kW)	
	Agricultural C_{ag}	Commercial C_{cm}	Industrial C_{in}	Residential C_{rs}	Load Point L1	Load Point L2
1.00	0.649	8.552	9.085	0.482	4.64	5.09
3.33	1.77	26.38	21.99	3.61	13.93	14.73
4.00	2.064	31.317	25.163	4.914	16.60	17.45
5.00	2.58	42.86	32.52	7.14	22.48	23.46
5.31	2.74	46.64	34.85	7.90	24.40	25.41
5.34	2.75	47.02	35.07	7.97	24.58	25.60
5.36	2.76	47.26	35.22	8.02	24.71	25.73
5.37	2.77	47.39	35.30	8.05	24.77	25.79
6.32	3.26	59.59	42.57	10.57	30.94	32.06
6.37	3.28	60.25	42.95	10.71	31.28	32.38
6.38	3.29	60.38	42.03	10.74	31.35	32.47
6.42	3.31	60.92	43.34	10.85	31.62	32.74
6.44	3.32	61.18	43.50	10.91	31.75	32.87
6.50	3.35	61.99	43.96	11.08	32.16	33.29
6.88	3.54	67.14	46.93	12.19	34.76	35.92
6.91	3.56	67.56	47.16	12.28	34.97	36.13
6.96	3.59	68.24	47.55	12.43	35.31	36.48
6.99	3.60	68.67	47.79	12.52	35.52	36.69
7.00	3.61	68.80	47.87	12.54	35.59	36.76
7.02	3.62	69.07	48.03	12.61	35.73	36.90
7.04	3.63	69.35	48.18	12.67	35.87	37.04
7.05	3.63	69.49	48.26	12.70	35.94	37.11
8.00	4.12	83.008	55.808	15.69	42.75	43.98

Appendix D

LOAD POINT INDICES FOR EXTREME WEATHER SEVERITY ANALYSIS

Tables D.1-D.6 present the load point indices associated with the distribution system shown in Figure 6.1 for various extreme weather frequencies.

Case (a): 40% of the total failures occurring in bad weather and 10% of the bad weather failures in extreme weather

- Load point failure rates

Table D.1 Load point failure rates (failures/year), Case (a)

Load point	Number of extreme weather events		
	One per year	Two per year	Three per year
1	0.239	0.247	0.255
2	0.252	0.261	0.269
3	0.252	0.261	0.269
4	0.239	0.247	0.255
5	0.252	0.261	0.269
6	0.249	0.258	0.266
7	0.252	0.261	0.269
8	0.140	0.145	0.150
9	0.140	0.145	0.150
10	0.243	0.251	0.259
11	0.252	0.261	0.269
12	0.256	0.264	0.273
13	0.252	0.261	0.269
14	0.256	0.264	0.273
15	0.243	0.251	0.259
16	0.252	0.261	0.269
17	0.243	0.251	0.259
18	0.243	0.251	0.259
19	0.256	0.264	0.273
20	0.256	0.264	0.273
21	0.252	0.261	0.269
22	0.256	0.264	0.273

- Load point unavailabilities

Table D.2 Load point unavailabilities (hours/year), Case (a)

Load point	Number of extreme weather events		
	One per year	Two per year	Three per year
1	1.219	1.571	1.923
2	1.358	1.761	2.165
3	1.358	1.761	2.165
4	1.219	1.571	1.923
5	1.358	1.761	2.165
6	1.323	1.714	2.104
7	1.258	1.623	1.988
8	1.107	1.507	1.907
9	1.018	1.379	1.741
10	1.220	1.573	1.925
11	1.358	1.761	2.165
12	1.392	1.809	2.225
13	1.234	1.587	1.939
14	1.269	1.634	2.000
15	1.220	1.573	1.925
16	1.358	1.761	2.165
17	1.254	1.619	1.984
18	1.220	1.573	1.925
19	1.359	1.763	2.166
20	1.359	1.763	2.166
21	1.234	1.587	1.939
22	1.269	1.634	2.000

- Load point average outage durations

Table D.3 Load point average outage durations (hours), Case (a)

Load point	Number of extreme weather events		
	One per year	Two per year	Three per year
1	5.095	6.352	7.530
2	5.378	6.748	8.032
3	5.378	6.748	8.032
4	5.095	6.352	7.530
5	5.378	6.748	8.032
6	5.310	6.653	7.911
7	4.982	6.219	7.378
8	7.908	10.391	12.707
9	7.266	9.508	11.599

Table D.3 Continued…

Load point	Number of extreme weather events		
	One per year	Two per year	Three per year
10	5.031	6.271	7.433
11	5.378	6.748	8.032
12	5.444	6.841	8.149
13	4.889	6.081	7.196
14	4.962	6.182	7.325
15	5.031	6.271	7.433
16	5.378	6.748	8.032
17	5.168	6.455	7.660
18	5.031	6.271	7.433
19	5.314	6.667	7.934
20	5.314	6.667	7.934
21	4.889	6.081	7.196
22	4.962	6.182	7.325

Case (b): 80% of the total failures occurring in bad weather and 40% of the bad weather failures in extreme weather

Table D.4 Load point failure rates (failures/year), Case (b)

Load point	Number of extreme weather events		
	One per year	Two per year	Three per year
1	0.239	0.309	0.380
2	0.252	0.327	0.401
3	0.252	0.327	0.401
4	0.239	0.309	0.380
5	0.252	0.327	0.401
6	0.249	0.322	0.396
7	0.252	0.327	0.401
8	0.139	0.183	0.227
9	0.139	0.183	0.227
10	0.242	0.314	0.385
11	0.252	0.327	0.401
12	0.256	0.331	0.407
13	0.252	0.327	0.401
14	0.256	0.331	0.407
15	0.242	0.314	0.385
16	0.252	0.327	0.401
17	0.242	0.314	0.385
18	0.242	0.314	0.385
19	0.256	0.331	0.407
20	0.256	0.331	0.407
21	0.252	0.327	0.401
22	0.256	0.331	0.407

- Load point unavailabilities

Table D.5 Load point unavailabilities (hours/year), Case (b)

Load point	Number of extreme weather events		
	One per year	Two per year	Three per year
1	3.605	6.448	9.291
2	4.093	7.351	10.608
3	4.093	7.351	10.608
4	3.605	6.448	9.291
5	4.093	7.351	10.608
6	3.974	7.128	10.282
7	3.733	6.682	9.632
8	3.844	7.071	10.297
9	3.483	6.402	9.321
10	3.608	6.452	9.296
11	4.093	7.351	10.608
12	4.213	7.574	10.935
13	3.616	6.463	9.310
14	3.735	6.686	9.636
15	3.608	6.452	9.296
16	4.093	7.351	10.608
17	3.725	6.671	9.618
18	3.608	6.452	9.296
19	4.096	7.354	10.613
20	4.096	7.354	10.613
21	3.616	6.463	9.310
22	3.735	6.686	9.636

- Load point average outage duration

Table D.6 Load point average outage durations (hours), Case (b)

Load point	Number of extreme weather events		
	One per year	Two per year	Three per year
1	15.094	20.844	24.462
2	16.228	22.493	26.432
3	16.228	22.493	26.432
4	15.094	20.844	24.462
5	16.228	22.493	26.432
6	15.982	22.123	25.982
7	14.799	20.448	23.999
8	27.560	38.555	45.302
9	24.975	34.909	41.006
10	14.882	20.550	24.117
11	16.228	22.493	26.432
12	16.467	22.854	26.869
13	14.335	19.776	23.196
14	14.601	20.174	23.678
15	14.882	20.550	24.117
16	16.228	22.493	26.432
17	15.364	21.250	24.953
18	14.882	20.550	24.117
19	16.010	22.191	26.077
20	16.010	22.191	26.077
21	14.335	19.776	23.196
22	14.601	20.174	23.678